ผลของตัวเร่งของโลหะต่อการเกิดซิลิกอนไนไตรด์จากเถ้าแกลบด้วยกระบวนการ
คาร์โบเทอร์มอลรีดักชันและไนไตรด์เดชัน

นาย ประพัฒน์ ทนงคงสวัสดิ์

CATALYTIC EFFECTS OF METALS ON THE FORMATION OF SILICON NITRIDE FROM RICE HUSK ASH VIA CARBOTHERMAL REDUCTION AND NITRIDATION PROCESS

Mr. Praphat Thanongkongsawad
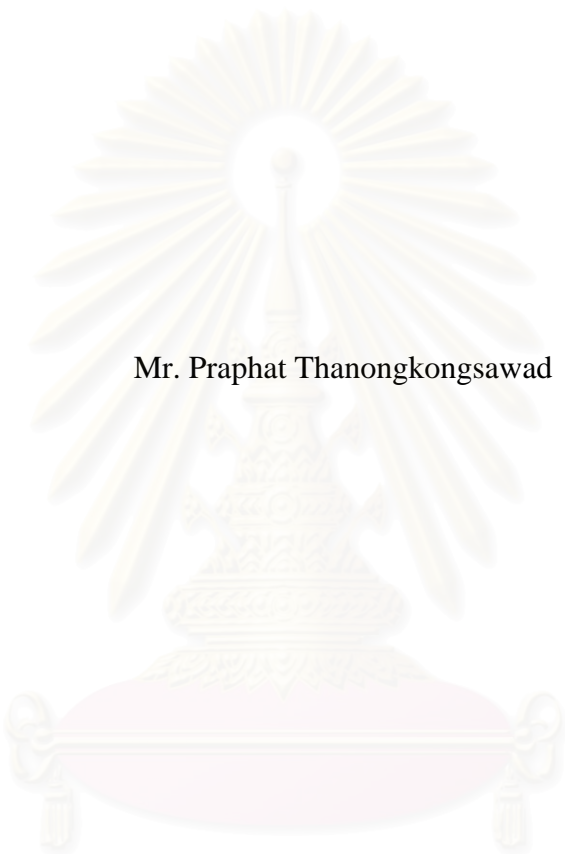
A Thesis Submitted in Partial Fulfillment of the Requirements
for the Degree of Master of Engineering Program in Chemical Engineering
Department of Chemical Engineering
Faculty of Engineering
Chulalongkorn University
Academic Year 2005
ISBN 974-17-6945-8

Thesis Title	CATALYTIC EFFECTS OF METALS ON THE FORMATION OF SILICON NITRIDE FROM RICE HUSK ASH VIA CARBOTHERMAL REDUCTION AND NITRIDATION PROCESS
By	Mr. Praphat Thanongkongsawad
Field of study	Chemical Engineering
Thesis Advisor	Assistant Professor Varong Pavarajarn, Ph.D.

Accepted by the Faculty of Engineering, Chulalongkorn University in Partial Fulfillment of the Requirements for the Master's Degree

.... Dean of the Faculty of Engineering

(Professor Direk Lavansiri, Ph.D.)

THESIS COMMITTEE

.... Chairman

(Associate Professor Tawatchai Charinpanitkul, Ph.D.)

.... Thesis Advisor

(Assistant Professor Varong Pavarajarn, Ph.D.)

.... Member

(Assistant Professor Sarawut Rimdusit, Ph.D.)

.... Member

(Assistant Professor Bunjerd Jongsomjit, Ph.D.)

.... Member

(Okorn Mekasuwandumrong, Ph.D.)

ประพัฒน์ ทนงคงสวัสดิ์ : ผลของตัวเร่งของโลหะต่อการเกิดซิลิกอนไนไตรด์จากเถ้าแกลบด้วย
กระบวนการคาร์โบเทอร์มอลรีดักชันและไนไตรด์เดชัน (CATALYTIC EFFECTS OF
METALS ON THE FORMATION OF SILICON NITRIDE FROM RICE HUSK
ASH VIA CARBOTHERMAL REDUCTION AND NITRIDATION PROCESS)
อ.ที่ปรึกษา : ผศ.ดร.วรงค์ ปวราจารย์, 120 หน้า. ISBN 974-17-6945-8.

แกลบถูกนำมาใช้ในการผลิตซิลิคอนไนไตรด์โดยวิธีคาร์โบเทอร์มอลรีดักชั่นและไนไตรด์
เดชั่น ซึ่งเป็นกระบวนการหนึ่งที่ใช้ในการผลิตซิลิคอนไนไตรด์อย่างแพร่หลาย ดังนั้นงานวิจัยนี้ได้
ทำการศึกษาอิทธิพลของโลหะต่อกระบวนการคาร์โบเทอร์มอลรีดักชั่นและไนไตรด์เดชั่นของเถ้า
แกลบ โดยทำการเผาแกลบภายใต้บรรยากาศอาร์กอนที่อุณหภูมิ 600 องศาเซลเซียสเป็นเวลา 3
ชั่วโมง เพื่อผลิตเถ้าแกลบก่อนที่จะเติมโลหะอันได้แก่ เหล็ก อลูมิเนียม แมกนีเซียม คอปเปอร์
และอิทเทรียม ลงไปในเถ้าแกลบในช่วงปริมาณ 1-3 เปอร์เซ็นต์โดยมวล ผลิตภัณฑ์ที่ได้จาก
กระบวนการคาร์โบเทอร์มอลรีดักชั่นและไนไตรด์เดชั่นที่ 1450 องศาเซลเซียสนั้นสามารถจำแนก
ได้เป็น 2 ส่วน ได้แก่ ผงสีเทาเข้มที่มีคาร์บอนปะปนอยู่ที่ก้นของภาชนะใส่สารตัวอย่าง และลักษณะ
เป็นเส้นใยสีขาวอยู่ด้านบนของผงสีเทาเข้ม ยังพบอีกว่าปริมาณของเฟสอัลฟาในซิลิกอนไนไตรด์
โดยทั่วไปนั้นจะลดลงเมื่อมีการเติมโลหะลงไป มีเพียงอิทเทรียมที่สามารถเพิ่มปริมาณของ
เฟสอัลฟาได้ นอกจากนั้นยังได้ทำการศึกษาผลของการบำบัดเถ้าแกลบด้วยไฮโดรเจนที่ 1450 องศา
เซลเซียส ก่อนการทำปฏิกิริยาที่เวลาต่างๆ พบว่าสภาวะของการบำบัดด้วยไฮโดรเจนเป็นปัจจัย
สำคัญที่ส่งผลต่อการเกิดซิลิกอนคาร์ไบด์หรือซิลิกอนไนไตรด์ในผลิตภัณฑ์

ภาควิชา	วิศวกรรมเคมี	ลายมือชื่อนิสิต	
สาขาวิชา	วิศวกรรมเคมี	ลายมือชื่ออาจารย์ที่ปรึกษา	
ปีการศึกษา	2548	ลายมือชื่ออาจารย์ที่ปรึกษาร่วม	

PRAPHAT THANONGKONGSAWAD: CATALYTIC EFFECTS OF METALS ON THE FORMATION OF SILICON NITRIDE FROM RICE HUSK ASH VIA CARBOTHERMAL REDUCTION AND NITRIDATION PROCESS THESIS ADVISOR: ASST. PROF. VARONG PAVARAJARN, Ph.D., 120 pp. ISBN 974-17-6945-8

Rice husk was used in silicon nitride synthesis by the carbothermal reduction and nitridation which has been recognized as one of the common methods for producing silicon nitride. In this study, catalytic effects of metals in the carbothermal reduction and nitridation of rice husk ash for silicon nitride synthesis were investigated. Rice husk was first pyrolyzed at 600°C for 3 h in argon atmospheres to produce rice husk ash (RHA) before impregnated with 1-3% by mass of iron, aluminium, magnesium, copper and yttrium. The product obtained could be categorized into two forms, i.e. carbon containing dark gray powder at the bottom of sample holder and white fibrous material on the top of dark gray powder. It is found that the fraction of α-silicon nitride is generally decreased when a metal is added to RHA. Only yttrium can enhance in the product, the fraction of α-phase. Hydrogen pretreatment of RHA at 1450°C and various time are also investigated. It is suggested that the condition of the pretreatment is a crucial factor to control the formation of the crystalline phases, i.e. silicon carbide and silicon nitride in the product.

Department __Chemical Engineering__ Student's signature _Praphat Thanongkongsawad_

Field of study _Chemical Engineering_ Advisor's signature _Varong P._

Academic year ____2005____ Co-advisor's signature _____

ACKNOWLEDGEMENTS

The author would like to express him greatest gratitude to him advisor, Assistant Professor Varong Pavarajarn, for his help, invaluable suggestions and guidance throughout the entire of this work. His precious teaching the way to be good in study and research has always been greatly appreciated. Although this work had obstacles, finally it could be completed by his advice. In addition, his friendliness motivated the author with strength and happiness to do this work.

The author wish to express him thanks to Associate Professor Tawatchai Charinpanitkul who has been the chairman of the committee for this thesis, as well as Assistant Professor Sarawut Rimdusit and Assistant Professor Bunjerd Jongsomjit, who have been him committee members. He would also like to register him thanks to Miss. Ruttairat Precharyutasin for their help during him study. To the many others, not specifically named, in Center of Excellence on Catalysis and Catalytic Reaction Engineering, Department of Chemical Engineering, who have provided him with encouragement and co-operate along this study, please be ensured that he thinks of you.

Moreover, the author would like to thank the Thailand Research Fund (TRF), the Thailand-Japan Technology Transfer Project (TJTTP) as well as the Graduate School of Chulalongkorn University for their financial support. Finally, he would like to dedicate the achievement of this work to him dearest parents. Their unyielding support and unconditional love have always been in him mind.

CONTENTS

page

Chapter **page**

Chapter   **page**

LIST OF TABLES

Table   **page**

LIST OF FIGURES

Figure **page**

Figure **page**

Figure **page**

Figure   **page**

Figure   **page**

CHAPTER I

INTRODUCTION

The world rice production as paddy is more than 550,000,000 tons/year. About 20% of the paddy (100,000,000 tons) is rice husk. In Thailand, about 4,000,000 tons of rice husk are produced every year. By this huge abundance, it has been interested in the utilization of rice husk. Rice husk has nutritive properties, resistance to degradation and high ash content. The major constituents of rice husk are cellulose (38%), lignin (22%), ash (20%), pentosan (18%) and other minor elements, such as sodium, potassium, calcium, magnesium, iron, copper, manganese and zinc [James et al., 1986]. This compositions are varied by geographical factors, year of harvest and sample preparation [Della et al., 2002].

Endeavour to use rice husk have been obstacled by their woody and sharp characteristic as well as toughness. So, current applications of rice husk are in low-value agricultural areas or to be used as fuel. However, rice husk has been recognized as high silica–content agricultural product. Silica contained in rice husk is mainly localized in the tough interlayer of the husk and fills in the spaces between the epidermal cell [Houston 1972; Ding 1986; Krishnarao et al., 1992]. Burning rice husk results in the waste product, namely rice husk ash (RHA). RHA is rich in silica (60-98%, depending on burning conditions) and can be an economically viable raw material for production of silica gels and silica powders (Kamath and Proctor, 1998; Chakraverty and Kaleemullah, 1991). Silica containing in RHA has been used as an adsorbent for minor vegetable oil components (Proctor et al., 1995; Proctor and Palaniappan, 1990). Moreover, silica in RHA has been directly used to synthesize various siliceous species, such as silicon, silicon nitride, silicon carbide and magnesium silicide [Real et al., 1996]

Silicon nitride (Si_3N_4) is one of the most promising structural materials for high-temperature and high mechanical stress applications because of its excellent properties such as high strength retention at elevated temperature, low thermal expansion coefficient, good thermal shock resistance and high corrosion resistance. It

has much higher creep resistance than metals and its thermal shock resistance is much better than other ceramics. Silicon nitride is also inert to many chemicals. Thus, another benefit of silicon nitride is its corrosion resistance. For these good properties, technology of silicon nitride materials has been studied intensively for more than 40 years in order to use silicon nitride instead of stainless steel or nickel-based alloy which is inferior in both properties and life-time.

Silicon nitride has two common crystal structures, i.e. α-phase and β-phase, both appearing to be hexagonal [Turkdogan et al., 1958]. β-silicon nitride is more desirable structure for high-temperature engineering applications because of its high temperature strength and excellent thermal shock resistance [Lange 1979]. The fabrication of β-silicon nitride parts usually starts from α-silicon nitride powder mixed with sintering additives before sintering at high temperature. During sintering process, the transformation of α-phase to β-phase occurs, providing desirable microstructure having high mechanical and thermal strength [Lange 1979; Ault et al., 1994].

Applications of silicon nitride depend upon its high temperature strength, good thermal shock resistance and chemical inertness. Reports on the use of silicon nitride as a refractory material appeared in the early 1950s. At that time, silicon nitride was produced by either the carbothermal reduction of silica in the presence of nitrogen or by the direct nitridation of silicon. Silicon nitride has also been used as high-temperature and unlubricated rollers and ball bearing for various applications, such as in oil drilling, sterilizable and unlubricated dental drills, and vacuum pumps, because of its high wear-resistance, low friction and high stiffness [Datton et al., 1986].

The development of silicon nitride ceramics as potential high-temperature structural engine materials markedly accelerated in the early 1960s. It was an outcome of a deliberate and structure search for new materials with good high-temperature properties, especially the resistance to thermal shock. This led to the development and subsequent testing of a wide range of silicon nitride components such as piston and gas turbine blade for internal combustion engine. It was also found that the low specific density of silicon nitride turbo charger could improve the engine response

during acceleration, comparing to the heavier metal parts. The nozzles of certain rockets have already been prepared by using silicon nitride [Tsuruto et al., 1990]. It should be noted that these applications are not very-high-temperature applications originally envisaged, but they rely on low density (mass and inertia) of the silicon nitride components coupled with high strength and toughness required to withstand impact damaged. In the past 30 years, during which most of the considerable developments on silicon nitride has been conducted primarily in the ceramics and electronics communities, many different aspects have been explored. Current development concerns further introduction of silicon nitride components to diesel and spark-ignited engines in the location where low mass and improved wear resistance are required. Examples of such components are exhaust valves, valve spring retainers, bucket tappets, stator blades, valve springs and rocker arm pads [Ziegler et al., 1987]

The well-known techniques for silicon nitride synthesis are direct reaction between silicon (Si) and nitrogen (N_2), and carbothermal reduction of silica (SiO_2) with a source of carbon and nitridation nitrogen gas at the same time [Segal 1986; Ziegler et al., 1987; Sugahara et al., 1988].

Nitridation of silicon powder:

$$3Si\,(s) + 2N_2\,(g) \xrightarrow{\;1200-1500^o C\;} Si_3N_4\,(s) \tag{1.1}$$

Carbothermal reduction of SiO_2 in nitrogen atmosphere:

$$3SiO_2\,(s) + 6C\,(s) + 2N_2\,(g) \xrightarrow{\;1200-1700^o C\;} Si_3N_4\,(s) + 6CO\,(g) \tag{1.2}$$
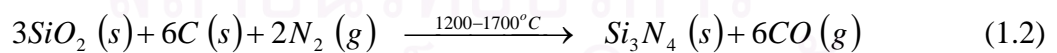
Production of silicon nitride powder via the carbothermal reduction and nitridation process has been commonly practiced [Li et al., 1991; Wang et al., 1996]. However, this method requires high reactivity and good distribution of raw materials, i.e. silica and carbon, to achieve satisfactory extent of the reaction. Therefore, RHA which naturally contains both silica and carbon is considered as good candidate for this reaction. In general, silicon nitride powder can be prepared from RHA at temperature in the range of 1260 to 1500°C under a flow of nitrogen. The process has

been known for more than 20 years, but it has not yet been industrialized. The main reason is that silicon nitride obtained is usually accompanied by other by-products, such as silicon carbide or silica. Moreover, the reaction is kinetically slow, requiring many hours to complete. It has also been reported that the rate of the reaction depends upon the treatment of rice husk before the carbothermal process.

It has been known that presence of metallic compound in rice husk can regulated the carbothermal reduction and nitridation process [Rahman et al., 1989], yet no additive or catatalyst has been used to control the formation of silicon nitride from RHA. On the contrary, catalytic effect of metal additive has been thoroughly investigated for silicon nitride synthesis via the direct nitridation of silicon [Pavarajarn et al., 2001]. Although the detailed mechanisms of these processes are different, it is generally accepted that both reactions involve the generation of silicon monoxide (SiO) and the reaction between SiO and N_2 consequently yields silicon nitride. By this similarity, it is expected that same metals can have similar catalytic effect toward both the direct nitridation of silica and the carbothermal reduction and nitridation of RHA. It is therefore the objective of this research to investigate effect of various metals which have been previously applied in the direct nitridation process, on the production silicon nitride from RHA via the carbothermal reduction and nitridation process. The scopes of this study are as following:

1. Rice husk ash is used as raw material for silicon nitride synthesis via the carbothermal reduction and nitridation process. Metals investigated in this research are iron, aluminium, magnesium, copper and yttrium. The content of metal is in the range of 0.5-3.0% by mass. The reaction was conducted at temperature of $1450^{o}C$.

2. Besides the catalytic effect of metal, effects of reaction parameters are also investigated. The parameters of the reaction investigated include reaction time, content of metal and duration time of hydrogen pretreatment. The reaction times investigated are 1, 3 and 6h, respectively. Duration times of hydrogen pretreatment investigated are 0, 1 and 3h, respectively.

This thesis is divided into five parts. The first three parts describe general information about the study, while the following two parts emphasize on the results and discussion from the present study. The background and scope of the study are presented in Chapter I. Chapter II consists of the theory and literature survey, while the experimental systems and procedures used in this study are shown in Chapter III. The experimental results, including an expanded discussion, are given in Chapter IV. Finally, in the last chapter, the overall conclusion from the results and some recommendations for future work are presented.

CHAPTER II

THEORY AND LITERATURE SURVEY

2.1 Properties of Rice Husk

Rice husk consists of cellulose, lignin, small quantities of proteins and vitamins, inorganic compounds rich in silicon and small amount of other metals [Mehta 1996]. The quantity of each composition depends on various factors, such as soil type, plant variety and climatic conditions. Figure 2.1 shows SEM micrographs of rice husk [Liou 2004].

(a)   (b)
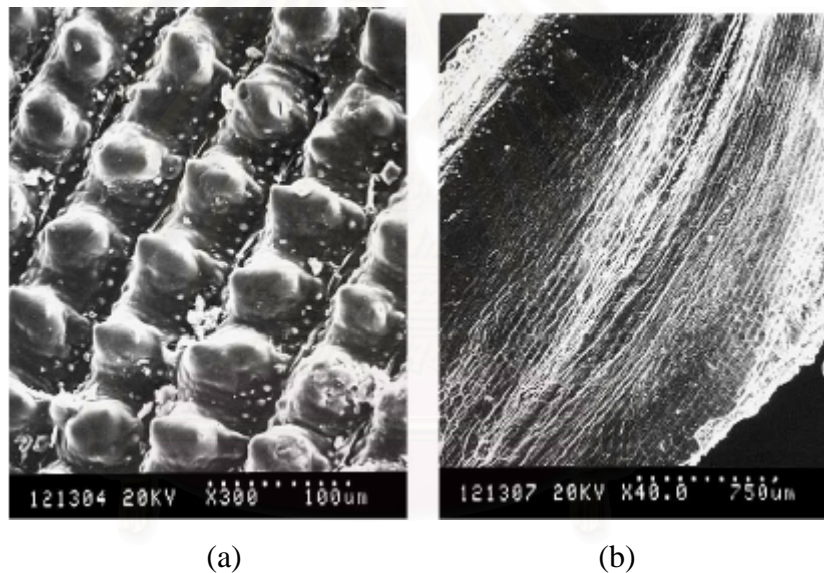
Figure 2.1 Scanning electron micrographs of rice husk: (a) outer epidermis of rice husk; (b) inner epidermis of rice husk

Figure 2.1a shows corrugated structure of the outer epidermis of rice husk, while Figure 2.1b shows the inner epidermis. Silica in rice husk is mainly localized in the tough interlayer of the husk and also filling in the spaces between the epidermal cells [Sharma et al., 1984; Krishnarao et al., 1992]. The typical analysis data of rice husk are shown in Table 2.1 [Fang et al., 2004].

Table 2.1 Rice husk analysis data.

Proximate Analysis:	% by mass
Moisture	6%
Ash	16.92%
Volatile	51.98%
Fixed carbon	25.10%
Ultimate Analysis:	
Carbon	37.60%
Hydrogen	4.89%
Sulphur	0.01%
Nitrogen	1.89%
Oxygen	32.61%
Ash	16.92%
Gross Calorific Value	13.4 MJ/kg
Physical Properties:	
Diameter range	0-10 mm
Equivalent mean diameter	1.60 mm
Natural packing density	122 kg/ m^3
Real density	500 kg/ m^3

2.2 Crystal Structure of Silicon Nitride

It has been generally accepted that there are two common forms of crystalline silicon nitride, designated as α and β forms. Detailed X-ray diffractometry (XRD) examinations in the mid-1950s have proved that the crystal structure of both α and β polymorphs are hexagonal [Turkdogan et al., 1958]. However, their respective structural dimensions are different. The structure of β-phase and α-phase shown in Figure 2.2 and Figure 2.3 respectively.
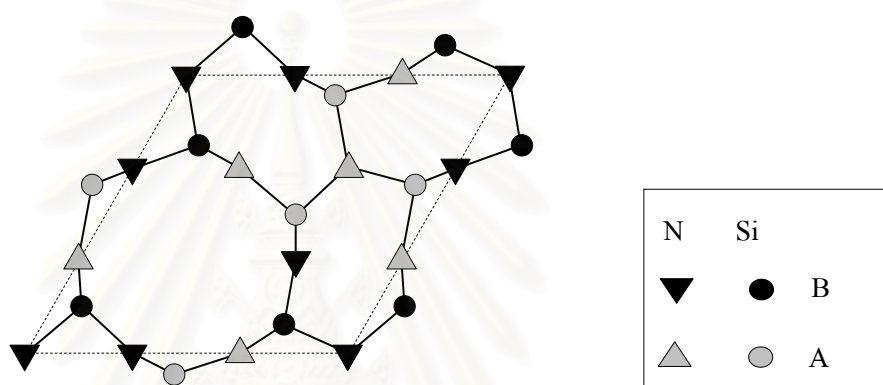
Figure 2.2 β-Si_3N_4 unit cell: the structure of β-Si_3N_4 can be described as a stacking of Si-N layers in …ABAB… sequence.
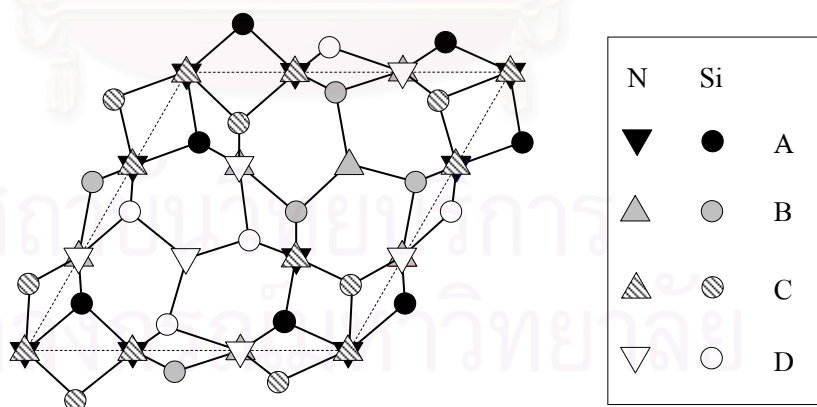
Figure 2.3 α-Si_3N_4 unit cell: the structure of α-Si_3N_4 can be described as a stacking of Si-N layers in …ABCDABCD… sequence.

In both the forms, the basic building unit is the silicon-nitrogen tetrahedron in which a silicon atom lies at the center of a tetrahedron, and four nitrogen atoms at each corner. Each nitrogen atom is shared among three tetrahedral so that each silicon atom has four nitrogen atoms as nearest neighbors [Ruddlesden et al., 1958]. The structures also can be regarded as puckered eight-membered rings of alternating silicon and nitrogen atoms. Basal planes are formed by the joining of six of these rings forming a larger central void encapsulated by six silicon atoms. Stacking of the basal planes forms the structure of β-phase, as shown in Figure 2.2. The large void between the hexagonal arrangement of atoms is continuous through the β-phase lattice forming a *c*-axis channel that has an equivalent cylindrical radius of 1.5 Å Theoretically, it may enable large atoms to diffuse readily through the lattice [Thomson et al., 1967].

The structure of α-Si_3N_4 was determined to be closely related to that of β-Si_3N_4, consisting of alternate basal layers of β-Si_3N_4 and its mirror image, as shown in Figure 2.3. Because of the operation of a *c*-glide plane, the continuous voids are interrupted to form a series of large interstices, which are roughly spherical in shape with a radius of approximately 1.5 Å, linked by tunnels having a radius of 0.7 Å. Consequently, large foreign atoms or molecules could be trapped within the lattice while small ones, such as oxygen, will be able to diffuse within the lattice [Thomson et al., 1967].

The fabrication of β-Si_3N_4 parts usually starts from α-Si_3N_4 powder mixed with sintering additives, which is then sintered at high temperature. During sintering process, the transformation of α-phase to β-phase occurs, providing desirable microstructure having high mechanical and thermal strength [Lange 1979; Ault et al., 1994]. On the contrary, the reverse β-phase to α-phase has never been observed experimentally, but it has been expected to be too slow to be detected at temperature lower than 1400°C [Jennings 1983; Riley 2000]. Silicon nitride does not melt but dissociates into silicon and nitrogen, with the nitrogen dissociation pressure reaching 1 bar (10^5 Pa) at about 1880°C [Riley 2000].

2.3 **Commercial Techniques for Mass-Producing Silicon Nitride Powder**

Silicon nitride is not found in nature, but can be synthesized by a number of different techniques. Pure silicon nitride is difficult to produce as a fully dense material. For industrial production of silicon nitride powder, silicon, silica (SiO_2) and silicon tetrachloride ($SiCl_4$) are the three commonly used starting materials because they are available in high purity on an economic basis or can be easily purified.

Silicon nitride powders are mainly produced in commercial scale by three methods: direct nitridation of silicon, high-temperature decomposition of silicon diimide and carbothermal reduction and nitridation of silica [Alcala et al., 2001].

2.3.1 Direct Nitridation of Silicon

This process is based on contacting elemental silicon with nitrogen at temperature in the range of 1200-1400°C. Although the true mechanism is unknown, the overall reaction of this process can be represented by the following equation:

$$3Si\ (s) + 2N_2\ (g) \leftrightarrow Si_3N_4\ (s) \tag{2.1}$$
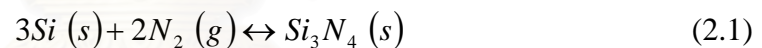
The reaction is highly exothermic. Extreme care must be taken to prevent temperature run-away, which results in melting of silicon particles. The direct nitridation process is more complicated than Equation (2.1) implies. Several models have been proposed to describe the nitridation of silicon [Atkinson et al., 1976; Jennings 1983; Pigeon et al., 1993], but there is no general agreement regarding the mechanism of the nitridation.

The production cost for this process is low, compared to other processes mentioned earlier, since the process is one simple step using inexpensive reactants. However, the quality of product obtained is low. This process is an inexpensive option for the applications in which metal impurities, originating from silicon, contained in the product silicon nitride can be tolerated.

2.3.2　High-Temperature Decomposition of Silicon Diimide

This process could be described as a two-step process. The first step is the liquid phase reaction between silicon tetrachloride and ammonia at room temperature, as follows:

$$SiCl_4\ (l) + 6NH_3\ (l) \leftrightarrow Si(NH)_2\ (s) + 4NH_4Cl\ (s) \qquad (2.2)$$
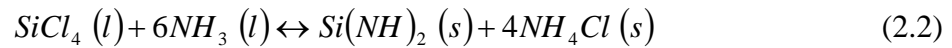
In principle, the liquid phase reaction of silicon tetrachloride with ammonia can be performed in three different ways: (a) liquid $SiCl_4$ with liquid NH_3, (b) gaseous $SiCl_4$ with liquid NH_3 and (c) liquid $SiCl_4$ and gaseous NH_3. In all three cases, fine silicon diimide and ammonium chloride particles are formed. The ammonium chloride can be removed by series of washing with liquid ammonia.

After removing the ammonium chloride, the silicon diimide is given a polymerization via heat treatment in nitrogen or ammonia [Yamada 1993]. The polymer is then pyrolized at 1100°C in nitrogen to produce amorphous silicon nitride. Subsequent heat treatment at temperature higher than 1430°C initiates conversion of amorphous product into α-crystalline form, which may be represented by an overall stoichiometric equation as:

$$3Si(NH)_2\ (s) \leftrightarrow Si_3N_4\ (s) + N_2\ (g) + 3H_2\ (g) \qquad (2.3)$$
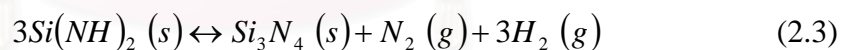
Since reactants are liquids or gases, very pure silicon nitride with a high content of α-form (> 95%) can be prepared [Ault et al., 1994]. However, the production cost is high due to complexities of the process and extensive efforts to purify the intermediate silicon diimide.

2.3.3 Carbothermal Reduction and Nitridation of Silica

The carbothermal reduction of silica powder under nitrogen was the earliest method used for silicon nitride production [Riley 2000]. It produces silicon nitride according to the following overall reaction [Segal 1986]:

$$3SiO_2\,(s) + 6C\,(s) + 2N_2\,(g) \;\leftrightarrow\; Si_3N_4\,(s) + 6CO\,(g) \tag{2.4}$$

This reaction also occurs via a gas-solid mechanism. The mechanism of reaction (2.4) is believed to involve multiple steps, where silicon monoxide acts as an intermediate [Arik 2003]. It is proposed that silicon monoxide is produced by reduction of silica by either carbon or carbon monoxide.

$$SiO_2\,(s) + C\,(s) \;\leftrightarrow\; SiO\,(g) + CO\,(g) \tag{2.5}$$

$$SiO_2\,(s) + CO\,(g) \;\leftrightarrow\; SiO\,(g) + CO_2\,(g) \tag{2.6}$$
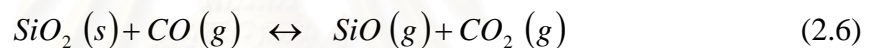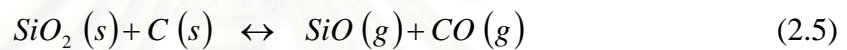
Carbon dioxide generated from reaction (2.6) can further react with carbon to produce more carbon monoxide:

$$CO_2\,(g) + C\,(s) \;\leftrightarrow\; CO\,(g) \tag{2.7}$$
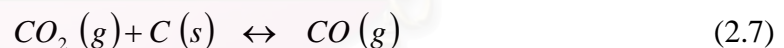
Silicon nitride is then produced by reaction of silicon monoxide, nitrogen gas and either solid carbon or carbon monoxide according to reaction (2.8) and (2.9). It has been believed that the carbothermal reduction and nitridation synthesis of α-Si$_3$N$_4$ crystals via reaction (2.8) and growth of the crystals by gas phase process according to reaction (2.9). It was also reported that the formation of the nuclei occurs through the formation of fine amorphous Si-O-C intermediate [Weimer et al., 1997].

$$3SiO\,(g) + 3C\,(s) + 2N_2\,(g) \;\leftrightarrow\; Si_3N_4\,(s) + 3CO\,(g) \tag{2.8}$$

$$3SiO\,(g) + 3CO\,(g) + 2N_2\,(g) \;\leftrightarrow\; Si_3N_4\,(s) + 3CO_2\,(g) \tag{2.9}$$
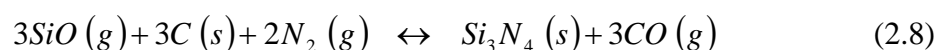
The overall process of the carbothermal reduction and nitridation is usually performed at temperature in the range of 1200-1450°C, depending on the reactivity of raw materials. Nevertheless, the reaction is reported to be slow, requiring up to 12 hours to complete [Weimer et al., 1997]. As seen from the reaction (2.5), physical contact between carbon and silica is essential for SiO vapor formation. Full conversion using a stoichiometric ratio of SiO_2:C, according to reaction (2.4), can occur only if the contact between carbon and silica particles is perfect. Hence, in practice, an excess amount of carbon is required for full transformation of silica to silicon nitride, and free carbon usually remains in silicon nitride powder. Although the remaining carbon can be removed by heat treatment in air, the silicon nitride would be oxidized as well. Consequently, the powder synthesized by this method often suffers from purity problem associated with residual carbon and oxygen content.

As mentioned earlier, the problem of this method is also associated with product contamination by silicon carbide, Silicon carbide can be formed either by the reaction between silicon monoxide and carbon (Eq 2.10) or by further reaction of silicon nitride product with the remaining carbon (Eq 2.11).

$$SiO\,(g) + 2C\,(s) \quad \leftrightarrow \quad SiC\,(s) + CO\,(g) \tag{2.10}$$

$$Si_3N_4\,(s) + 3C\,(s) \quad \leftrightarrow \quad 3SiC\,(s) + 2N_2\,(g) \tag{2.11}$$
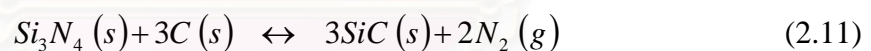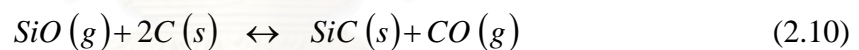
However, the reaction condition suitable for reactions 2.8, 2.9, 2.10 and 2.11 are slightly different. Therefore, controlling the operating conditions is particularly important in establishing which compound will be formed.

2.4 <u>Synthesis of Silicon Nitride from Rice Husk Ash</u>

Many raw materials have been used for producing silicon nitride via the carbothermal process, e.g. mixture of silica and carbon, diatomite [Arik 2003] and rice husk ash [Cutler 1974; Hanna et al., 1985; Rahman et al., 1989; Kuskonmaz et al., 1996; Alcala et al., 2001]. The production of silicon nitride from RHA was first reported in a U.S. patent [Cutler 1974]. It employs the carbothermal reduction and nitridation process in the same manner as previously discussed in section 2.3.3. The reaction temperature used was within the range of 1100-1350°C [Cutler 1974], which is relatively lower than the temperature for the process using conventional silica-carbon mixture. The nitridation rate of RHA is also faster than that of the SiO_2/C mixture [Hanna et al., 1985; Liou et al., 1996], most probably because of the superior homogeneity in mixing between silica and carbon in RHA. The silicon nitride can be in the form of powder, fibers or a needle-like shape. The shape of the silicon nitride particles is the result of nucleation mechanism.

Similar to the process using physically mixed silica and carbon, silicon nitride obtained from the carbothermal reduction of RHA is usually accompanied by silicon carbide and other metallic impurities. As the result, many researchers have emphasized on the production of silicon nitride-silicon carbide composites instead. It has been reported that the carbothermal reduction and nitridation at temperature in the range of 1450-1500°C for 6 h under nitrogen flow results in the silicon nitride and silicon carbide composites [Yamaguchi 1986; Kuskonmaz et al., 1996].

For the synthesis of pure silicon nitride from RHA, effective removal of impurities before reaction and controlling the reaction conditions are important. The study of the carbothermal reduction of rice husks by simultaneously controlling reaction rate and concentration of CO generated showed that the reaction depends upon CO concentration [Alcala et al., 2001]. Extensive studies have also been conducted to control the properties of RHA to suit the production of silicon nitride. Nevertheless, silicon nitride obtained from the carbothermal reduction of RHA is usually accompanied by silicon carbide (SiC) and other metallic impurities. The excess carbon is necessary component in the carbothermal reduction for production of

silicon nitride because a full conversion according to the stoichiometric ratio can only be achieved in the case of a full contact between the carbon and the silica particles, which is unlikely to occur under actual reaction conditions [Kuskonmaz et al., 1996].

2.5 Catalytic Effects of Metal in Silicon Nitride Synthesis

There are many variables that influence the extent of the nitridation process, such as starting materials, temperature, particle size, reaction time, heating rate and reactant gas composition. Another interesting variable is the catalytic effect of metal additive.

For the direct nitridation process, many researchers have studied the effects of several transition metals on the nitridation of silicon by intentionally adding metals into silicon before the nitridation. Aluminium, titanium, hafnium, zirconium and chromium are known as metals that accelerate the growth of β-Si_3N_4 [Lin 1977; Mitomo 1977; Mukerji et al., 1981; Pigeon et al., 1993; Cofer et al., 1994]. Calcium is known to promote the development of α-Si_3N_4 [Pigeon et al., 1993]. Copper aids silicon nitride production and the formation of α-Si_3N_4 at $1200^{\circ}C$ but enhances the β-Si_3N_4 formation at higher temperatures [Deckwerth et al., 1994; Pavarajarn et al., 2001]. Effect of yttrium on the direct nitridaiton of silicon has been recently reported. It has been found that an addition of yttrium 2% by mass leads to the overall conversion over 98% with α-phase content about 97% [Pavarajarn et al., 2001].

For the carbothermal reduction and nitridation process, catalytic effect of iron has been widely investigated. However, there has been no general agreement. Bartnitskaya et al. reported that pure silicon nitride could only be formed if small amount of Fe was added to the raw materials [Bartnitskaya et al., 1983], whereas showed that Fe promote silicon carbide formation over silicon nitride [Siddiqi et al., 1985]. Recently, it was reported that silicon nitride powder with a predominant β-phase was produced from a fine silica-carbon mixture at $1540^{\circ}C$, in the presence of iron as catalyst. Below this temperature, a mixture of β-Si_3N_4, SiC and Si_2ON_2 was formed [Bondyopadhyay et al., 1991]. For other metals, addition of nickel (II) oxide was found to promote the competitive formation of silicon carbide at temperature as

low as 1300°C [Rahman et al., 1989]. In the presence of vanadium (V) oxide and aluminium (III) oxide favour formation of β-Si$_3$N$_4$. TiO$_2$ and CeO$_2$ appeared to accelerate silicon nitride formation, and led to higher overall yields [Rahman et al., 1989]. Fe$_2$O$_3$ and NiO are readily reduced under low oxygen partial pressure to the metals, which in turn yield the liquid silicides at the nitridation temperature. The nitridation of Fe$_2$O$_3$-PRH (pretreatment of rice husk) resulted in production of a mixture of SiC and Si$_3$N$_4$ [Rahman et al., 1989].

2.6 Mechanisms for Crystal Growth from Gas Phase

Two types of mechanism are often used to explain the crystal growth associated with gas phase, as shown in Figure 2.4 [Kawai et al., 1998]. In the vapor-solid (VS) mechanism, Figure 2.4(a), chemical species diffuse toward a substrate through an interfacial gas layer, and adsorbed on the surface of the substrate. The adsorbed species may be mobile on the surface. Subsequently, nucleation and crystal growth occur, accompanied by the elimination of any by-product. In VS mechanism, the diffusion of the chemical species in the gas phase and surface migration on the substrate are fast. Therefore, high deposition rate will be obtained if the reaction between chemical species is fast enough. On the other hand, there are few studies focusing on the use of the vapor-liquid-solid (VLS) mechanism. As shown in Figure 2.4(b), if liquid-phase exists on a substrate, chemical species must be first dissolved in the liquid phase for crystal growth. Next, they diffuse in liquid and adsorbed on the substrate. Finally, crystal growth occurs via nucleation in the liquid phase. The diffusion rates of the chemical species in the liquid phase are probably much slower than in gas phase. Therefore, the rate of the supplement of chemical species to nucleus for crystal growth is very small. This results in high nucleation density and the formation of the finer crystals than those through the VS mechanism.
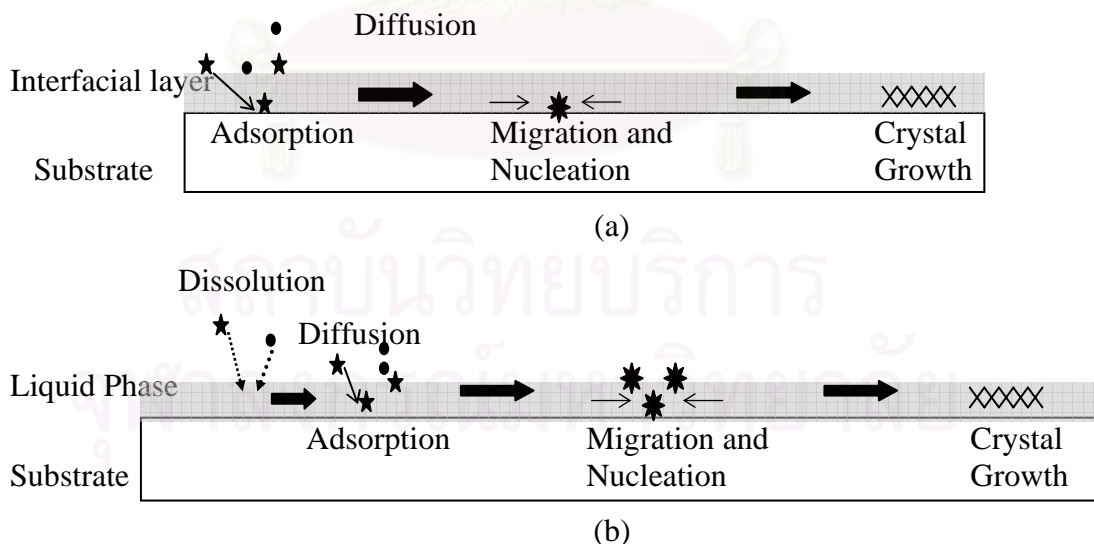
Figure 2.4   Mechanism of two types of gas phase process:
(a) VS mechanism.
(b) VLS mechanism.

CHAPTER III

EXPERIMENTAL

This chapter describes the experimental systems and procedures used in this study. The first section is preparation raw material for the carbothermal reduction and nitridation. Pyrolysis process, preparation of metal impregnated rice husk ash, the carbothermal reduction and nitridation process and analysis of physical and chemical properties of products are explained in the section 3.2, 3.3, 3.4 and 3.5, respectively.

3.1 Raw Material Preparation

Rice husk used in this work was obtained from Nakornratchasima province in Thailand. It was thoroughly washed with distilled water to remove dust, before soaked distilled water at 90°C for 3 hours to remove its impurities. Then, it was dried in an oven at 110°C for 24 hours to ensure the elimination of all possibly remaining moisture.

3.2 RHA Preparation

After thoroughly washed, rice husk obtained was pyrolyzed at 600°C for 3 h under argon flow rate of 10 ml/sec in a horizontal tubular flow reactor which is an alumina tube (49 mm inside diameter × 1.2 m long) placed inside a high temperature furnace (Carbolite-STF 15/--/180). In this study, the pyrolysis was done at 600°C for 3 hours under argon (flow rate of 10 ml/sec) because this condition has been reported to result in high amount of amorphous silica [Yalcin et al., 2001; Alcala et al., 2001 ; Fang et al., 2004]. The product obtained is rice husk ash (RHA)

3.3 Metal Impregnation on RHA

To prepare metal impregnated RHA, about 2 g of RHA was immersed in 10 mL of solution of metal nitrate compounds, e.g. $Fe(NO_3)_3.9H_2O$, $Mg(NO_3)_2.6H_2O$, $Y(NO_3)_3.6H_2O$, $Al(NO_3)_3.9H_2O$ and $Cu(NO_3)_2.2.5H_2O$, in 99.9% methanol, followed by natural evaporation of all methanol at room temperature. The content of metal impregnated was adjusted to be 0.50%, 1.00% and 3.00%wt. respectively, based on mass of reduced metal. The sample was put into an oven at 110^oC for 24 h to ensure the elimination of all possibly remaining methanol and moisture.

3.4 Carbothermal Reduction and Nitridation of RHA

For silicon nitride synthesis via the carbothermal reduction and nitridation process, about 0.2 mg of RHA was put into an alumina tray (25 mm ×15 mm × 5 mm deep). The alumina trays were placed in the uniform temperature zone of the horizontal tubular flow reactor (Figure 3.1). The uniform temperature zone was 5 cm in length. The reactor was purged with a mixture of 90% argon and 10% hydrogen and heated to desire temperature at constant heating rate of 10°C/min. Hydrogen in the feed stream was used to convert metal nitrate into reduced metal before the nitridation. The period whereas H_2/Ar mixture was supplied to the reactor is referred to as the pretreatment period. For most of the runs, the pretreatment was carried out until the prescribed reaction temperature (1450^oC) was reached. However, in some cases, the pretreatment was conveyed further at 1450^oC for desired period of time. After the pretreatment, the nitridation was initiated by feeding a gas mixture of 90% nitrogen and 10% hydrogen to the reactor. The overall flow rate of the gas mixture was 50 l/h (measured at room temperature). The reaction time was held at constant temperature for 6 h.
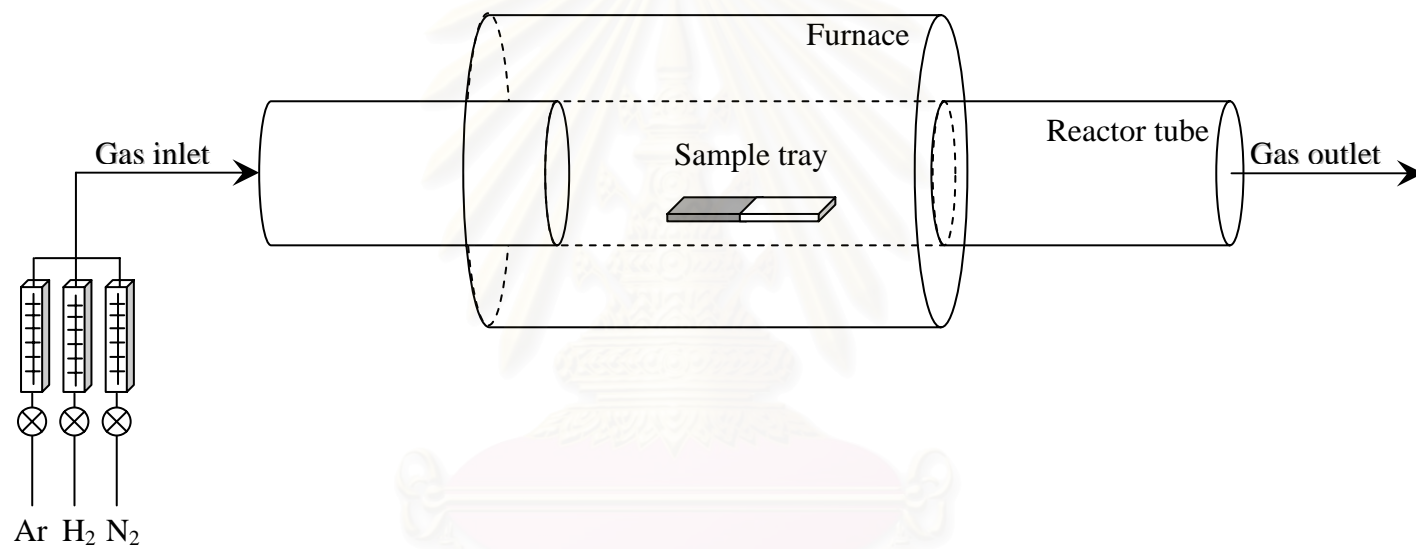
Figure 3.1 Schematic diagram of the tubular flow reactor system

3.5 <u>Characterization of Products</u>

The products obtained from each step of the experimental procedures were characterized by using various techniques, as following:

3.5.1 X-ray Diffraction Analysis (XRD)

The crystalline structures of reactant and obtained products were determined from X-ray Diffraction analysis (XRD), using a SIEMENS D5000 diffractometers with Cu-Kα radiation. Each sample was scanned in the range of $2\theta = 20\text{-}50^{o}$ with a step size of $2\theta = 0.02^{o}$.

3.5.2 Scanning Electron Microscopy (SEM)

The microstructure of a solid sample was determined using a scanning electron microscope (SEM), (JSM-6400, JEOL Co., Ltd.) at the Sciencetific and Technological Research Equipment Center (STREC), Chulalongkorn University.

3.5.3 Fourier Transform Infrared Spectrometry (FT-IR)

The sample was mixed with KBr with ratio of sample:KBr equal to 1:100. Then, the mixture was grounded into a fine powder and pressed into a thin wafer. Infrared spectra were recorded between 4000 and 400 cm^{-1} with Nicolet Impact 400 FT-IR spectrometer, Nicolet Instrument Corporation, U.S.A. The spectra were used to study the functional group of product of Si_3N_4.

3.5.4 Thermo Gravimetric Analysis (TGA)

The residual carbon content and thermal behaviors of RHA and obtained products were determined by using TG/DTA analysis on a Diamond TG/DTA thermo gravimetric instrument. The analysis was performed at a heating rate of 20°C/min in 100 ml/min flow of oxygen.

3.5.5 Analysis by the Temperature Programmed Reduction (TPR)

Temperature programmed reduction (TPR) technique was used to verify the temperature, at which the impregnated metal-contains compound could be reduced to metal. The analysis was done by heating the sample up to $850^{o}C$, with heating rate of $10^{o}C/min$ under flow of $10\%H_2$ in Ar.

CHAPTER IV

RESULTS AND DISCUSSION

This chapter describes about results of the research, including effect of hydrogen pretreatment for RHA before the carbothermal reduction and nitridation, catalytic effects of metals on the formation of silicon nitride from rice husk ash, effect of catalyst concentration and effect of catalyst for different reaction time. This chapter is divided into two sections. Effects of hydrogen pretreatment are firstly discussed in section 4.1. The effects of each metal catalyst, including effect of catalyst concentration and effect of reaction time are given in section 4.2.

4.1 Effect of Hydrogen Pretreatment

4.1.1 Pretreatment at Constant Temperature

It has been generally acknowledged that hydrogen accelerates the carbothermal reduction and nitridation of RHA [Pavarajarn et al., 2005]. Although the actual role of hydrogen remains unclear, it is believed that the presence of hydrogen in the nitridation atmosphere assists the reduction of silica, according to Equation 4.1 [Silva and Figueiredo, 2001]:

$$SiO_2\left(s\right)+H_2\left(g\right)\leftrightarrow SiO\left(g\right)+H_2O\left(g\right) \tag{4.1}$$
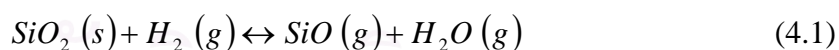
In this research, the effect of hydrogen was further investigated. Hydrogen pretreatment was applied to RHA prior to the carbothermal process, in order to learn about the effect of hydrogen to RHA without the presence of nitrogen. The pretreatment was conducted by supplying the gas mixture consisting of 90% argon and 10% hydrogen to the reactor, after the system had been heated up to 1450°C under flow of pure argon. The pretreatment time was varied from 0, 1 and 3 h. Then, the carbothermal reduction and nitridation process was carried out at 1450°C for 6 h, by using nitrogen mixed with 10% hydrogen as the reaction gas mixture

The XRD patterns of products obtained after the nitridation, using hydrogen pretreatment at constant temperature for various time, are shown in Figure 4.1 and 4.2. It is confirmed that, the product obtained without hydrogen pretreatment is similar to the results reported earlier in literature [Pavarajarn et al., 2005]. Namely, the product residing in the sample holder could be categorized into two portions, i.e. dark gray powder at the bottom of the sample holder and thin layer of white fibrous material on the top, all of which were confirmed by XRD analysis to have silicon nitride as the major crystalline phase (Figure 4.1a and 4.2a, respectively). Mass fraction of the dark gray portion of the product was much greater than that of the top layer, as shown in Table 4.1.

For the products obtained using hydrogen pretreatment for 1 and 3 h, they could be categorized into two portions as well as the product without hydrogen pretreatment. Mass fraction of the dark gray portion of the product was also much greater than that of the top layer, as shown in Table 4.1. However, the XRD analysis showed that both portions consisted of silicon carbide as the major crystalline phase (Figure 4.1b, c and 4.2b, c, respectively). No silicon nitride was obtained. According to TG/DTA experiments, whereas the samples were heated to 1000°C under flow of oxygen, it was found that amount of residual carbon the bottom portion of the sample decreased as the pretreatment was prolonged. It means that the remaining carbon in the bottom portion was consumed in the greater amount by the reaction with silica, when the pretreatment was extended. In the other words, the activity of RHA was increased by the pretreatment. For the top layer, no such trend was observed. However, it should be noted that fraction of the top portion of the sample was negligibly small, especially when the hydrogen pretreatment was employed.
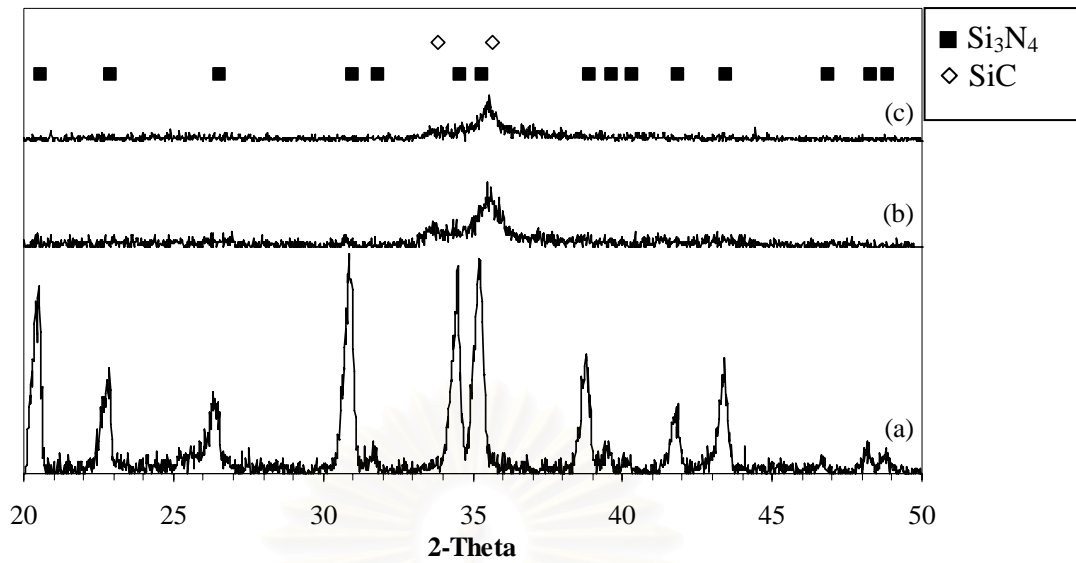
Figure 4.1 XRD patterns of top portion of the product obtained from the carbothermal reduction and nitridation of RHA that was pretreatment at 1450°C for various durations: (a) no hydrogen pretreatment, (b) 1 h and (c) 3 h pretreatment.

Figure 4.2 XRD patterns of bottom portion of the product obtained from the carbothermal reduction and nitridation of RHA that was pretreatment at 1450°C for various durations: (a) no hydrogen pretreatment, (b) 1 h and (c) 3 h pretreatment.

Table 4.1 Mass fraction of each portion of the product from the carbothermal reduction and nitridation of RHA, which was pretreated by hydrogen at 1450°C for various durations, and the mass loss observed from TGA analysis.

Pretreatment duration (h)	Mass fraction (%)		TGA analysis results: mass loss (%)	
	Top portion	Bottom portion	Top portion	Bottom portion
No-pretreatment	11.93	88.07	42.25	57.43
1	0.66	99.34	53.56	48.51
3	0.15	99.85	40.84	38.64

It is easy to understand that silicon carbide is formed by the reaction between silicon dioxide and free carbon in rice husk ash according to the following equation, where as silicon monoxide has been identified as the reaction intermediate [van Dijen et al., 1996];

$$SiO_2 + 3C \rightarrow SiC + 2CO \qquad (4.2)$$

The change in Gibbs free energy for reaction in Equation 4.2 can be calculated from:

$$\Delta G_T^o = 604000 - 339.4T \qquad ,[J] \qquad (4.3)$$

From equation (4.3), at 1450°C, ΔG_T^o has the value of -62,734.7 J. The negative value of ΔG_T^o indicates that silicon carbide can be spontaneously formed at this temperature. Found that, carbon monoxide was generated between hydrogen pretreatment and decrease when time increase. The formation of silicon nitride depend on generate of carbon monoxide, when amount of carbon monoxide generate are very much, it will send effect to formation of silicon nitride, by increasing formation of silicon nitride [Shimada et al., 2001]. From experimental, when time for hydrogen pretreatment is long time, products obtained are silicon carbide. These result supports with Gas Chromatography (GC) because amount of carbon monoxide

was detected from GC, it will decrease when time for hydrogen pretreatment are increase as showed in Figure 4.3. These results make the carbon remain in sample (residual carbon). So, the carbon remain in sample was reacted with silica produced to silicon carbide following equation (4.2). These result supports that, the reaction between silica and carbon to form silicon carbide takes place at temperature higher than 1500°C [Krishnarao et al., 1992].
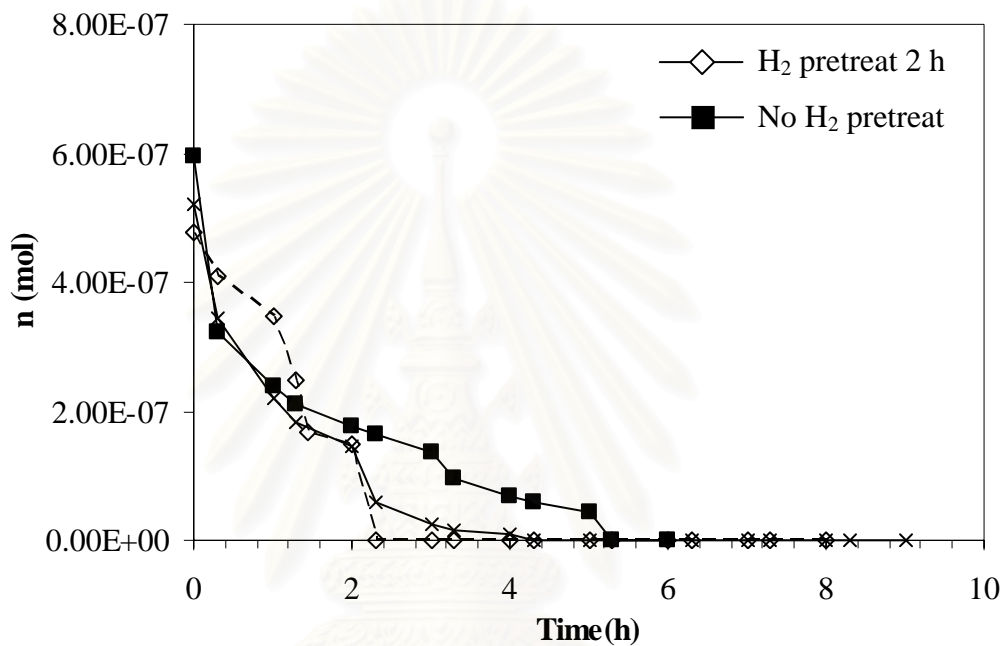
Figure 4.3 Relation between moles of product obtained from hydrogen pretreatment
0 h and 2 h hydrogen pretreatment before nitride with time.

The SEM micrographs of products from the carbothermal reduction and nitridation at 1450°C using RHA that was pretreated with hydrogen for 0, 1 and 3 h are shown in Figure 4.4, 4.5 and 4.6, respectively. It is clearly indicated that morphologies of the product in different portions are quite different. The dark gray powder in bottom layer consists of irregular-shape aggregates. The electron dispersive X-ray spectroscopy (EDX) analyzer equipped on SEM revealed that the aggregates were carbon-rich, while the rod-like grains were silicon-rich [Pavarajarn et al., 2005]. The top layer is generally fibrous material. Nevertheless, the morphology of the fibers depends upon the pretreatment. For sample without hydrogen pretreatment, it consists of short and thick fibers. These fibers have uniform width of approximately 0.27 μm and length around 5-10 microns. On the other hand, for the sample pretreated with hydrogen, the top layer consists of very thin and long fibers, similar to the strand of cotton thread. Since these fibrous materials were found on top of the bottom layer, it suggested that they were grown from vapor phase. Moreover, since the fibers were composed of silicon, it further suggested that siliceous vapor was generated from the RHA starting powder and reacted with nitrogen gas to form the fibers according to Eq. 2.9. No sign of liquid, e.g. melting of bead forming at the tip of the fiber, was observed from SEM images (Figure 4.4(a), 4.5(a) and 4.6(a)). This indicates that the fibers are grown via the VS mechanism, rather than the VLS mechanism.

Figure 4.4 SEM micrographs of product obtained from the carbothermal reduction
and nitridation of RHA without hydrogen pretreatment; (a) Top portion,
(b) Bottom portion
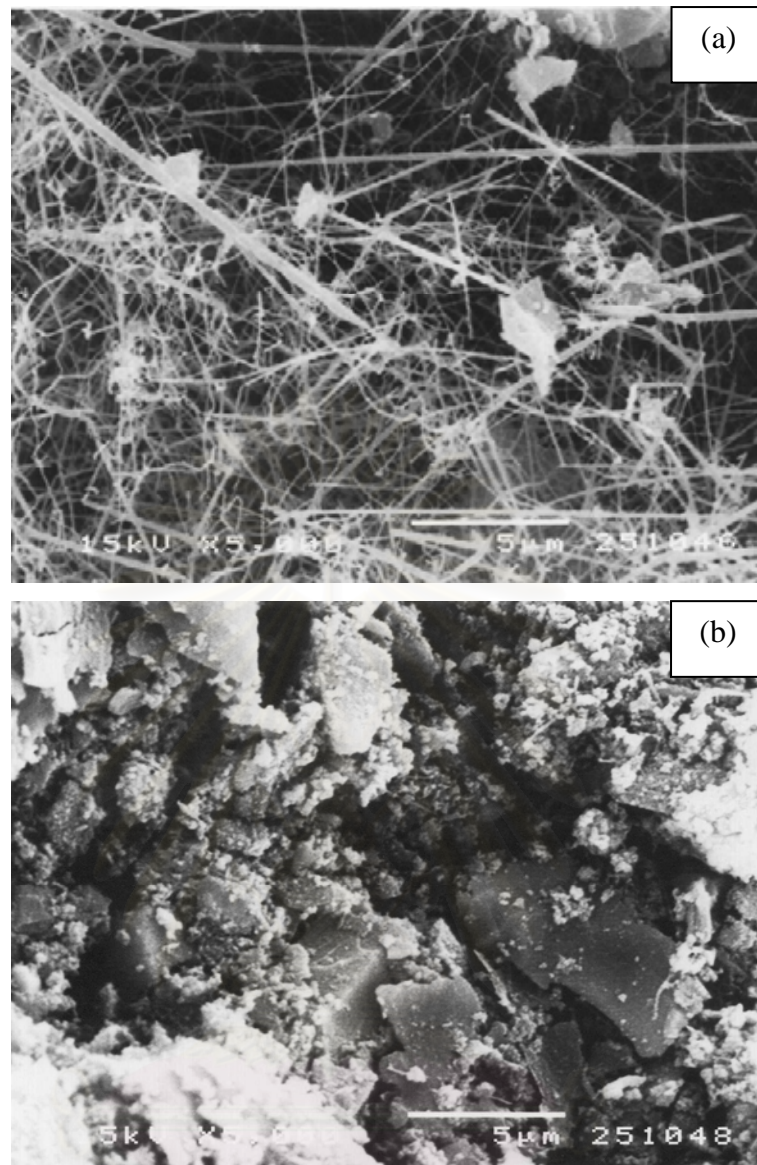
Figure 4.5 SEM micrographs of product obtained from the carbothermal reduction
and nitridation of RHA pretreated with hydrogen at 1450°C for 1 h;
(a) Top portion, (b) Bottom portion
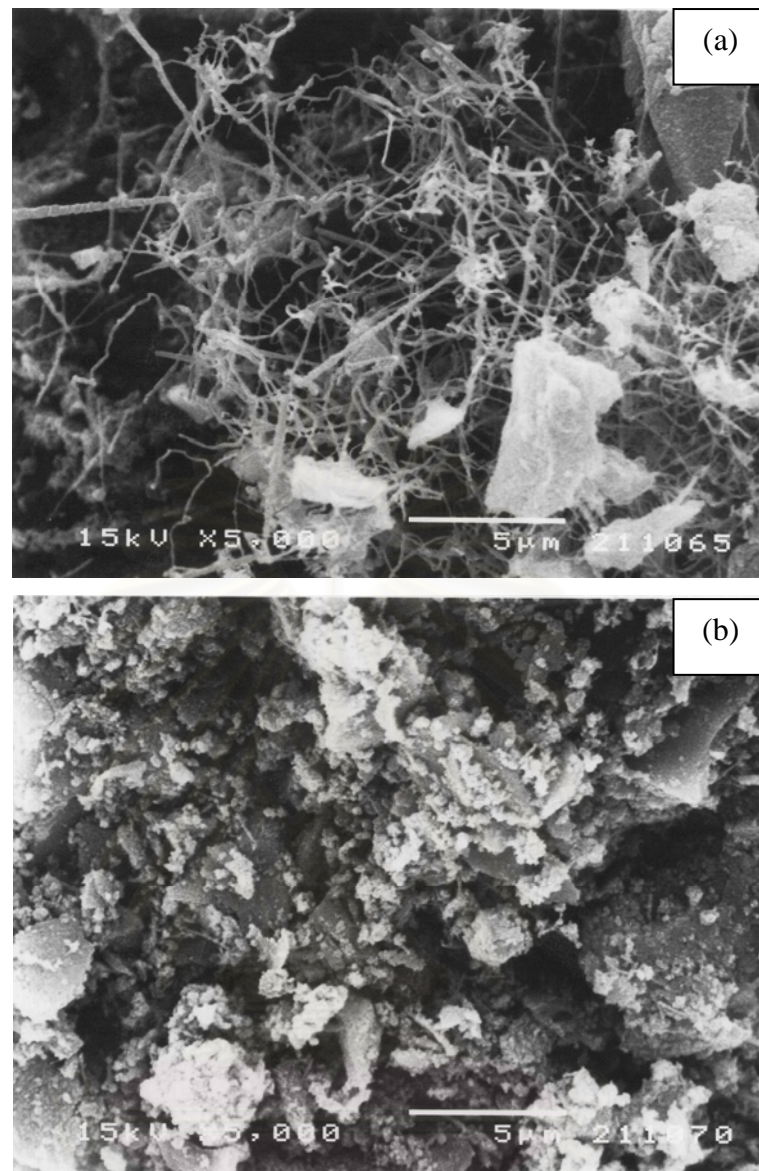
Figure 4.6 SEM micrographs of product obtained from the carbothermal reduction
and nitridation of RHA pretreated with hydrogen at 1450°C for 3 h;
(a) Top portion, (b) Bottom portion

4.1.2 Pretreatment during Heating up

In this section, hydrogen pretreatment was conducted at the same time as the RHA was heated up. The temperature, at which the pretreatment was started, was varied from room temperature, 600°C and 1000°C, respectively. The pretreatment was carried until the system had reached 1450°C. Then, the gas supplying to the reactor was switched to the mixture of 90% nitrogen and 10% hydrogen to instigate the carbothermal reduction and nitridation process. It should be noted that, for the runs with the pretreatment at 600 and 1000°C, pure argon was constantly supplied to the reactor during the heating up from room temperature to the pretreatment temperature.

The results from XRD analysis of the top and bottom portion of the nitrided are shown in Figure 4.7 and 4.8, respectively. It is confirmed that silicon nitride is the major crystalline phase in all product portions. No other apparent crystalline compound was detected.

According to the results shown in Figure 4.9, it is observed that mass fraction of the top portion of the sample, which has been pretreated from room temperature, is greater than that of the samples treated at higher temperatures.

Figure 4.10 (a) and (b) show the mass loss during the TGA analysis of the top and bottom portions of the nitrided product, respectively. The TGA analysis was conducted in the same manner as discussed in the previous section, i.e. the sample was heated to 1000°C at heating rate of 20°C under flow of oxygen. It is confirmed that the residual carbon in both top and bottom portions increases with temperature where hydrogen pretreatment was initiated. The mass loss of the product with hydrogen pretreatment since room temperature is less than that of the samples pretreated at 600°C and 1000°C, respectively. This result implies that the carbothermal reduction and nitridation can be enhanced by extending the conversion of hydrogen pretreatment to take place at the beginning of the heating up process. Although the duration of the pretreatment is the dominant factor contributing to such enhancement, as observed earlier in the previous section, the interesting aspect of the pretreatment during heating up is that the content of residual carbon in the top portion of the sample in this case is much lower than those shown in Table 4.1
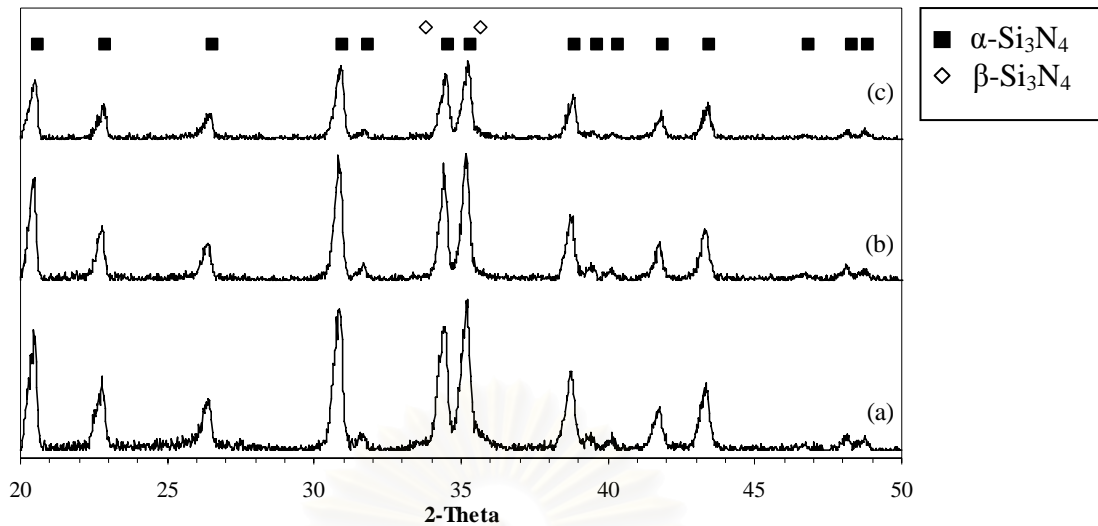
Figure 4.7 XRD patterns of top portion of theproducts obtained from the carbothermal reduction and nitridation of RHA that was pretreated during heating up from: (a) room temperature, (b) 600°C and (c) 1000°C, respectively.
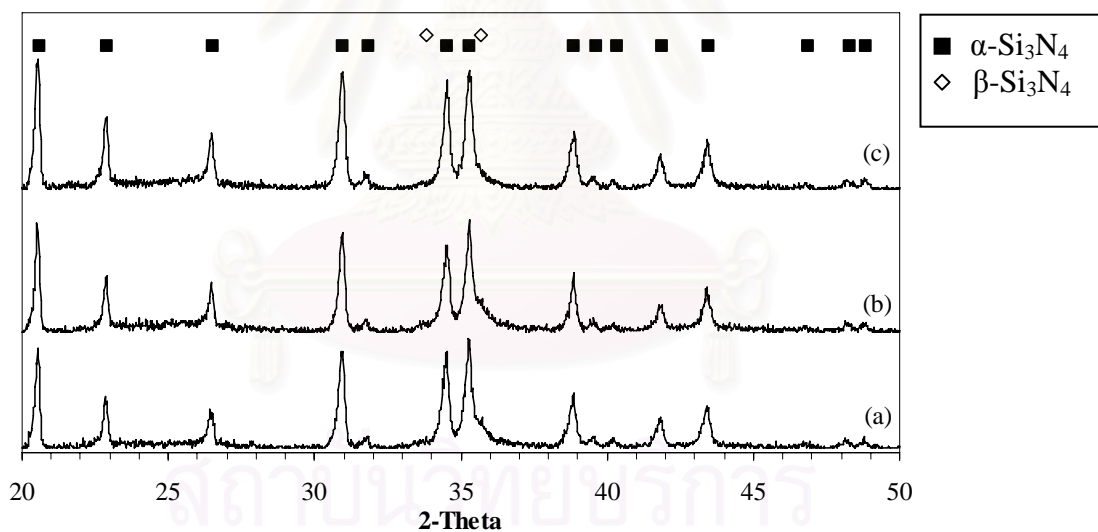
Figure 4.8 XRD patterns of bottom portion of theproducts obtained from the carbothermal reduction and nitridation of RHA that was pretreated during heating up from: (a) room temperature, (b) 600°C and (c) 1000°C, respectively.
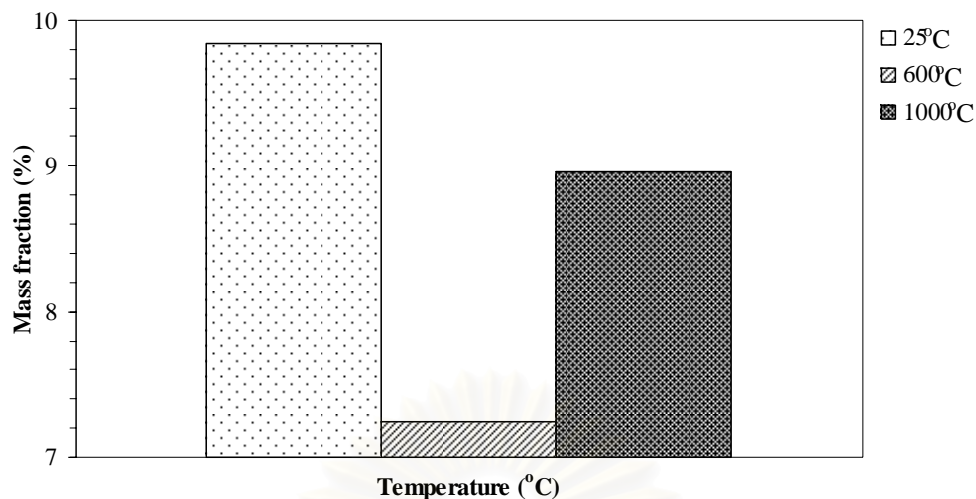
Figure 4.9 Mass fraction of the top portion of the products from the carbothermal
reduction and nitridation of RHA that was pretreated during heating up
from various temperatures.
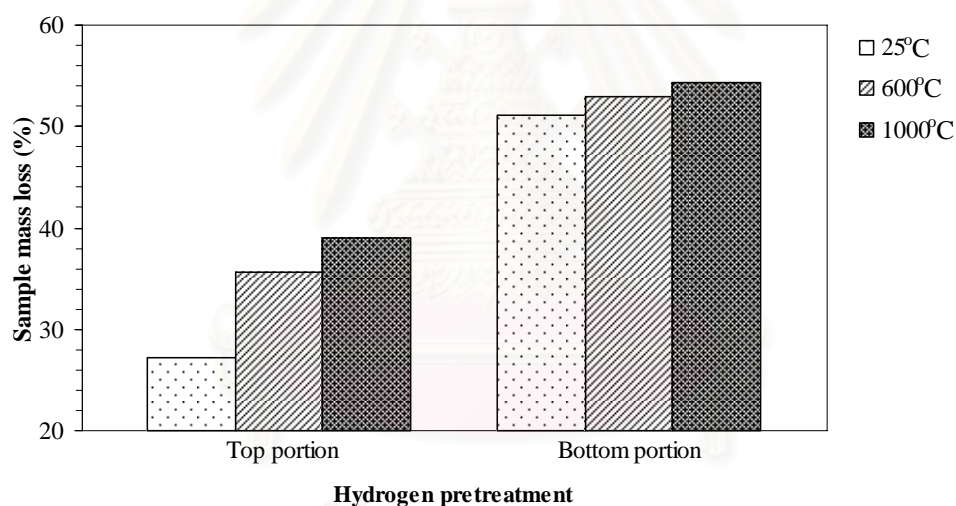
Figure 4.10 Results from TG/DTA analysis of the products from the carbothermal
reduction and nitridation of RHA that was pretreated during heating up
from various temperatures.

4.2 <u>Effect of Metals</u>

The main purpose of this section is to study α- and β-silicon nitride formation of the product from the carbothermal reduction and nitridation of RHA with the presence of metal. The effect of each metal was compared by using the content of metal impregnated of 0.5 wt.%. The carbothermal reduction and nitridation was done at $1450^{o}C$ for 6 h after the pretreatment conducted during heating up from room temperature. The results in term of α- and β-phase in top and bottom portion of the sample are presented in Figure 4.11 and 4.12, respectively. From Figure 4.11, it can be observed that the fraction of α-phase in the top portion is generally decreased when metal is added to RHA, especially for yttrium impregnated RHA (98% α-phase). It should be noted that the samples with iron and copper impregnation did not form into two distinguishable portions like others. Therefore, no data for top portion of Fe- and Cu-impregnated sample is presented in Figure 4.11-4.12. For bottom portion, α-phase is also decreased when a metal is added to RHA. It is widely known from the study of catalytic effect of metals on the direct nitridation of silicon that aluminium, titanium, hafnium, zirconium and chromium can accelerate the growth of β-silicon nitride [Lin 1977; Mitomo 1977; Mukerji et al., 1981; Pigeon et al., 1993; Cofer et al., 1994]. It is also reported that, for the direct nitridation of silicon, iron can form liquid phase providing an easy diffusion path for nitrogen to react with silicon and results in the enhancement of the formation of β-silicon nitride. For the carbothermal process investigated in this research, the similar behavior was also observed from iron impregnated RHA.
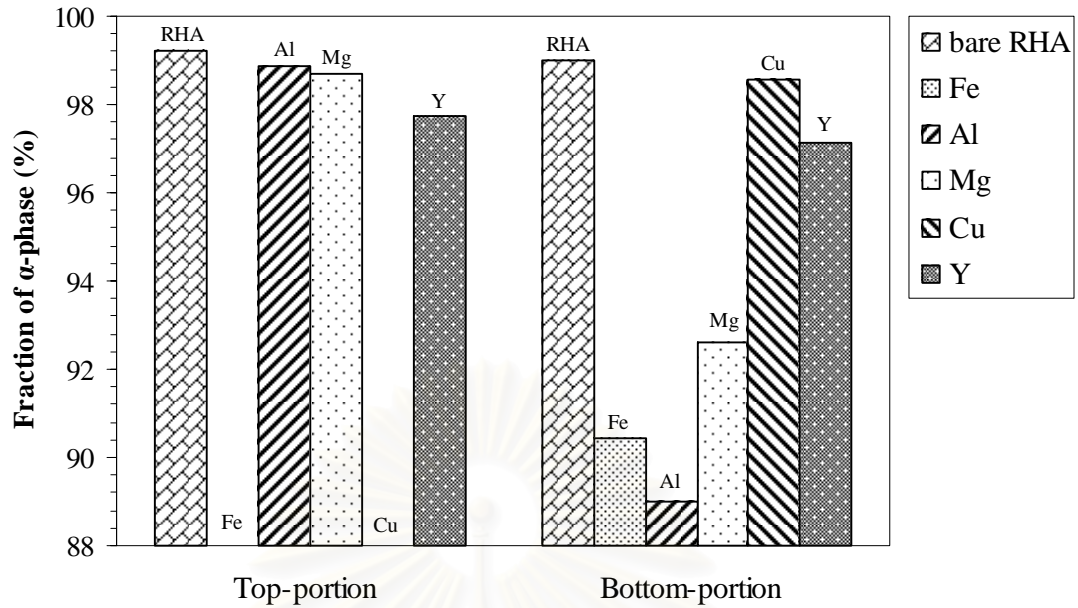
Figure 4.11 Fraction of α-phase in samples obtained from the carbothermal reduction and nitridation of RHA impregnated with 0.5% by mass of various kinds of metal at 1450°C.
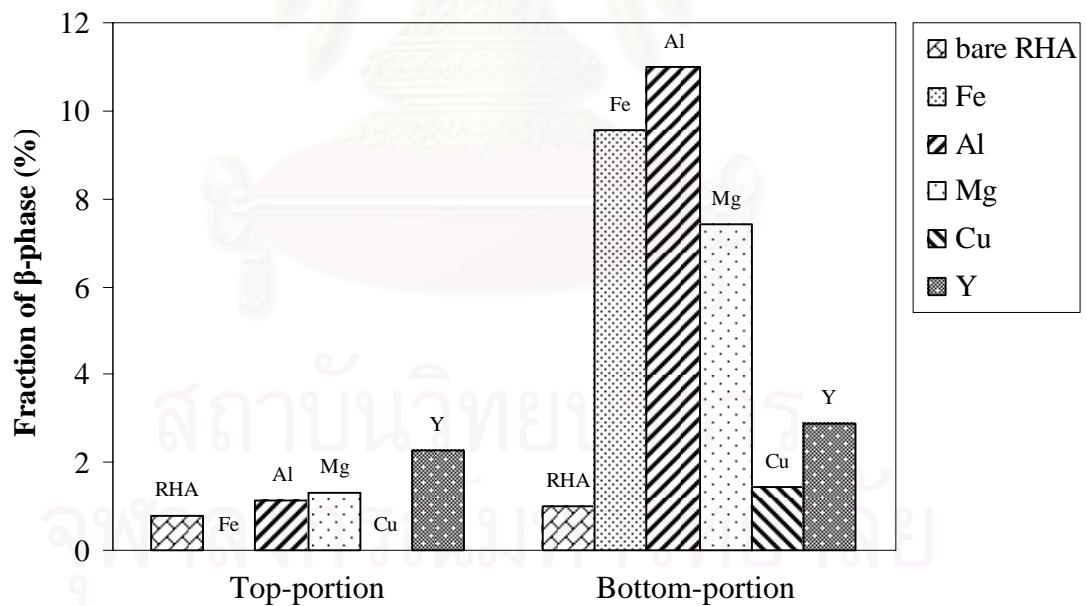
Figure 4.12 Fraction of β-phase in samples obtained from the carbothermal reduction and nitridation of RHA impregnated with 0.5% by mass of various kinds of metal at 1450°C.
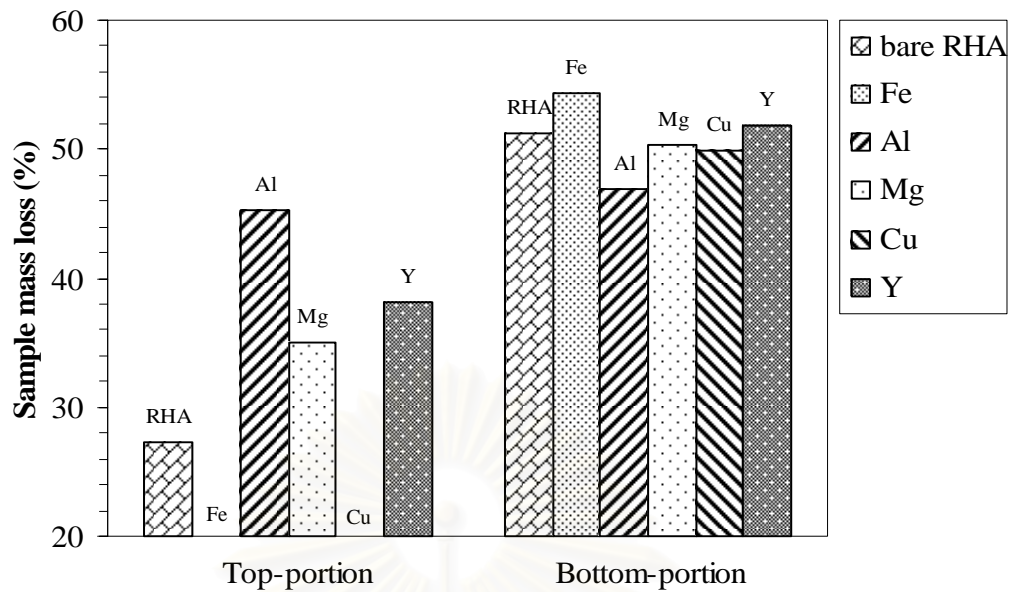
Figure 4.13 TG/DTA analysis of the products from the carbothermal reduction and nitridation of RHA impregnated with 0.5% by mass of various kinds of metal.

The results from TG/DTA analysis of each portion of the nitrided samples are shown in Figure 4.13. It is indicated that the amount of carbon residue in the top and bottom portions of the product are varied by an addition of have different metal. Yet, the mass fraction of carbon residue in the bottom portion of silicon nitride product is still higher than that of the top portion. It is clear that the bottom portion has a residual carbon remaining in product more than the top portion. In the top portion, more carbon was used in the reaction than the bottom portion, i.e. conversion of top portion is higher than the bottom portion.

Figure 4.14 shows the XRD patterns of silicon nitride products from RHA impregnated with various metals (0.5% wt). It is clear that metal has catalytic effect toward the phase formation of silicon nitride. Addition of iron, copper and yttrium enhances the formation of β-silicon nitride, especially in the bottom portion of the product because signal of β-silicon nitride was detected at $2\theta = 33.67^o$ and 36.05^o, respectively. Furthermore, it is observed that impregnation of iron, copper and yttrium also leads to the formation of silicon carbide in the bottom portion of the product.

Figure 4.14 XRD patterns of products from the carbothermal reduction and
nitridation of RHA impregnated with various metals: (a) top portion of
the product, (b) bottom portion of the product, ◆ α-Si$_3$N$_4$, ▲ β-Si$_3$N$_4$,
□ SiC.
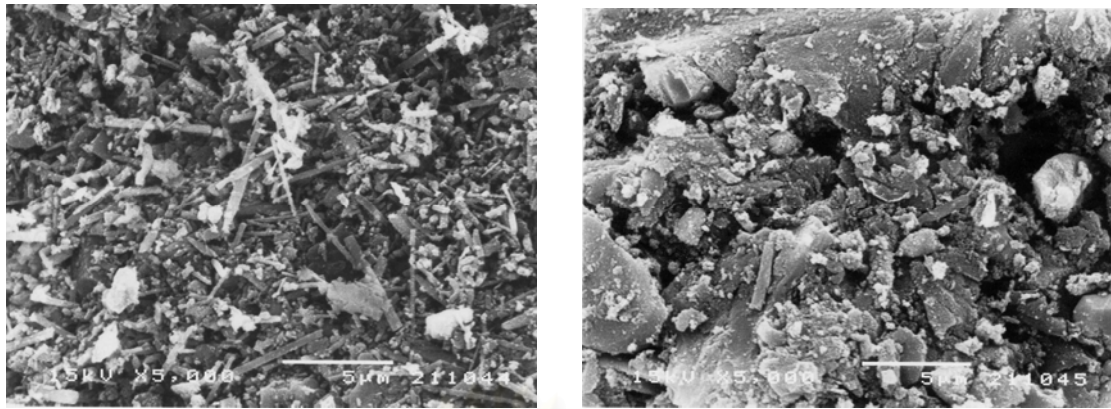
top portion

bottom portion

(a)

bottom portion

(b)
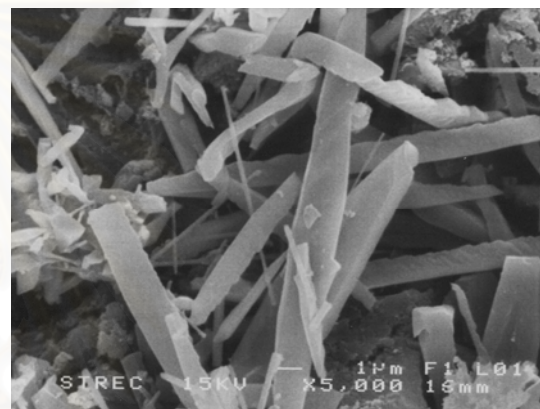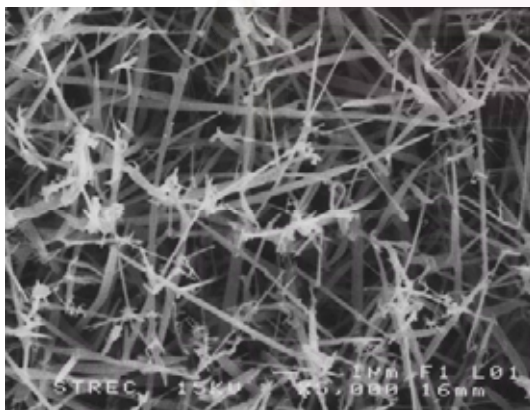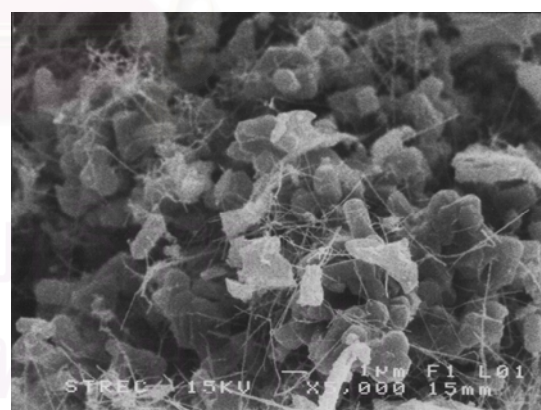
top portion

bottom portion

(c)

Figure 4.15 SEM micrographs of products from the carbothermal reduction and
nitridation at $1450^{o}C$ for 6 h of: (a) bare RHA, (b) RHA impregnated
with 0.5% iron, (c) RHA impregnated with 0.5% aluminium.
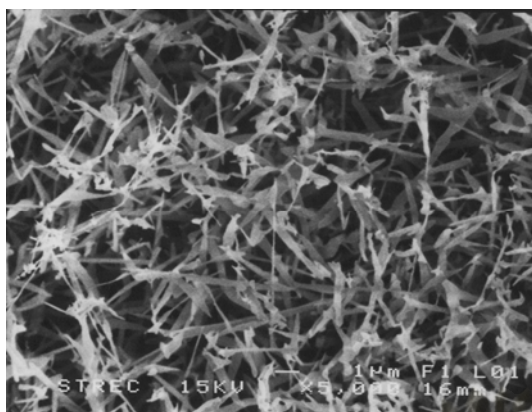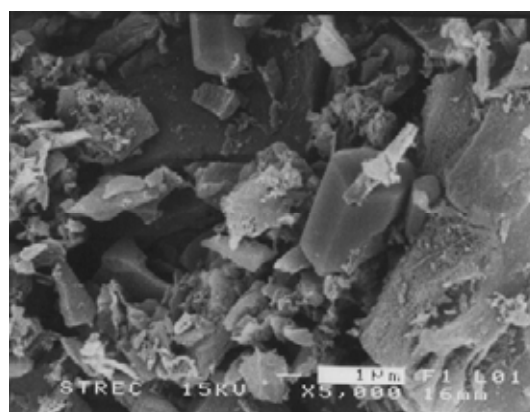
top portion   bottom portion

(d)

bottom portion

(e)
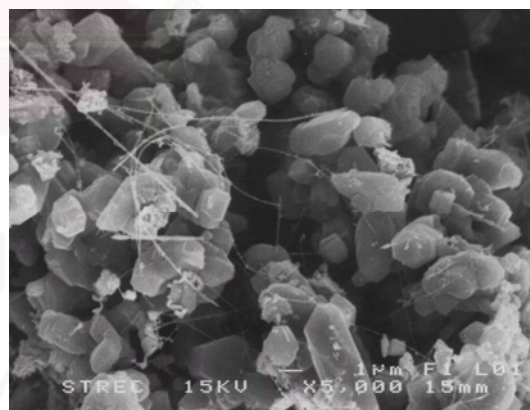
top portion   bottom portion

(f)

Figure 4.15 (continued) SEM micrographs of products from the carbothermal
reduction and nitridation at 1450°C for 6 h: (d) RHA impregnated with
0.5% magnesium, (e) RHA impregnated with 0.5% copper and (f) RHA
impregnated with 0.5% yttrium.

The SEM pictures for each portion of the silicon nitride products obtained from the nitridation at 1450°C and 6 h are shown in Figure 4.15. It can be observed that morphology of the silicon nitride product in top and bottom portions are quite different. The top portions of all silicon nitride products obtained are similar in morphology regardless of the kind of metal impregnated. The top portion is, in fact, consisted of lots of white fibrous materials which have diameter in submicron range. For the bottom layer, the sample with no metal impregnation consists of irregular shape aggregates. The top portion of the product of 0.5% aluminium impregnated RHA consists of very long fibers which is different from RHA impregnated with magnesium or yttrium. It is suggested that aluminium enhances the generation of silicon monoxide vapor. For the bottom portion, the sample with no metal impregnation is irregular-shaped aggregates. It can be observed that RHA impregnated with 0.5% aluminium, magnesium and yttrium result in product with different morphology from bare RHA, and they are not tightly aggregated as the product from bare RHA. It is suggested that the impregnation of metal affects the generation silicon monoxide, which decreases the contact between silica and carbon. For silicon nitride obtained from RHA impregnated with 0.5% iron or copper, the morphology is different that the others. It is suggested that reaction between silica and carbon in solid state occurs when iron or copper is impregnated to RHA. These results can be described by the vapour-solid (VS) and the vapor-liquid-solid (VLS) mechanism [Kawai et al., 1998]. For unimpregnated RHA and RHA impregnated with 0.5% aluminium, magnesium and yttrium, the presence of fibers has confirmed that the nitridation involves the reaction in gas phase which results in fiber growth.

4.2.1 Effect of Metal Content

In this section, effects of metal addition on the carbothermal reduction and nitridation of RHA are further investigated by using various contents of metal impregnation. The metal contents investigated are 0.5, 1 and 3% by mass.

The summary for the effects of metal content on the fraction of each phase of silicon nitride in top and bottom portions of the samples are presented in Figure 4.16 and 4.17, respectively. It can be observed that the fraction of α-phase is generally decreased when metal is added to RHA. The higher the metal content, the lower the fraction of α-phase in both top and bottom portion.
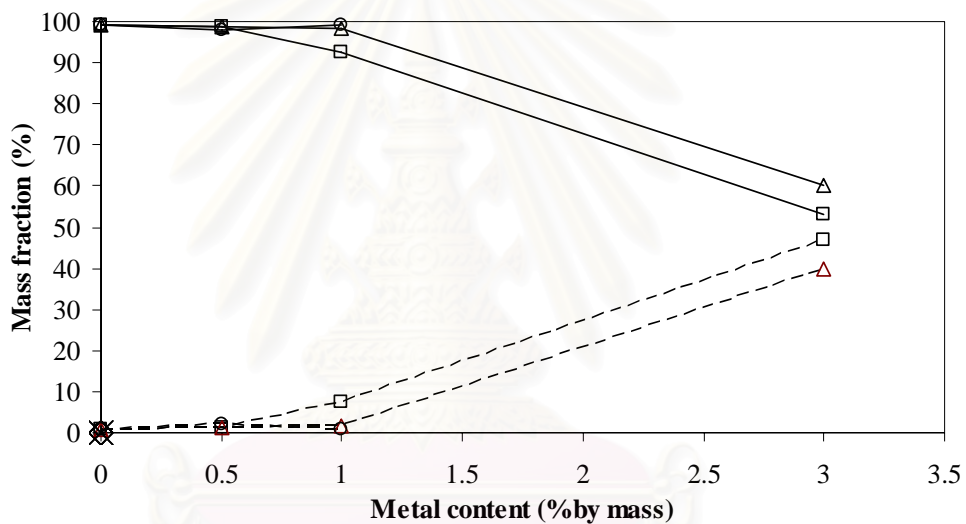
Figure 4.16 Fraction of each phase of silicon nitride in the top potion of the product
from the carbothermal reduction and nitridation of RHA impregnated
with metals at various metal content: (◇) iron; (□) aluminium;
(△) magnesium; (×) copper; (○) yttrium; (—) α-phase; (- - -) β-phase.
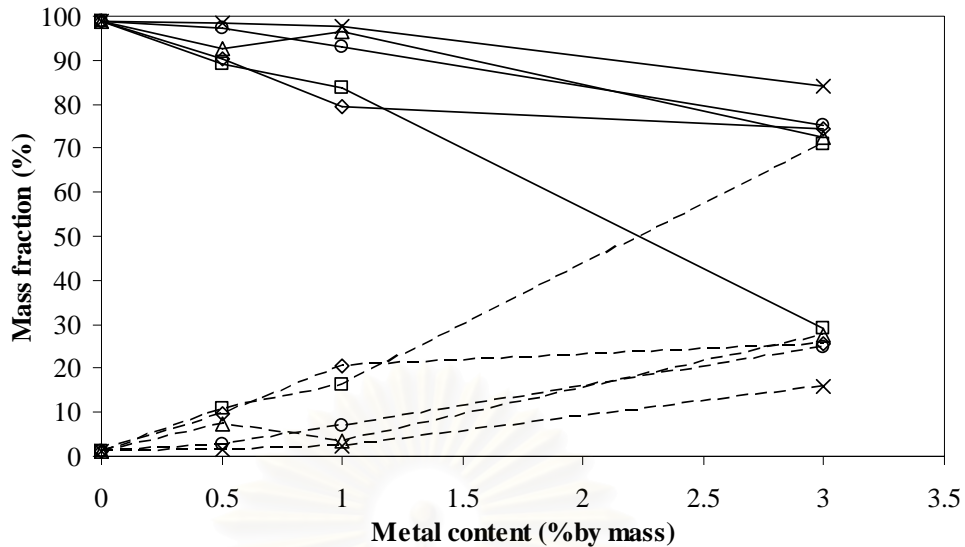
Figure 4.17 Fraction of each phase of silicon nitride in the bottom potion of the
product from the carbothermal reduction and nitridation of RHA
impregnated with metals at various metal content: (◇) iron;
(□) aluminium; (△) magnesium; (×) copper; (○) yttrium;
(—) α-phase; (- - -) β-phase.

The effects of each metal on the fraction of α- and β-phase in the product are
individually discussed in the following sections.

4.2.1.1 Addition of iron

Iron is investigated in this work because it has been found to be effective in
term of enhancing the formation of β-silicon nitride in the direct nitridation of silicon
[Boyer et al., 1978; Pigeon et al., 1993]. The effect of iron on the carbothermal
reduction and nitridation of RHA is shown in Figure 4.18. It indicates that iron affects
the reaction, such that it enhances the β-phase formation. Figure 4.18 shows the
tendency in decreasing the fraction of α-phase with an increase in the amount of iron
addition. In this work, the maximum fraction of β-phase obtained from iron
impregnated sample is 74.454%, when the content of iron is 3% by mass.

Figure 4.18 Fraction of α- and β-phase in silicon nitride obtained from the
Carbothermal reduction and nitridation of RHA impregnated with iron
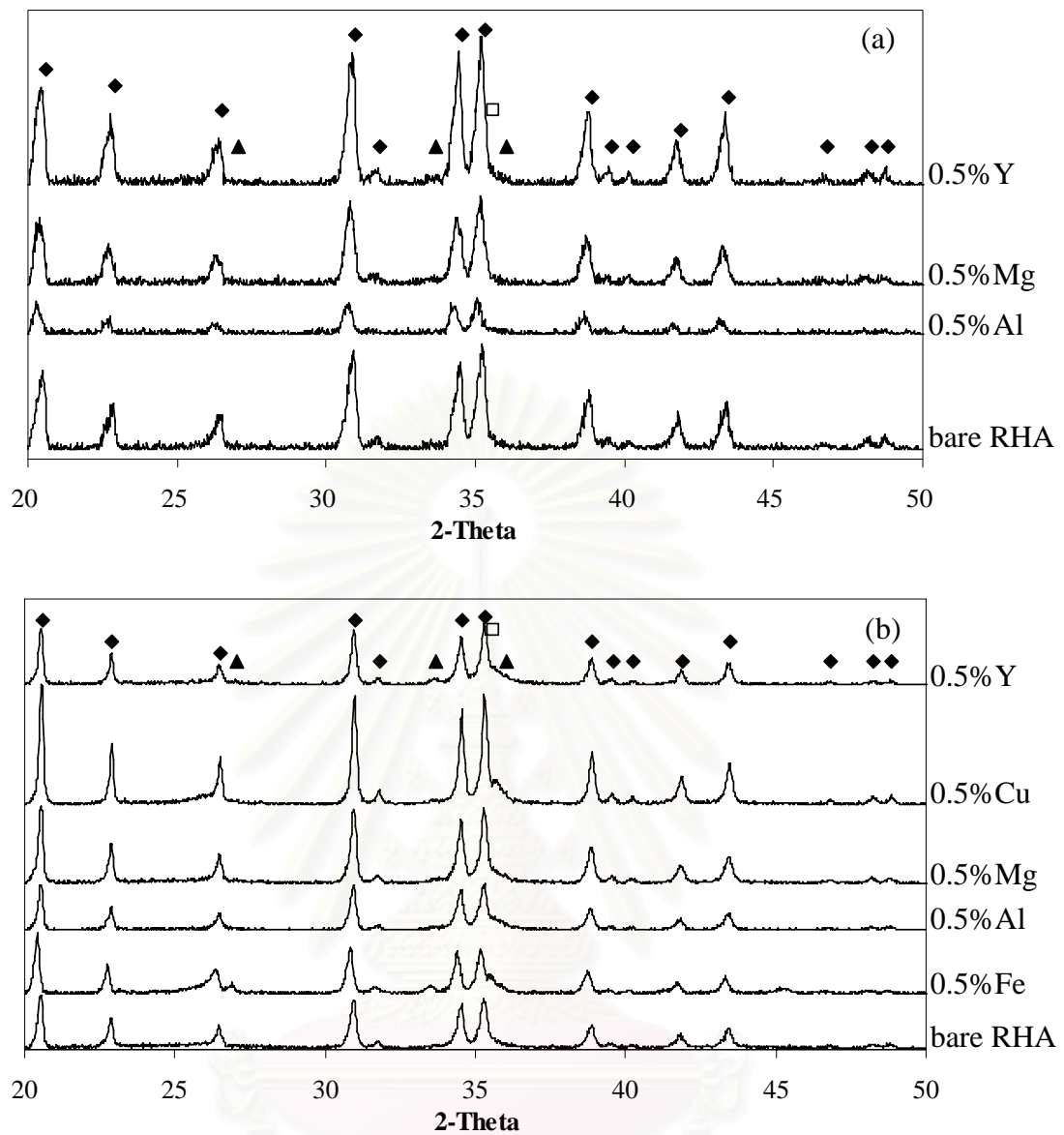at 1450°C for 6 h: (—) α-phase; (---) β-phase.

Figure 4.19 XRD patterns of products from the carbothermal reduction and
nitridation of RHA impregnated with iron at different concentrations:
◆ α-Si₃N₄, ▲ β-Si₃N₄, □ SiC.

Figure 4.20 Results from TG/DTA analysis of the product from the carbothermal reduction and nitridation of RHA impregnated with iron at various concentrations.

According to results shown in Figure 4.19, it can be observed that iron not only promotes β-silicon nitride formation, but also enhances silicon carbide. This effect is very strong when amount of iron impregnated to RHA is increased. Nevertheless, the TG/DTA analysis of the nitrided samples as shown in Figure 4.20 indicates that amount of residual carbon in the sample decreased with an increase in iron content. It means that the reaction between silica and carbon in RHA is enhanced by the presence of iron. It is suspected that the formation of silicon carbide in addition to silicon nitride further consumed carbon in the system. Therefore, it results in less carbon remaining in sample. The fact that silicon carbide was obtained from iron impregnated RHA supports with the report in literatures that iron promotes silicon carbide over silicon nitride [Siddiqi et al., 1985].

(a)

(b)

(c)

(d)

Figure 4.21 SEM micrographs of products from the carbothermal reduction and
nitridation at 1450°C for 6 h of: (a) unimpregnated RHA, (b) RHA
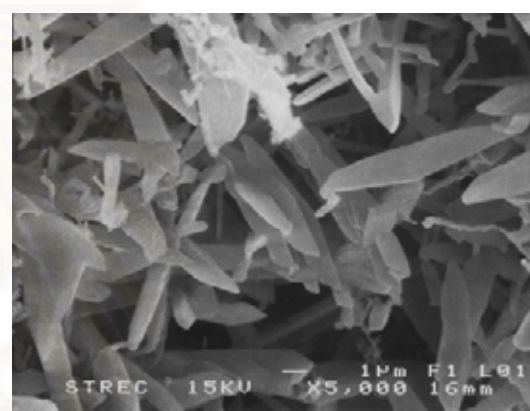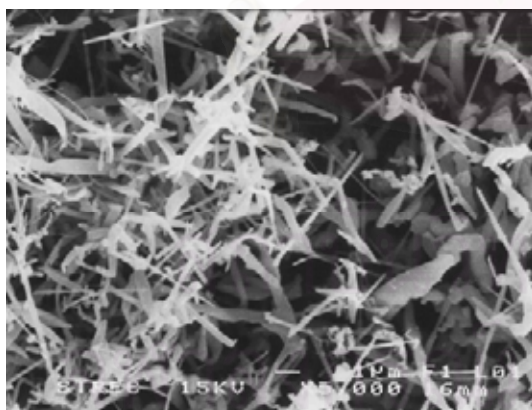impregnated with 0.5% iron, (c) RHA impregnated with 1.0% iron, and
(d) RHA impregnated with 3.0% iron.

The SEM pictures of the silicon nitride product are shown in Figure 4.21.
Since the nitrided product of iron-impregnated RHA was not consisted of two
distinguishable portions, only the SEM image for bottom portion of the nitrided
product of the unimpregnated RHA is used as the reference. For 0.5, 1.0 and 3.0%
iron impregnated RHA, the nitrided product are shown in Figure 4.21 (b), (c) and (d),
respectively. It can be described that when amount of iron impregnated to RHA is
increased, grains in silicon nitride product are generally much bigger than that in
sample with low content of iron. However, for 3.0% iron content, the morphology is
significantly different because the product is predominantly silicon carbide, as
observed from the XRD in Figure 4.19.

4.2.1.2 Addition of aluminium

Figure 4.22 shows the results from the carbothermal reduction and nitridation of RHA impregnated with aluminium at various concentration at 1450°C for 6h. The results obtained are similar to that of iron impregnated RHA. Figure 4.22 also shows the tendency in decreasing the fraction of α-phase with an increase in the amount of aluminium addition. However, for an addition of aluminium, the formation of β-silicon nitride is enhanced in much greater extent that the case of iron impregnation discussed earlier. The fraction of β-phase reaches as high as 70.7% in the bottom portion of the product.

The results from TG/DTA analysis of the nitrided product of aluminium impregnated RHA, in both top and bottom portions, are shown in Figure 4.24. It can be observed that the amount of residual carbon in the sample with low aluminium content (i.e. 0.5 and 1.0%) increases with the amount of aluminium, especially for the top portion of the sample. When the amount of aluminium addition is 3% by mass, the amount of residual carbon in sample after nitridation decreases. For bottom portion, it can be observed that amount of residual carbon is decreased when aluminium content is increased. This result can be described that the process consists of two mechanisms. For the first mechanism, the decrease in residual carbon indicates that carbon was consumed in the carbothermal reduction and nitridation process. High aluminium content yields high conversion of silicon nitride. The second mechanism is observed from the result that the formation of silicon carbide is increased with aluminium content. It means that carbon was consumed in reaction between silica and carbon to form silicon carbide. For top portion, it can be observed that residual carbon in RHA impregnated with 0.5% and 1.0% aluminium is higher than that of unimpregnated RHA. However, for RHA impregnated with 3.0% aluminium, the residual carbon is decreased. It is suggested that small amount of carbon was consumed in the carbothermal reduction and nitridation for RHA impregnated with 0.5% and 1.0% aluminium. The conversion is decreased by aluminium impregnated in low content. This result can be explained incorporating with XRD data (Figure 4.23) that the additional consumption of carbon takes place by the formation of silicon carbide, in the same manner as previously discussed for iron.
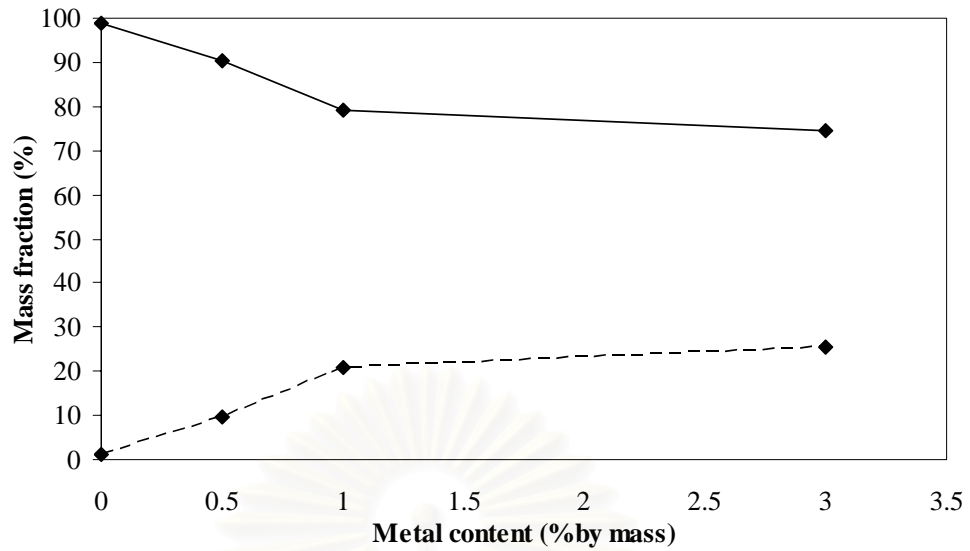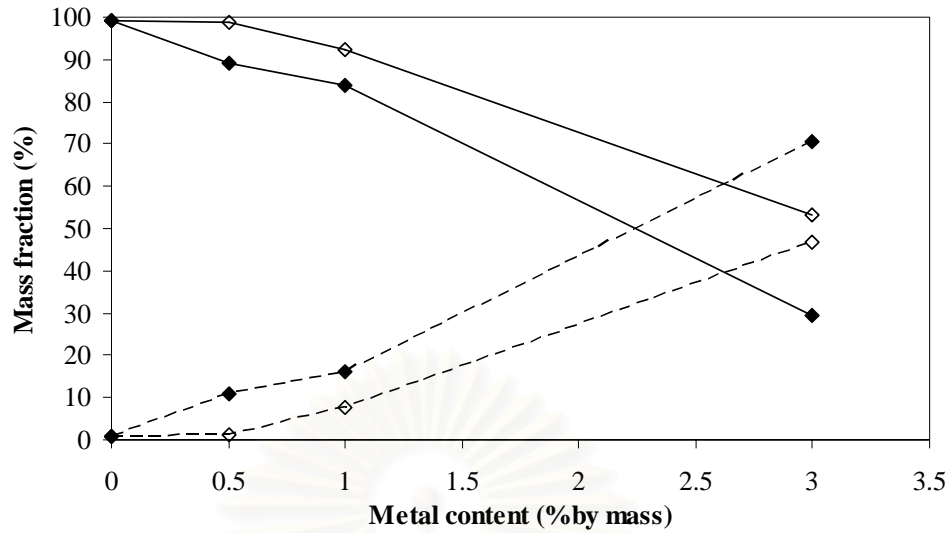
Figure 4.22 Fraction of α- and β-phase in silicon nitride obtained from the carbothermal reduction and nitridation of RHA impregnated with aluminium at 1450°C: (◇) top portion of the product, (◆) bottom portion of the product, (—) fraction of α-phase, (---) fraction of β-phase.

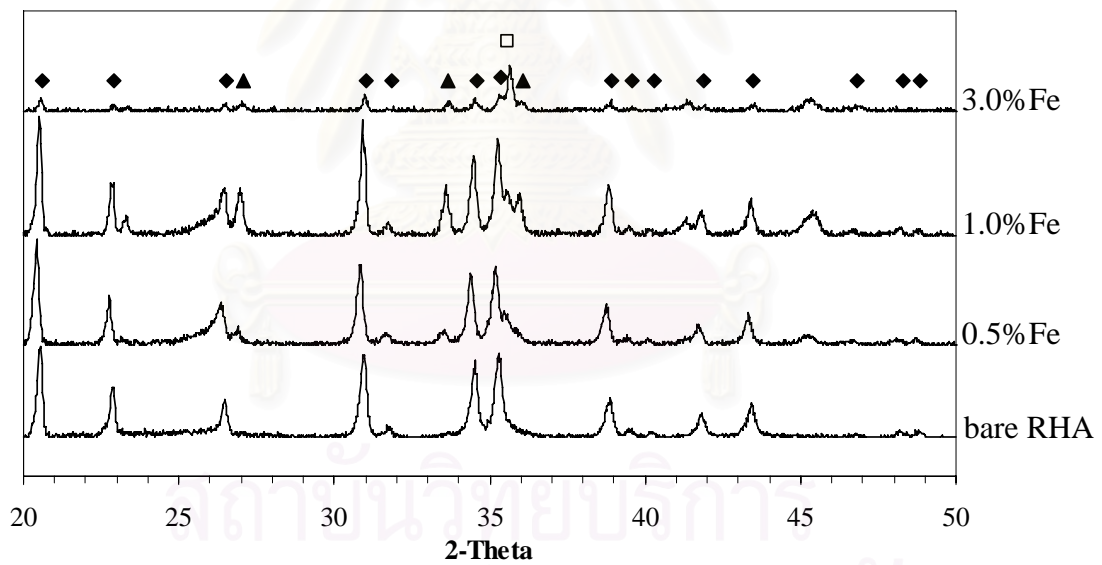สถาบันวิทยบริการ
จุฬาลงกรณ์มหาวิทยาลัย
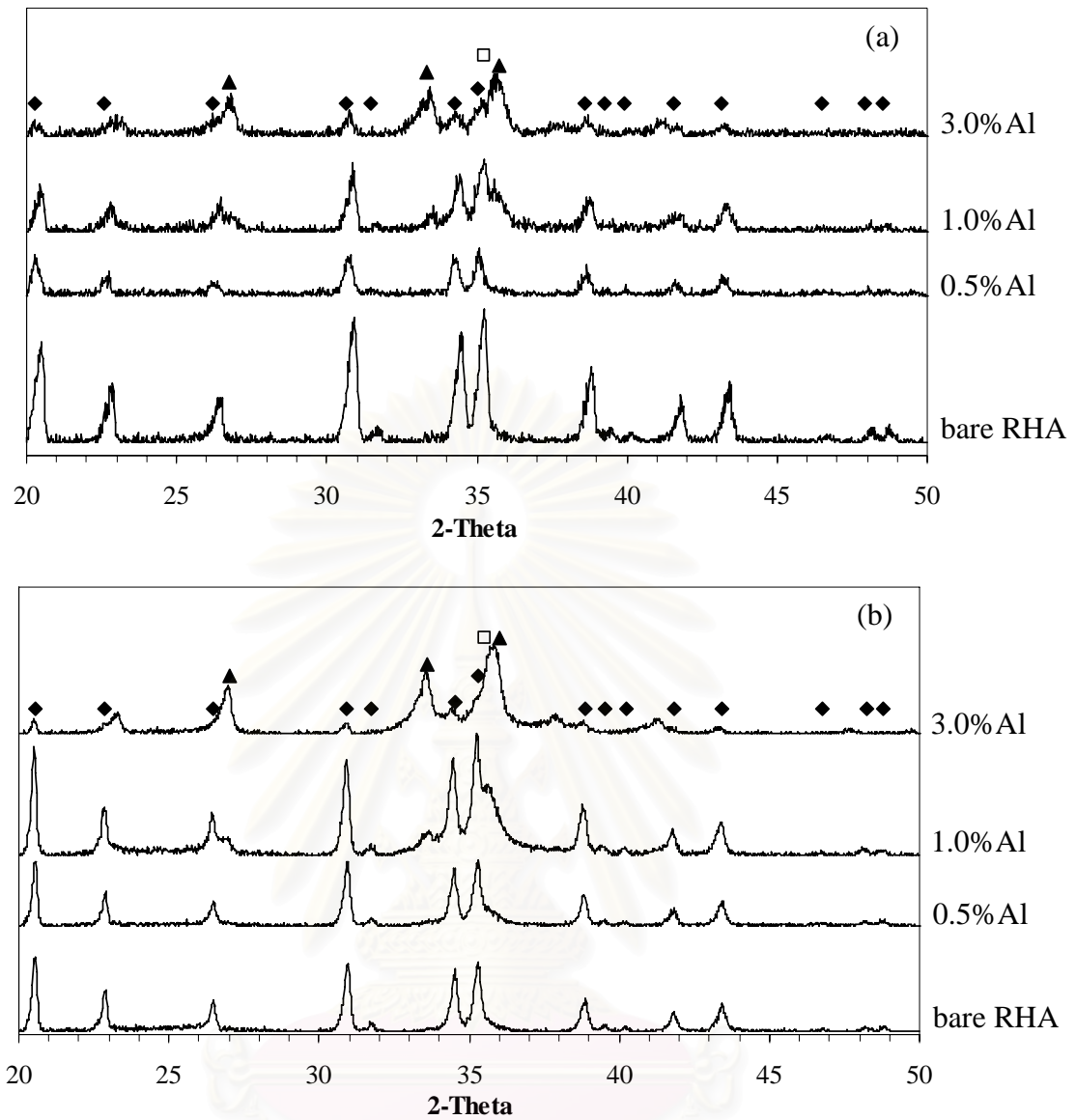
Figure 4.23 XRD patterns of products from the carbothermal reduction and nitridation of RHA impregnated with aluminium at different concentrations: (a) top portion of the product, (b) bottom portion of the product, ◆ α-Si_3N_4, ▲ β-Si_3N_4, □ SiC.
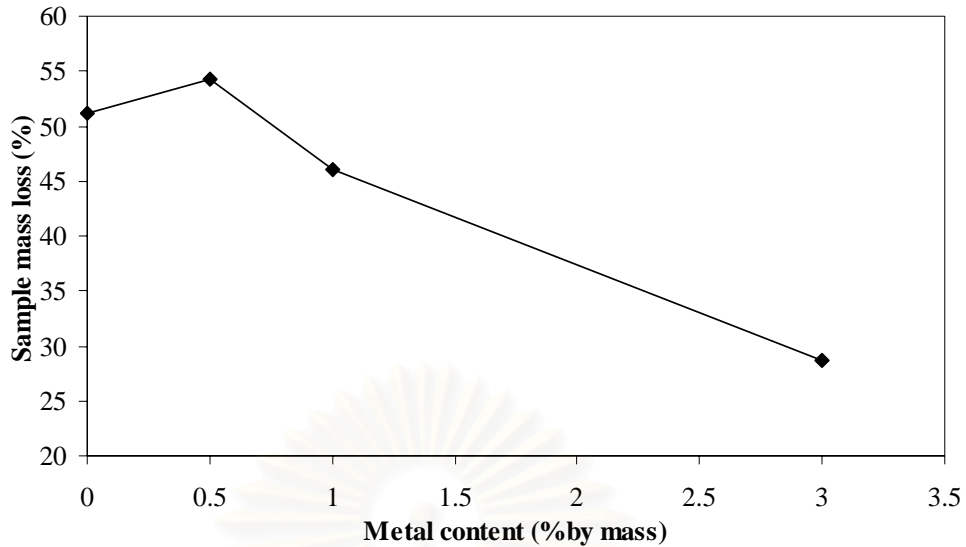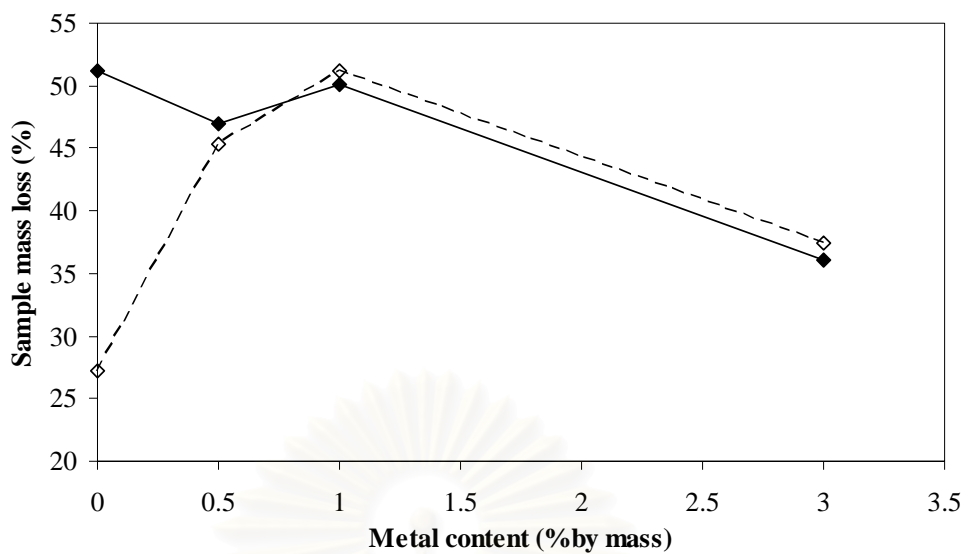
Figure 4.24 Result from TG/DTA analysis of the product from the carbothermal
reduction and nitridation of RHA impregnated with aluminium at various
concentrations: (◇) top portion of the product, (◆) bottom portion of
the product.

top portion   bottom portion

(a)

top portion   bottom portion
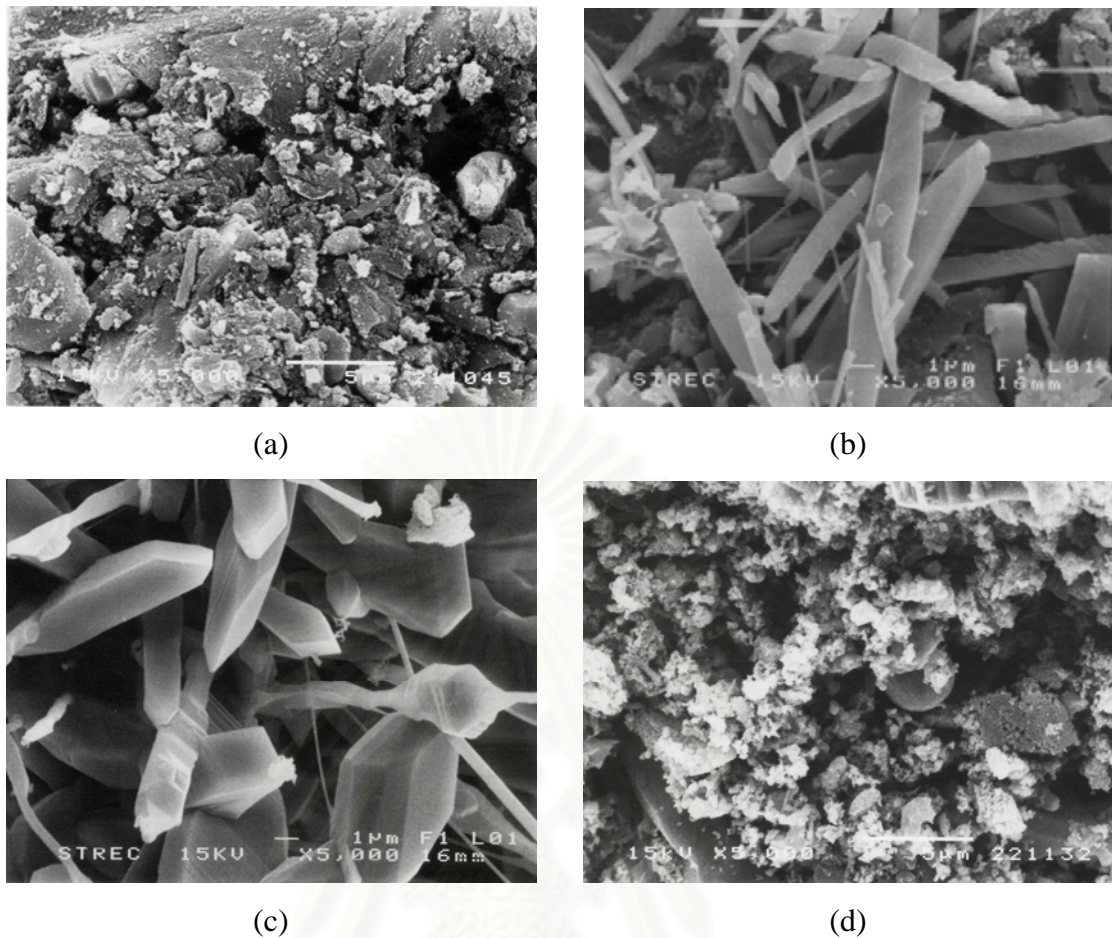
(b)

top portion   bottom portion

(c)
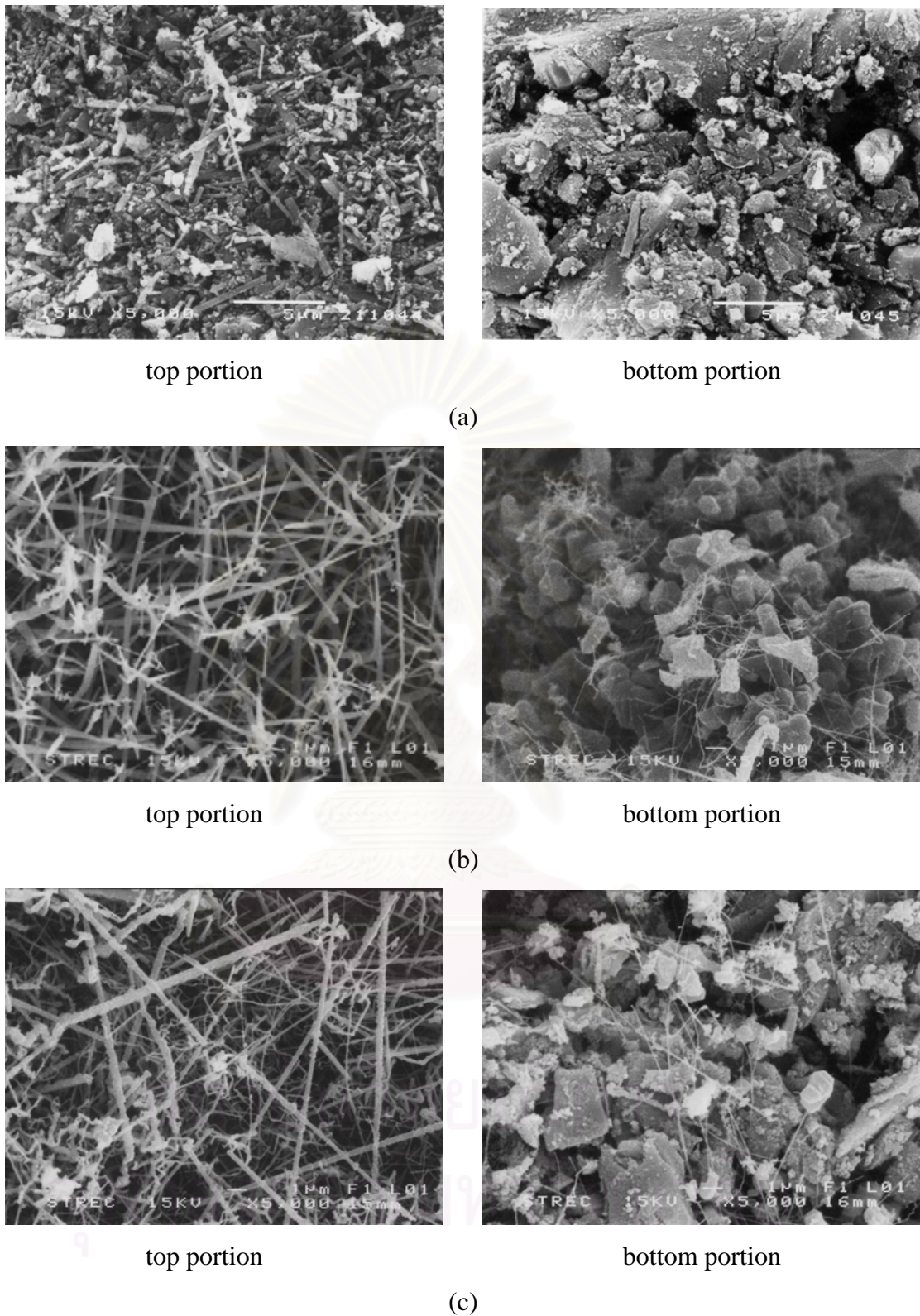
Figure 4.25 SEM micrographs of products from the carbothermal reduction and nitridation at $1450^{o}C$ for 6 h of: (a) bare RHA, (b) RHA impregnated with 0.5% aluminium, (c) RHA impregnated with 1.0% aluminium.

top portion	bottom portion

(d)
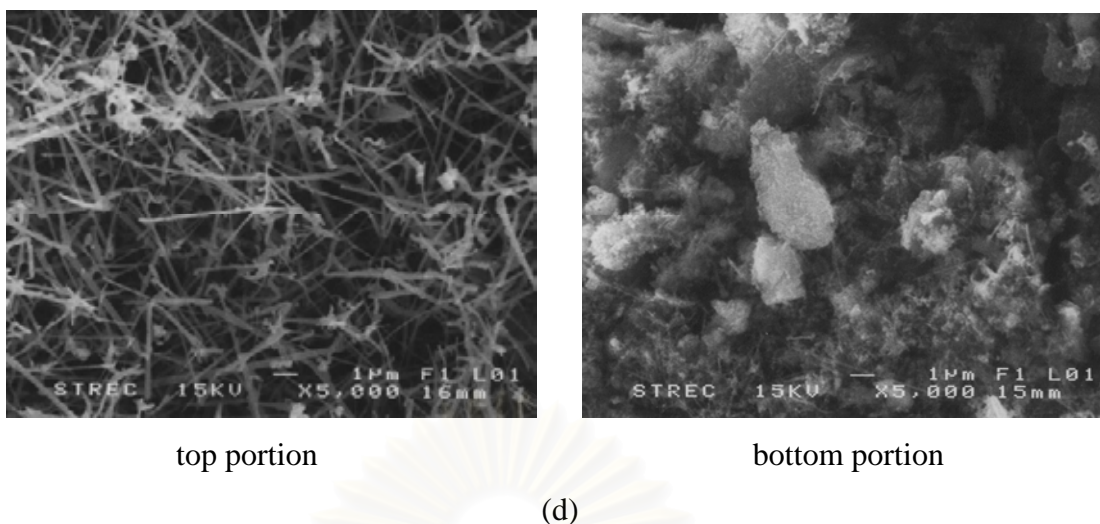
Figure 4.25 (continued) SEM micrographs of products from the carbothermal
reduction and nitridation at 1450°C for 6 h of: (d) RHA impregnated
with 3.0% aluminium.

The SEM pictures of each portion of the silicon nitride products obtained from
the nitridation at 1450°C and 6 h are shown in Figure 4.25. It can be observed that
morphology of silicon nitride product in top and bottom portions are quite different.
The top portion consists of lots of long fibers which have diameter in submicron
range. It means that aluminium enhances silicon monoxide production. For bottom
portion, product with an addition of aluminium has different morphology from that of
unimpregnated RHA because aluminium enhances silicon monoxide generation,
which decreases the contact between silica and carbon and results in less aggregated
samples.

4.2.1.3 Addition of magnesium

The effect of magnesium on the carbothermal reduction and nitridation is
similar to those of iron and aluminium. Figure 4.26 indicates that magnesium is
another metal that suppresses the β-silicon nitride formation. β-Phase is hardly
detected by XRD for RHA impregnated with 3.0% magnesium in both top and bottom
portions as shown in Figure 4.23 (a) and (b), respectively. Fraction of α-phase
decreases with magnesium content. The results show that RHA impregnated with
magnesium promotes the formation of β-silicon nitride with the absence of silicon

carbide. The fraction of β-phase of silicon nitride product at top and bottom portion is 39.72 and 27.41%, respectively.

Figure 4.26 Fraction of α- and β-phase in silicon nitride obtained from the
carbothermal reduction and nitridation of RHA impregnated with
magnesium at 1450°C: (◇) top portion of the product, (◆) bottom
portion of the product, (—) fraction of α-phase, (---) fraction of β-phase.

Figure 4.27 XRD patterns of products from the carbothermal reduction and nitridation of RHA impregnated with magnesium at different concentrations: (a) top portion of the product, (b) bottom portion of the product, ◆ α-Si$_3$N$_4$, ▲ β-Si$_3$N$_4$, □ SiC.

Figure 4.28 Result from TG/DTA analysis of the product from the carbothermal
reduction and nitridation of RHA impregnated with magnesium at
various concentrations: ($\diamond$) top portion of the product, ($\blacklozenge$) bottom
portion of the product.

For the TG/DTA analysis of the nitrided product of magnesium-impregnated
RHA, the results are shown in Figure 4.28. It can be observed that mass loss of the
sample in the bottom portion is much higher than the top portion. In the other words,
the top portion has less amount of residual carbon than the bottom portion. When
amount of magnesium impregnated was increased, the amount of residual carbon in
bottom portion decreased. However, the content of residual carbon in top portion is
lower than bottom portion because top portion is formed from vapor phase, which has
much higher purity than the bottom. When all carbon is removed, the sample turns
light gray which is corresponding to the color of silicon nitride. This result indirectly
confirms the XRD data in Figure 4.27 that no silicon carbide was formed.

top portion   bottom portion

(a)

top portion   bottom portion

(b)

top portion   bottom portion

(c)
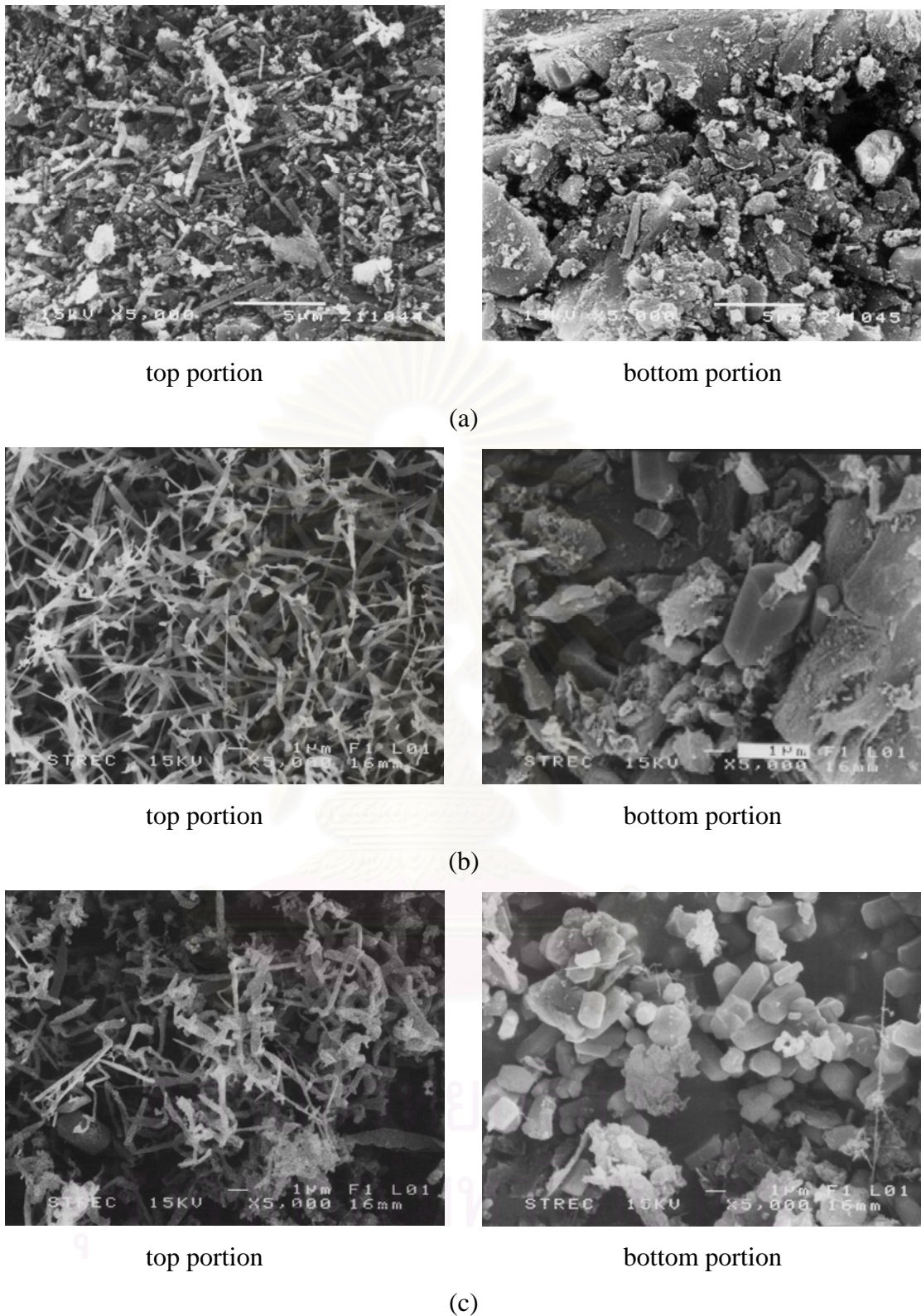
Figure 4.29 SEM micrographs of products from the carbothermal reduction and
nitridation at $1450^{o}C$ for 6 h of: (a) bare RHA, (b) RHA impregnated
with 0.5% magnesium, (c) RHA impregnated with 1.0% magnesium.

top portion   bottom portion

(d)
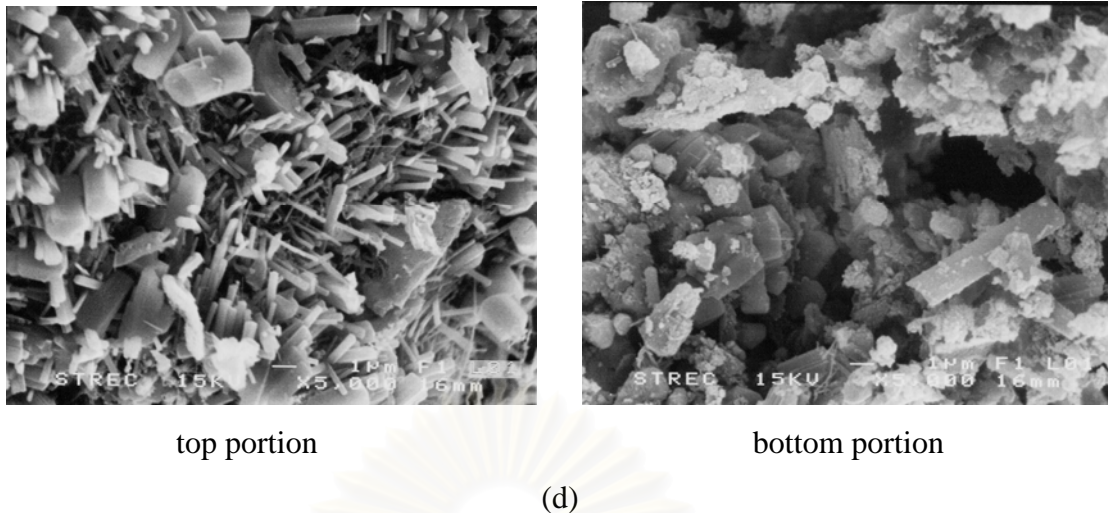
Figure 4.29 (continued) SEM micrographs of products from the carbothermal
reduction and nitridation at 1450°C for 6 h of: (d) RHA impregnated
with 3.0% magnesium.

SEM micrographs of each portion of the products are shown in Figure 4.29. It
is clearly indicated that morphology of product in different portions are quite
different. Both top and bottom portions has increased crystallinity as the magnesium
content is increased. It can be observed that top portion are short fibers. It is suggested
that magnesium enhances silicon monoxide in less extent than aluminium. For RHA
impregnated with 3.0% magnesium, the top portion has morphology similar to the
bottom portion, which means that silicon monoxide production is decreased when
magnesium content is increased. For bottom portion, the crystal structure of all
products doped with magnesium is hexagonal. On the other hand, for top portion, the
crystal structure is hexagonal only when magnesium content is 3.0%.

4.2.1.4 Addition of copper

Copper is investigated in this work because it is another metal recently studied
for the aid of silicon nitride production, even though the technique reported is not the
carbothermal process [Deckwerth et al., 1994]. Results of the carbothermal reduction
and nitridation of copper-impregnated RHA are shown in Figure 4.30. The results
obtained are similar to those for other metals. Fraction of α-phase tends to decrease
with an increase in the amount of copper addition. It indicates that copper tends to
enhance the formation of β-phase at high concentration of copper. The results are

further illustrated by XRD patterns shown in Figure 4.31. When amount of copper impregnated to RHA is increased, the signals for β-silicon nitride as well as silicon carbide can be clearly visible.

According to TG/DTA analysis as shown in Figure 4.32, the amount of residual carbon in the sample decreases when copper content is increased, mainly because silicon carbide is formed in greater amount. The higher the copper content, the higher signal of silicon carbide is detected.

The SEM pictures of the silicon nitride products obtained from the nitridation at 1450°C and 6 h are shown in Figure 4.33. However, when the content of copper is 3.0%, morphology of the product becomes different than that of the sample with low copper content, most probably because silicon carbide is formed together with silicon nitride. In general, it is indicated that copper has similar catalytic effect to iron.
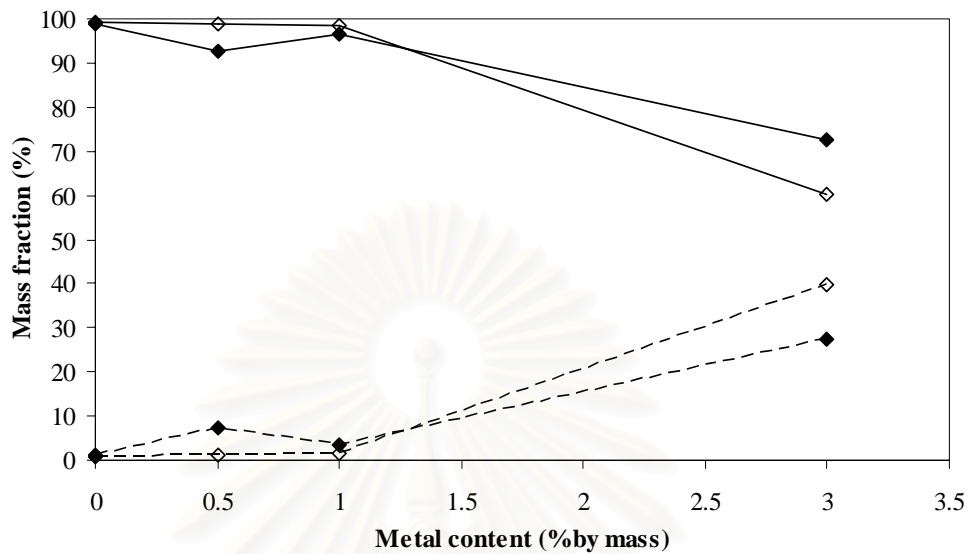

Figure 4.30 Fraction of α- and β-phase in silicon nitride obtained from the
Carbothermal reduction and nitridation of RHA impregnated with copper
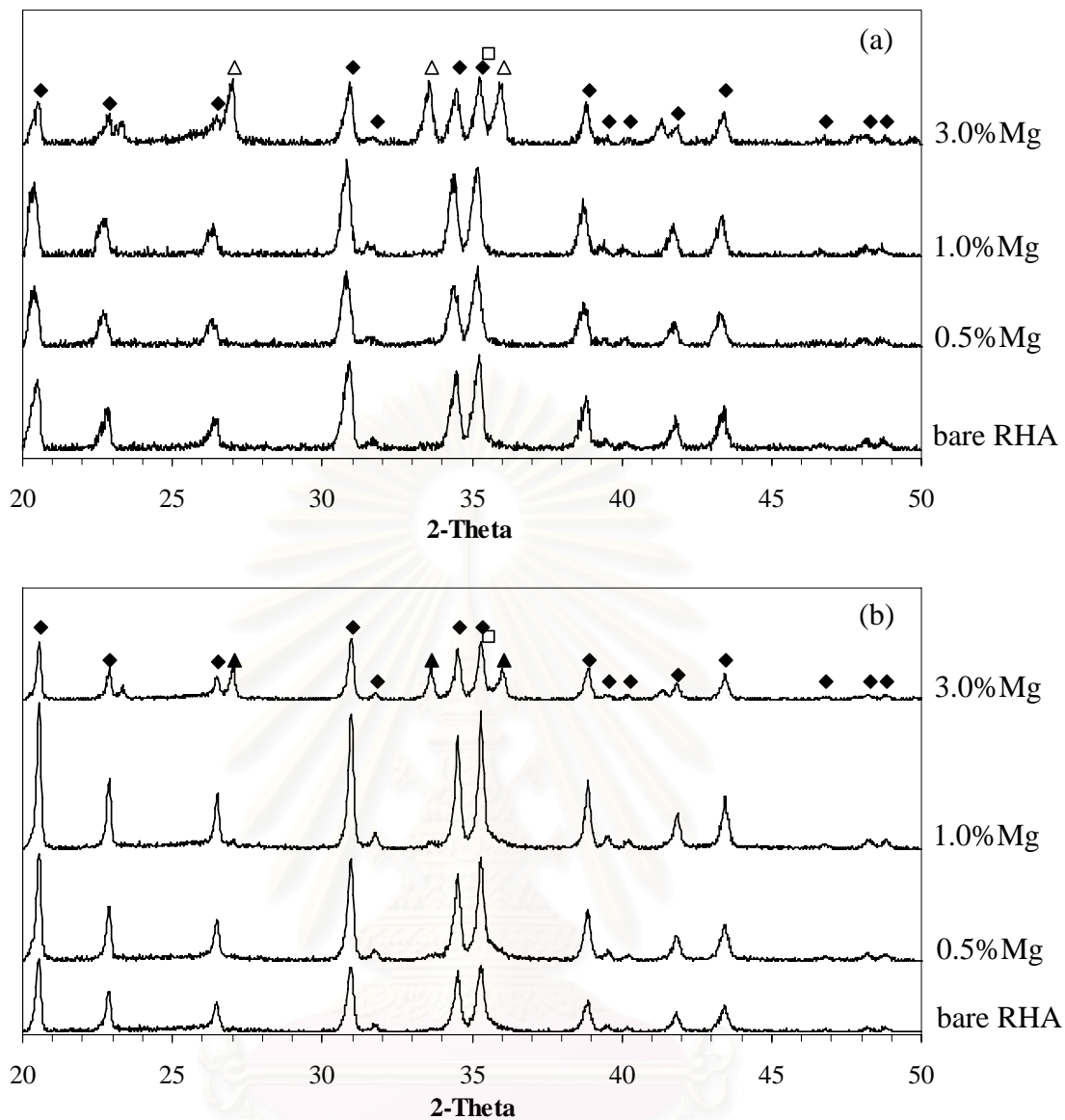at 1450°C for 6 h: (—) α-phase; (---) β-phase.
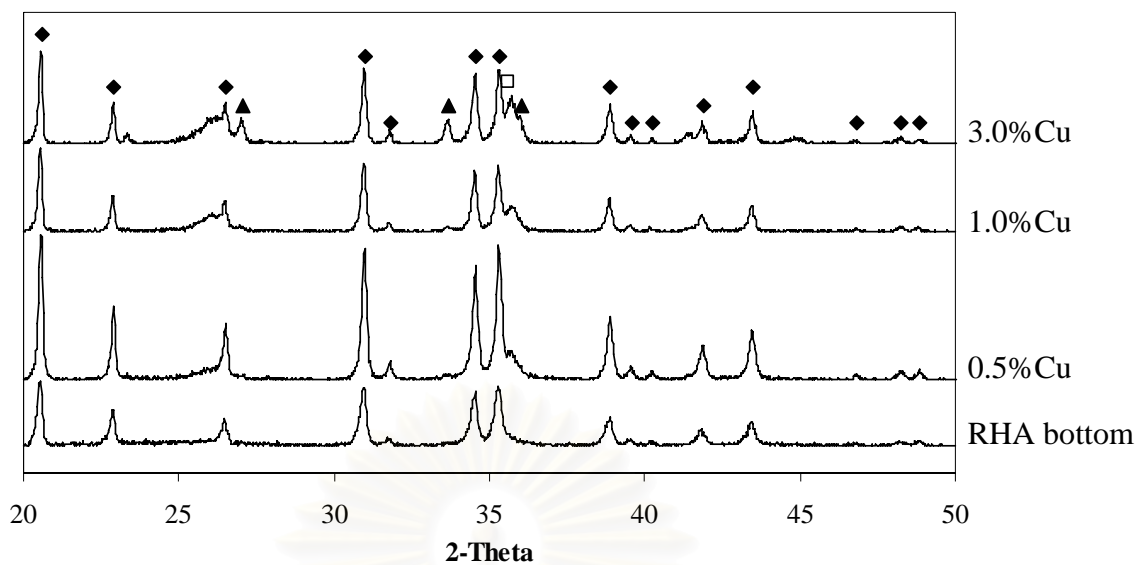
Figure 4.31 XRD patterns of products from the carbothermal reduction and nitridation of RHA impregnated with copper at different concentrations: ◆ α-Si$_3$N$_4$, ▲ β-Si$_3$N$_4$, □ SiC.
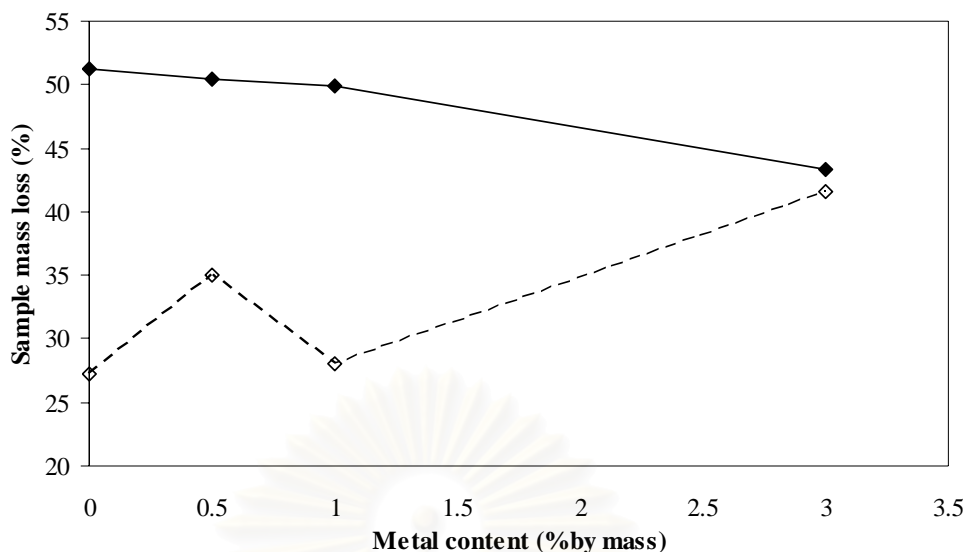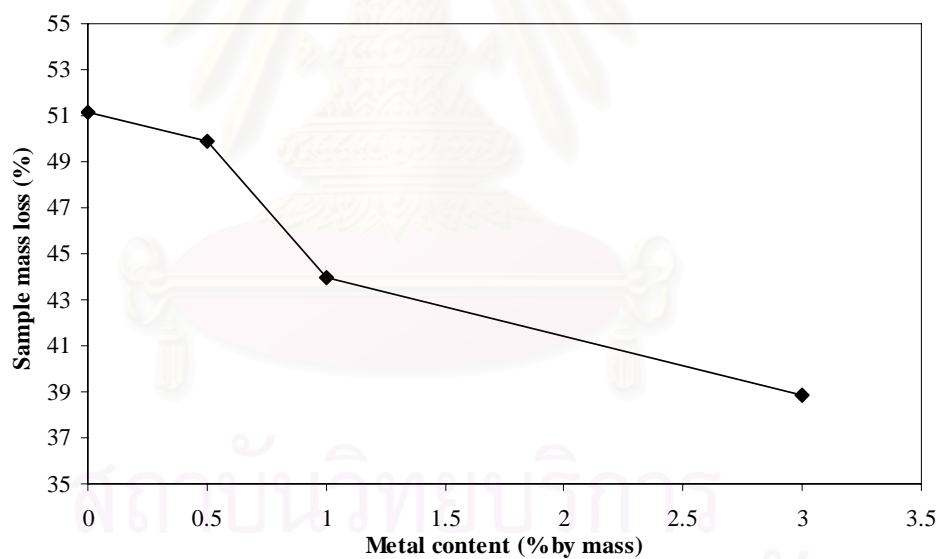

Figure 4.32 Results from TG/DTA analysis of the product from the carbothermal reduction and nitridation of RHA impregnated with copper at various concentrations.
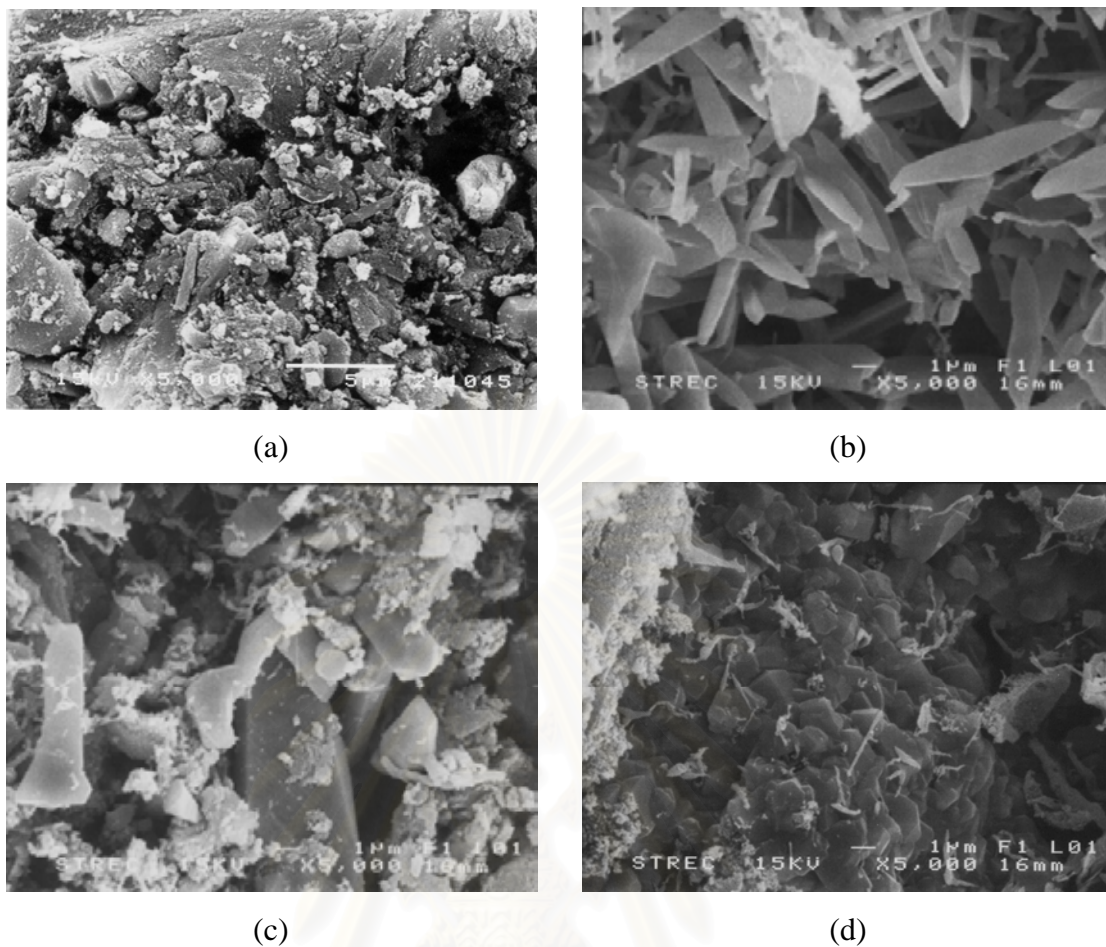
Figure 4.33 SEM micrographs of products from the carbothermal reduction and nitridation at 1450°C for 6 h of: (a) unimpregnated RHA, (b) RHA impregnated with 0.5% copper, (c) RHA impregnated with 1.0% copper, and (d) RHA impregnated with 3.0% copper.

4.2.1.5 Addition of yttrium

Yttrium is investigated in this work because it has been found to be effective in term of enhancing the formation of α-silicon nitride in the direct nitridation process. The effect of yttrium on the carbothermal reduction and nitridation are shown in Figure 4.34, which indicates that yttrium is another metal that increases the fraction of α-phase in top portion of the silicon nitride product. The content of α-phase obtained from 1.0% yttrium impregnated RHA is 99.3%, which is higher than other samples. For RHA impregnated with 3.0% yttrium, the amount of top portion is significantly less than other samples. The amount of top portion was too small to be

analyzed by TGA. Results from the bottom portion are similar to other metals. Figure 4.35 (a), confirms that yttrium enhances the formation of α-silicon nitride in the top portion. No silicon nitride in β-phase can be observed from the top portion of the nitride product of yttrium impregnated RHA. The results from TG/DTA analysis (Figure 4.36) show that residual carbon is decreased when yttrium content is increased. Since only small fraction of silicon carbide is formed, the decreased in the residual carbon indicates high conversion of the carbothermal reduction and nitridation process. However, top portion has conversion higher than bottom portion in the same manner as other metals.

Figure 4.34 Fraction of α- and β-phase in silicon nitride obtained from the
carbothermal reduction and nitridation of RHA impregnated with
aluminium at 1450°C: ($\diamondsuit$) top portion of the product, ($\blacklozenge$) bottom
portion of the product, (—) fraction of α-phase, (---) fraction of β-phase.

Figure 4.35 XRD patterns of products from the carbothermal reduction and
nitridation of RHA impregnated with yttrium at different
concentrations: (a) top portion of the product, (b) bottom portion of the
product, ◆ α-Si$_3$N$_4$, ▲ β-Si$_3$N$_4$, □SiC.

Figure 4.36 Result from TG/DTA analysis of the product from the carbothermal
reduction and nitridation of RHA impregnated with yttrium at
various concentrations: ($\diamondsuit$) top portion of the product, ($\blacklozenge$) bottom
portion of the product.

top portion   bottom portion

(a)

top portion   bottom portion

(b)

top portion   bottom portion

(c)
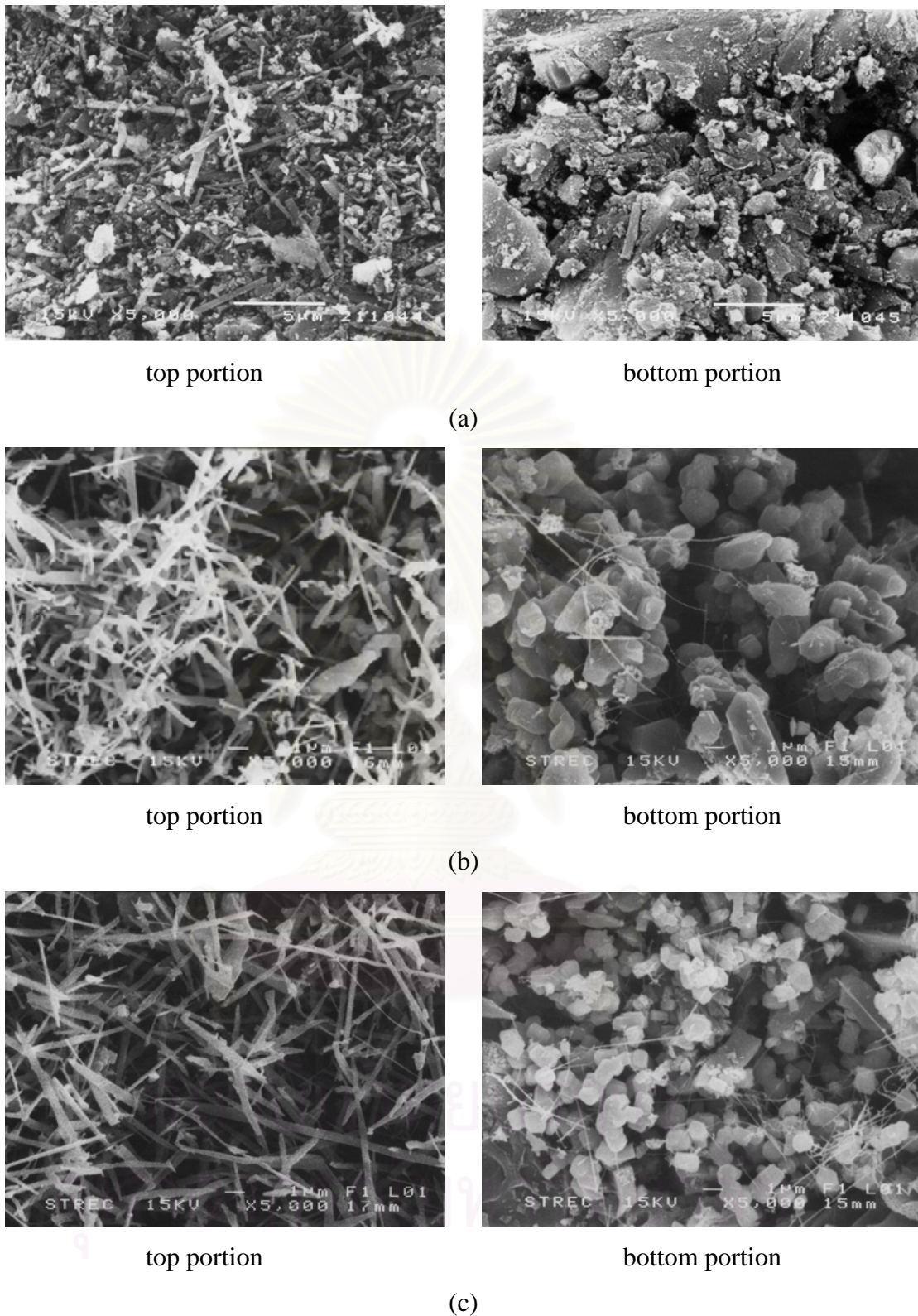
Figure 4.37 SEM micrographs of products from the carbothermal reduction and
nitridation at $1450^{\circ}C$ for 6 h of: (a) bare RHA, (b) RHA impregnated
with 0.5% yttrium, (c) RHA impregnated with 1.0% yttrium.

| top portion | bottom portion |

(d)
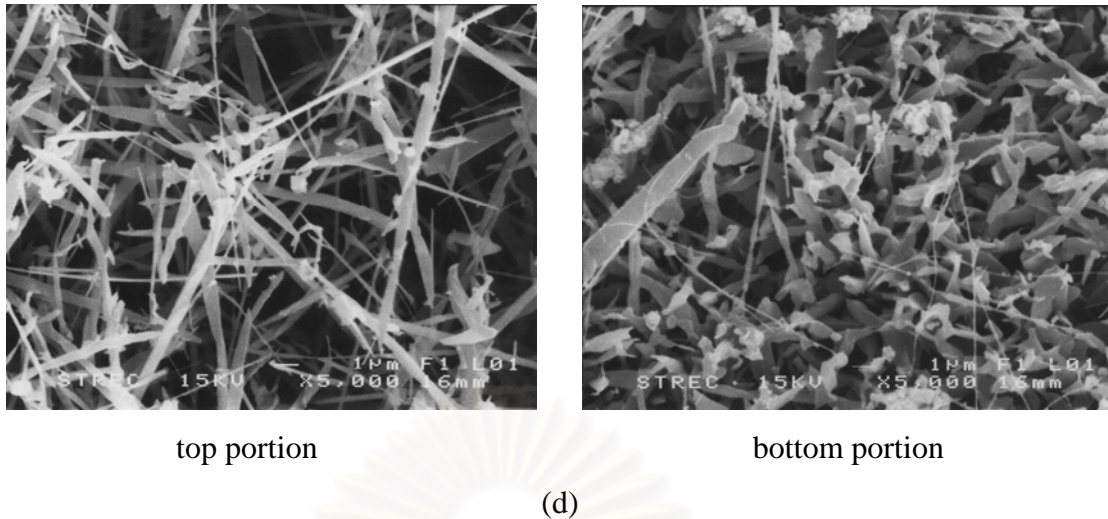
Figure 4.37 (continued) SEM micrographs of products from the carbothermal reduction and nitridation at 1450°C for 6 h of: (d) RHA impregnated with 3.0% yttrium.

The SEM pictures as shown in Figure 4.37 indicate that the top portion of the silicon nitride product consists of lots of short fibers, which have diameter in submicron range. When yttrium content are very high, the fibers grow longer. It means that high content of yttrium enhances silicon monoxide in higher extent than the low concentration of yttrium. The mechanism has already been discussed in the previous section. For bottom portion, it can be seen that, when amount of yttrium impregnated to RHA is increased, grains in silicon nitride product become much bigger. However, at higher content of yttrium impregnated to RHA, silicon carbide was found mixed with silicon nitride in the bottom portion of the product. This may alter the morphology of the grains of the product as observed by SEM.

4.2.2 Effect of Reaction Time

This section, effect of reaction time on the carbothermal reduction and nitridation of metal-impregnated RHA is investigated. Although the effects of various metals dominantly influence the carbothermal reduction and nitridation, the effect of reaction time is also discussed. The reaction time of 1, 3 and 6 h were investigated in this work. It should be noted that the content of metal impregnated in this section was kept constant at 0.5%. The effect of reaction time on the carbothermal reduction and nitridation are presented as follows:

4.2.2.1 Iron

Results from XRD analysis of the nitrided product of iron impregnated RHA from the reaction for different period of time are shown in Figure 4.38. It is indicated that silicon carbide is the dominant product at the beginning of the carbothermal reduction and nitridation process. Then, the formation of silicon nitride is favored as the reaction proceeds. It means that silicon carbide is converted to silicon nitride, which can be represented by the following equation:

$$3SiC\,(s) + 2N_2\,(g) \rightarrow Si_3N_4(s) + 3C\,(s) \tag{4.4}$$
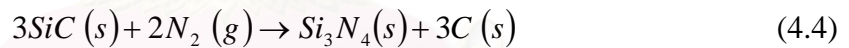
Figure 4.39 shows the fraction of α- and β-phase in silicon nitride synthesized from 0.5% iron impregnated to RHA. It can be observed that the fraction of α-phase is roughly unaffected by the reaction time. TG/DTA analysis as shown in Figure 4.40, it support with XRD pattern because 1 and 3 h nitridation are more silicon carbide mixed with silicon nitride than 6 h nitridation, mass loss at 6 h nitridation is higher than 3 h nitridation but 1 h nitridation has nearest value with 6 h nitridation because it is not silicon carbide whole of sample, it has higher residual carbon remain in product.

Figure 4.38 XRD patterns of products from the carbothermal reduction and
nitridation of RHA impregnated with iron under various reaction
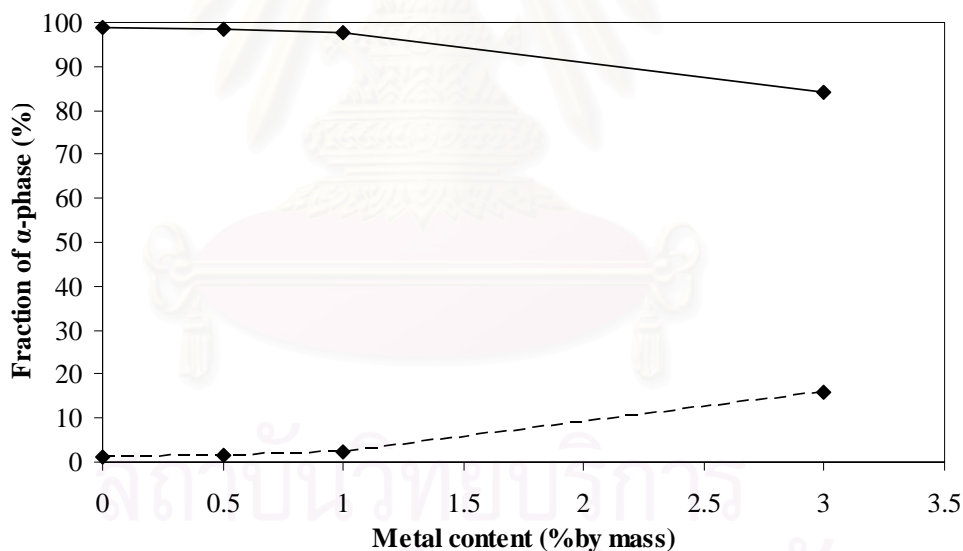times: ◆ α-Si$_3$N$_4$, ▲ β-Si$_3$N$_4$, □ SiC.

Figure 4.39 Fraction of α- and β-phase in silicon nitride obtained from the
carbothermal reduction and nitridation of RHA impregnated with iron
under various reaction times: (—) α-phase; (---) β-phase.

Figure 4.40 Results from TG/DTA analysis of the product from the carbothermal reduction and nitridation of RHA impregnated with iron under various reaction times.

4.2.2.2 Aluminium

It can be observed from the Figure 4.41 that, although silicon carbide is formed at the very beginning of the reaction, silicon carbide is not found in the product when reaction time reaches 6 h. Top portion of the product is pure α-silicon nitride, which the bottom portion is α-silicon nitride mixed with β-silicon nitride. Figure 4.42 shows the fraction of α- and β-phase as the reaction progresses. It is observed that the formation of α-phase in the top portion is slightly higher than the bottom portion for the whole period of the reaction. Results from the TG/DTA analysis shown in Figure 4.43 confirm that conversion of silicon nitride increases with reaction time. Amount of carbon remaining in silicon nitride product after 1 h nitridation is much higher than those nitrided for 3 and 6 h.

Figure 4.41 XRD patterns of products from the carbothermal reduction and nitridation of RHA impregnated with aluminium under various reaction times: (a) top portion of the product, (b) bottom portion of the product, ◆ α-Si_3N_4, ▲ β-Si_3N_4, □ SiC.
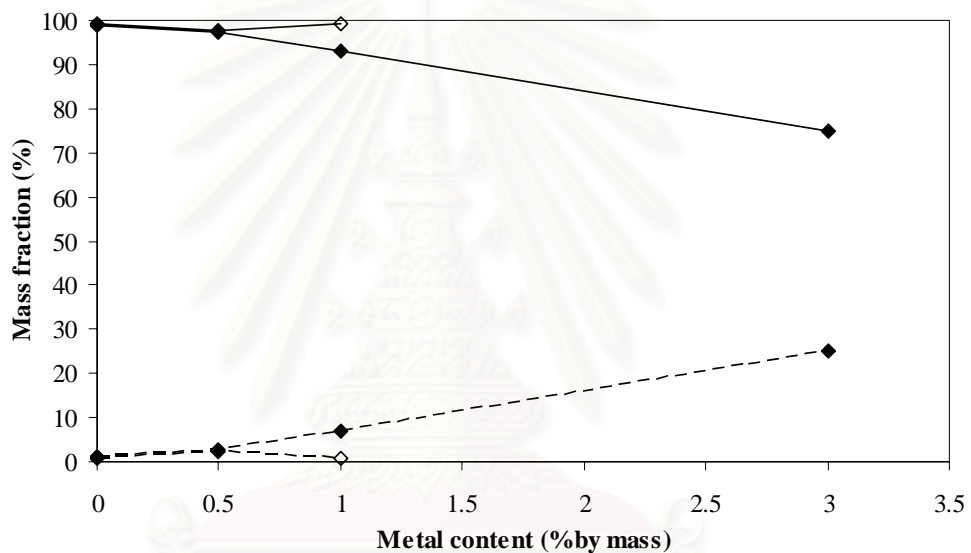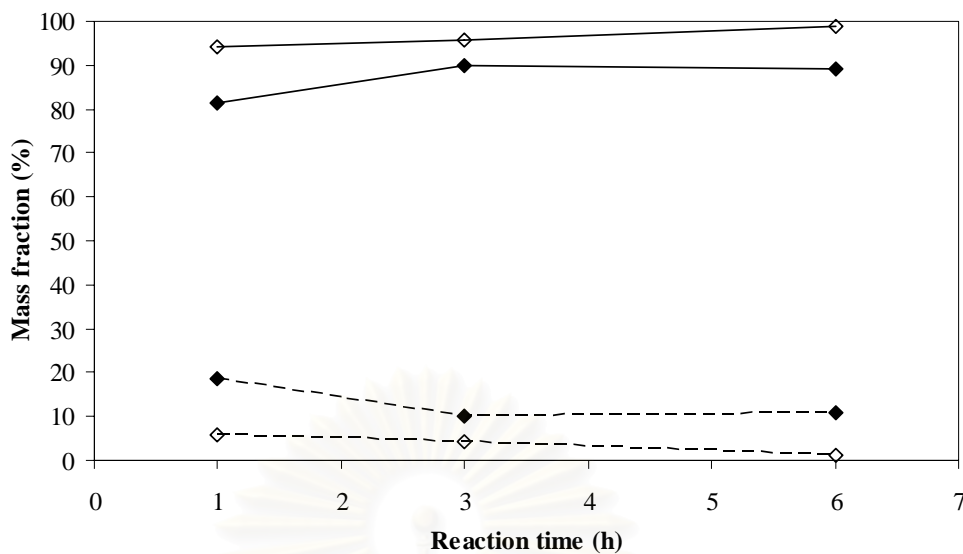
Figure 4.42 Fraction of α- and β-phase in silicon nitride obtained from the
carbothermal reduction and nitridation of RHA impregnated with
aluminium under various reaction times: (◇) top portion of the product;
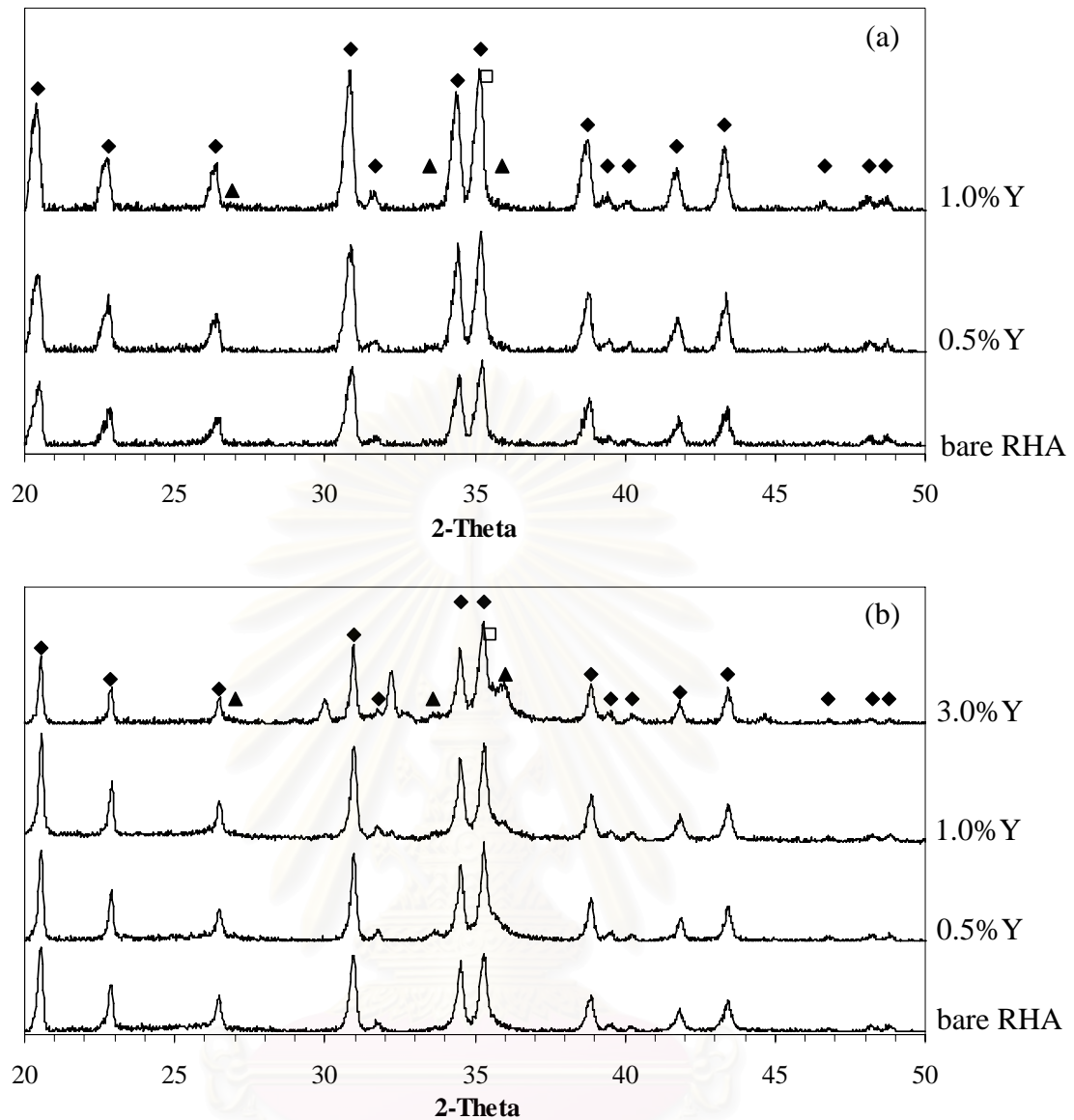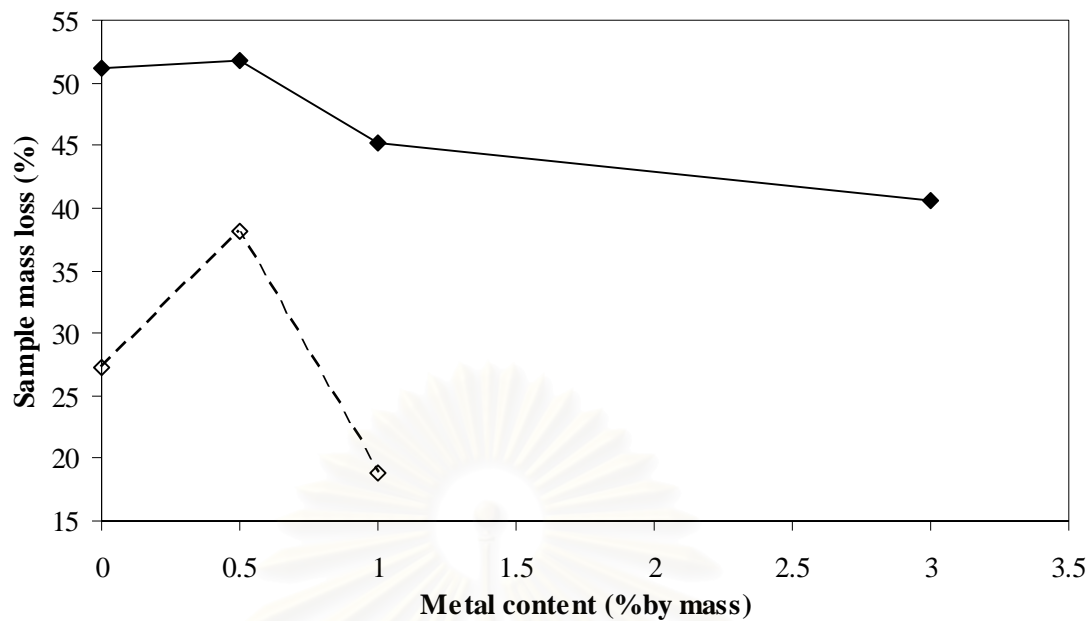(◆) bottom portion of the product; (—) fraction of α-phase; (---) fraction
of β-phase.

Figure 4.43 Results from TG/DTA analysis of the product from the carbothermal
reduction and nitridation of RHA impregnated with aluminium under
various reaction times: (◇) top portion of the product, (◆) bottom
portion of the product.

4.2.2.3 Magnesium

Figure 4.44 shows XRD patterns of the products of the carbothermal reduction and nitridation using magnesium-impregnated RHA under various reaction times. It is confirm that silicon carbide is not found in the product when reaction timed is prolonged, in the same manner as observed earlier for aluminium impregnated RHA. The effect of magnesium on the carbothermal reduction and nitridation of RHA is very similar to that of aluminium. Figure 4.45 indicates that magnesium is another metal that suppresses the β-silicon nitride formation. Although the product of short-time reaction has high fraction of β-silicon nitride, β-phase is hardly detected by XRD when reaction time is 6 h. TG/DTA analysis of magnesium-impregnated RHA is shown in Figure 4.46. It is confirmed that conversion of silicon nitride increases with reaction time.
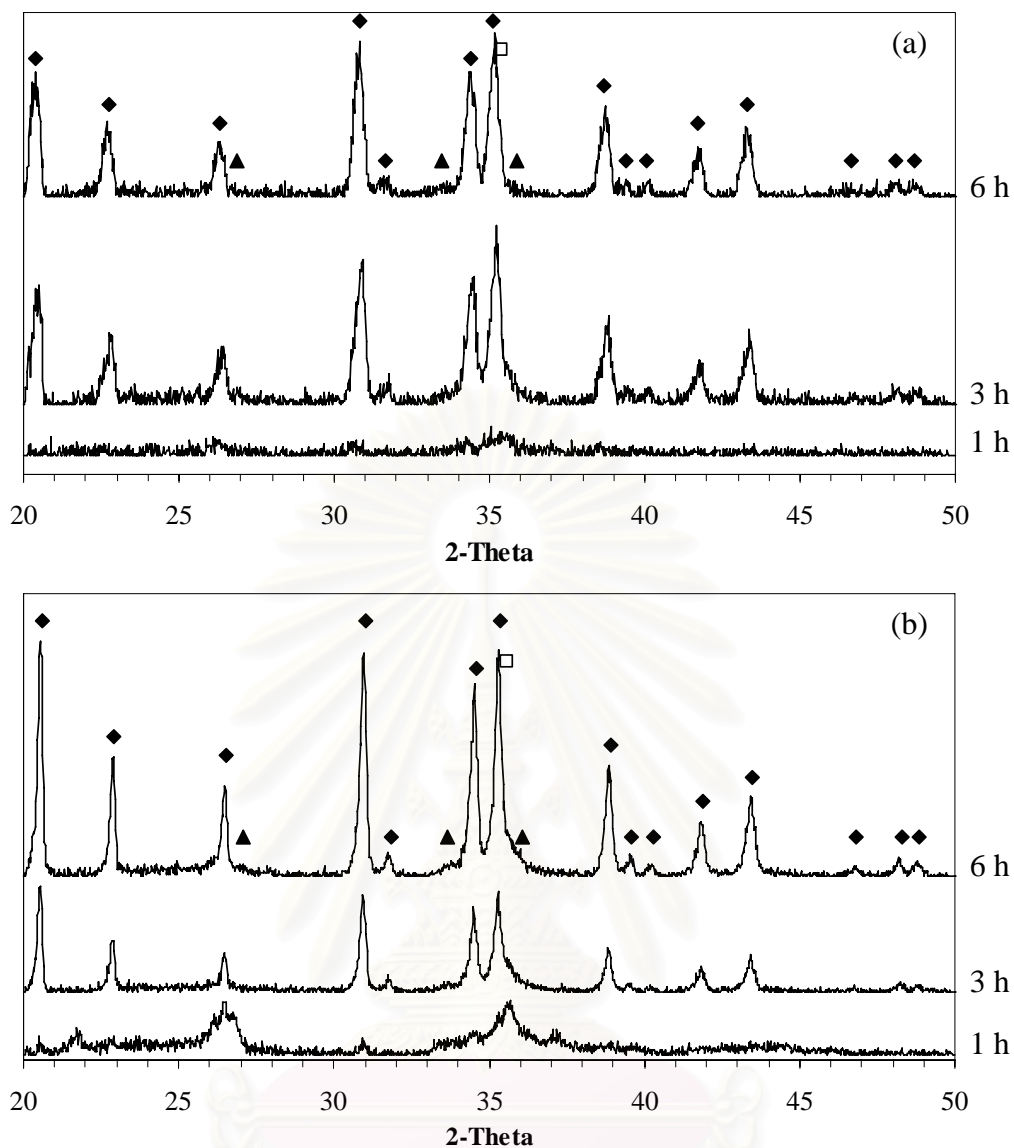
Figure 4.44 XRD patterns of products from the carbothermal reduction and nitridation of RHA impregnated with magnesium under various reaction times: (a) top portion of the product, (b) bottom portion of the product, ◆ α-Si$_3$N$_4$, ▲ β-Si$_3$N$_4$, □ SiC.
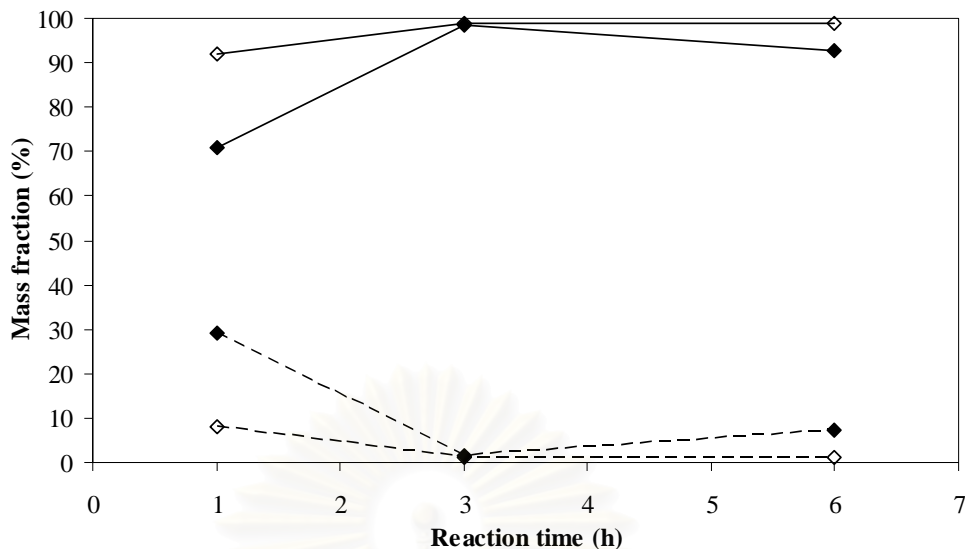
Figure 4.45 Fraction of α- and β-phase in silicon nitride obtained from the
carbothermal reduction and nitridation of RHA impregnated with
magnesium under various reaction times: (◇) top portion of the product;
(◆) bottom portion of the product; (──) fraction of α-phase; (---) fraction
of β-phase.
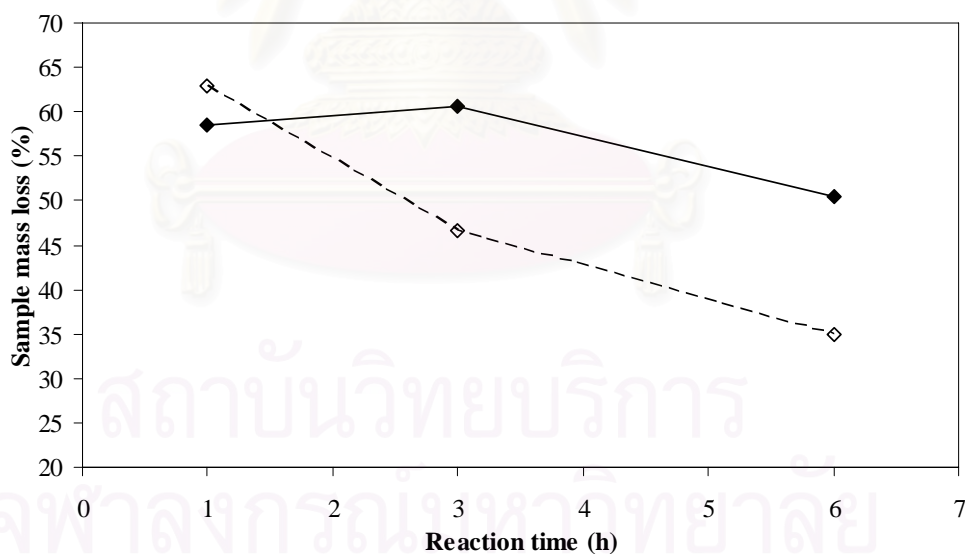
Figure 4.46 Results from TG/DTA analysis of the product from the carbothermal
reduction and nitridation of RHA impregnated with magnesium under
various reaction times: (◇) top portion of the product, (◆) bottom
portion of the product.

4.2.2.4 Copper

The effect of copper on the carbothermal reduction and nitridation of RHA is very similar to that of iron. Results from XRD analysis of the nitrided product of copper impregnated RHA are shown in Figure 4.47. It is indicated that copper promotes silicon nitride formation over silicon carbide, as the reaction time is increased, in the same manner as iron.

Figure 4.48 shows the fraction of α- and β-phase in the sample. It can be observed that the fractions of α-phase is increased when the reaction time is increased. TG/DTA analysis as shown in Figure 4.49 confirms that conversion of silicon nitride increases with reaction time.
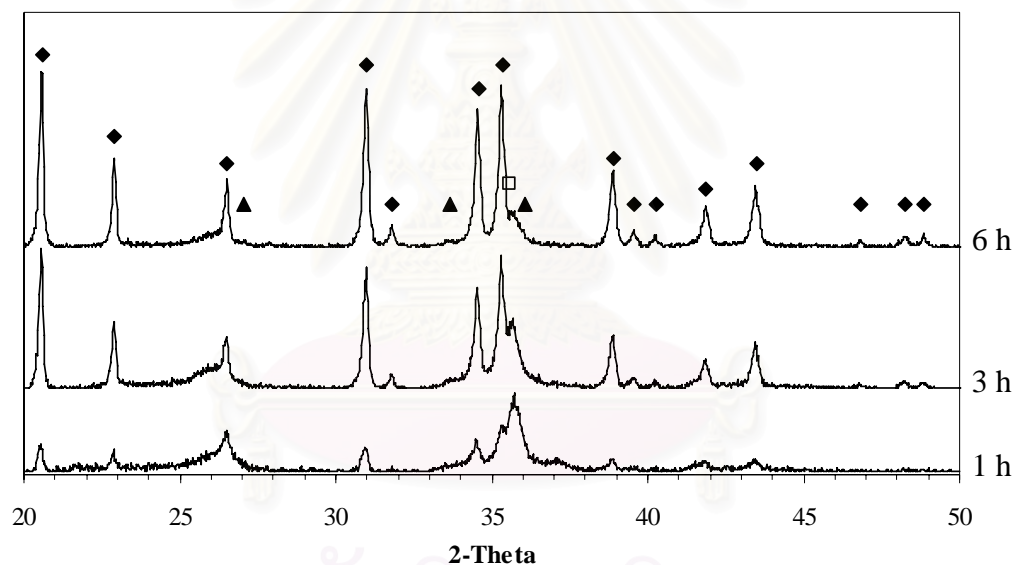
Figure 4.47 XRD patterns of products from the carbothermal reduction and nitridation of RHA impregnated with copper under various reaction times: ◆ α-Si$_3$N$_4$, ▲ β-Si$_3$N$_4$, □ SiC.
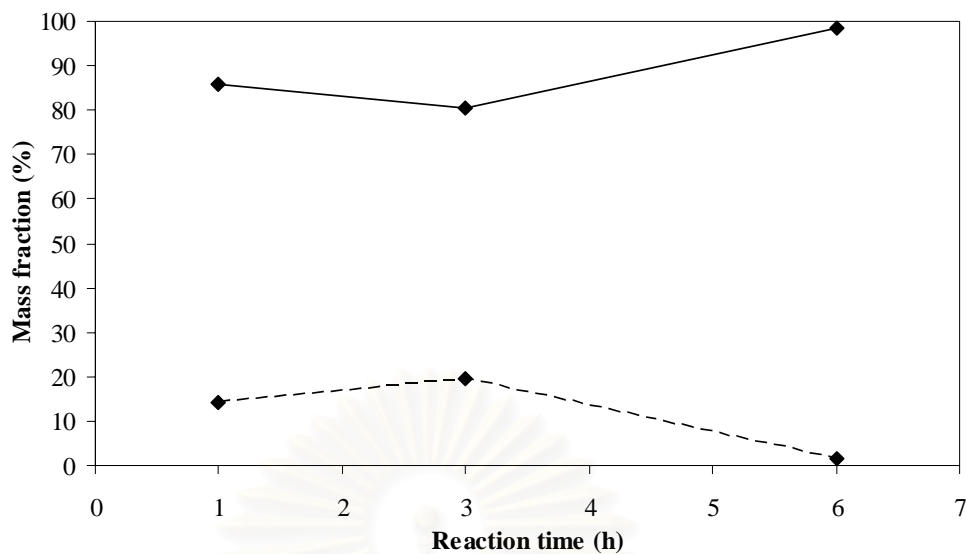
Figure 4.48 Fraction of α- and β-phase in silicon nitride obtained from the
carbothermal reduction and nitridation of RHA impregnated with copper
under various reaction times: (——) α-phase; (---) β-phase.
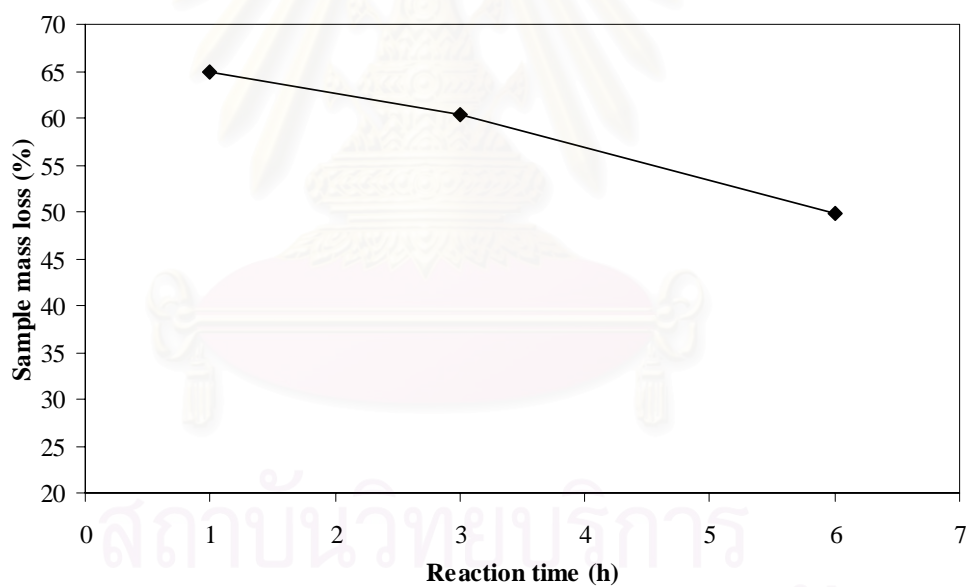
Figure 4.49 Results from TG/DTA analysis of the product from the carbothermal
reduction and nitridation of RHA impregnated with copper under
various reaction times.

4.2.2.5 Yttrium

Figure 4.50 indicates that silicon carbide is not found in the product when reaction time is increased in the same manner as aluminium and magnesium. Both top and bottom portions are α-silicon nitride mixed with β-silicon nitride, as shown in Figure 4.50 (a) and (b), respectively. Fractions of α- and β-phase in silicon nitride product are shown in Figure 4.51. It is observed that silicon nitride products are dominantly α-phase for the whole time. Results from the TG/DTA analysis are shown in Figure 4.52. It shows that carbon remaining in silicon nitride product after 1 h nitridation is higher than those nitrided for 3 and 6 h, respectively. It is confirmed that conversion of silicon nitride increases with reaction time.
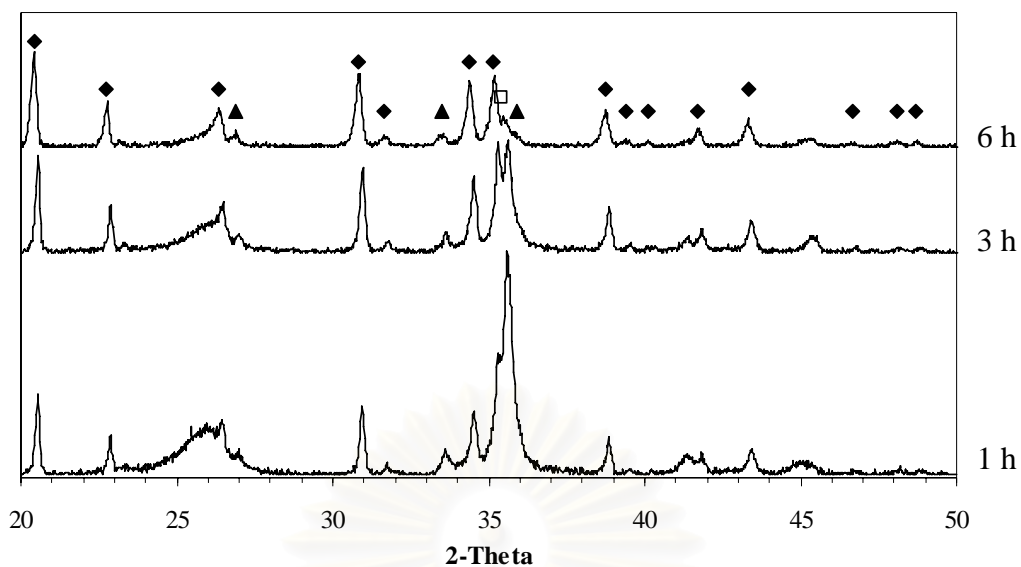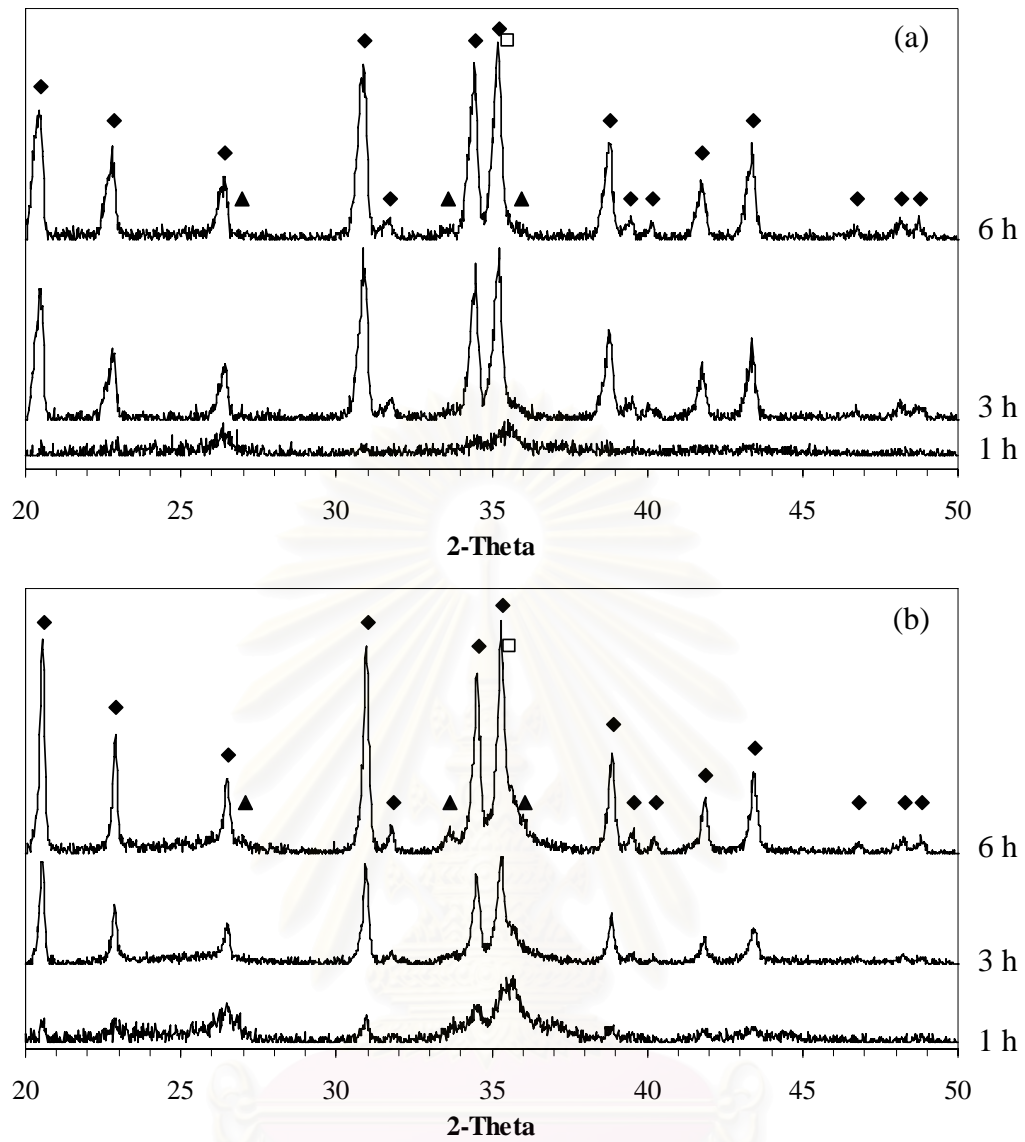
Figure 4.50 XRD patterns of products from the carbothermal reduction and nitridation of RHA impregnated with yttrium under various reaction times: (a) top portion of the product, (b) bottom portion of the product, ◆ α-Si$_3$N$_4$, ▲ β-Si$_3$N$_4$, □ SiC.
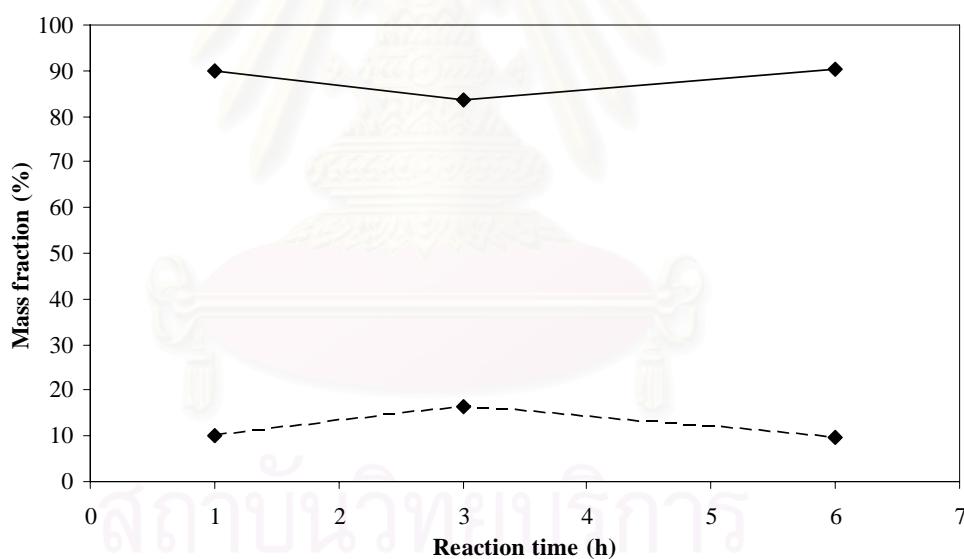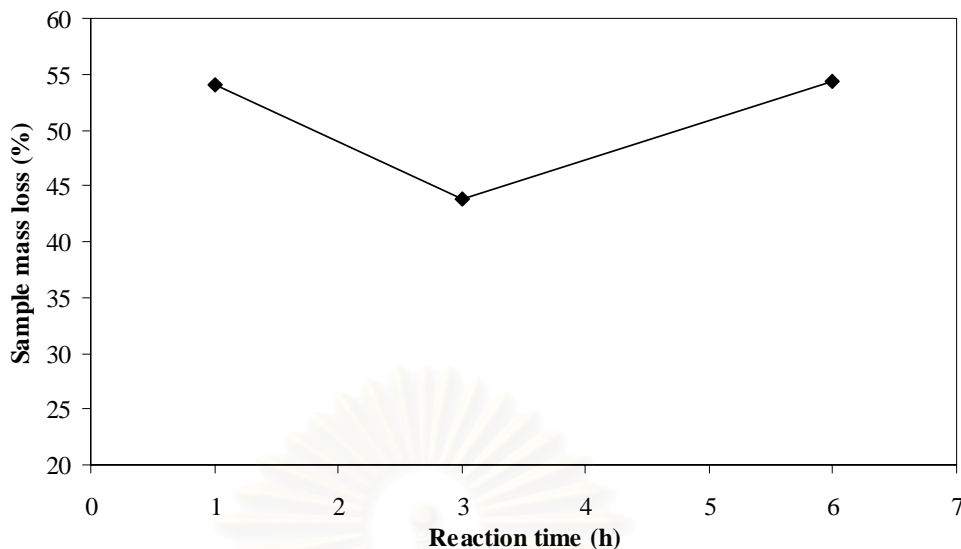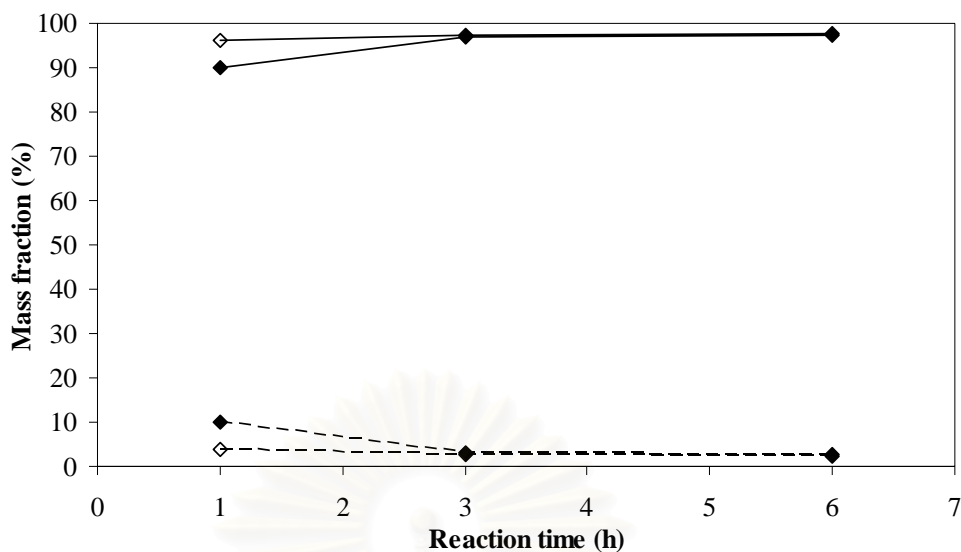
Figure 4.51 Fraction of α- and β-phase in silicon nitride obtained from the
carbothermal reduction and nitridation of RHA impregnated with
yttrium under various reaction times: (◇) top portion of the product;
(◆) bottom portion of the product; (—) fraction of α-phase; (---) fraction
of β-phase.
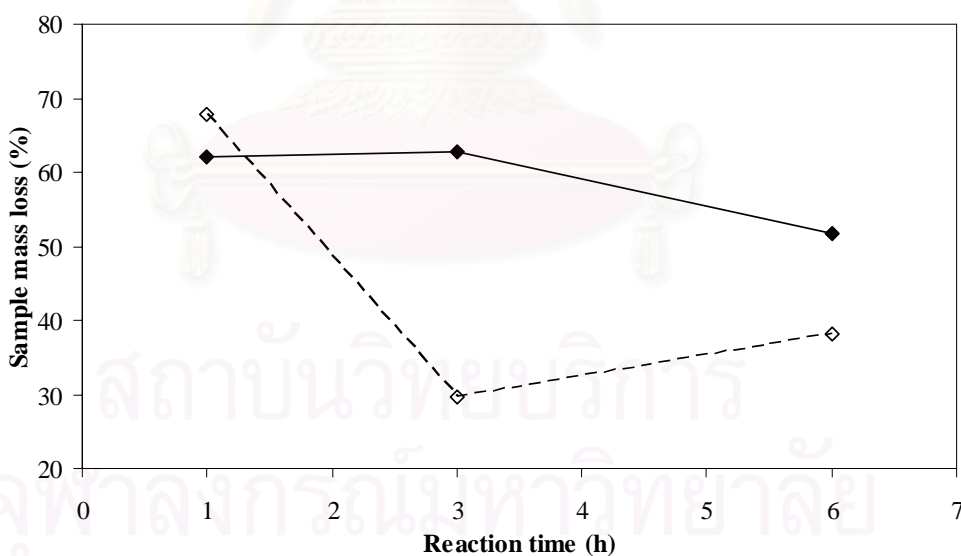
Figure 4.52 Results from TG/DTA analysis of the product from the carbothermal
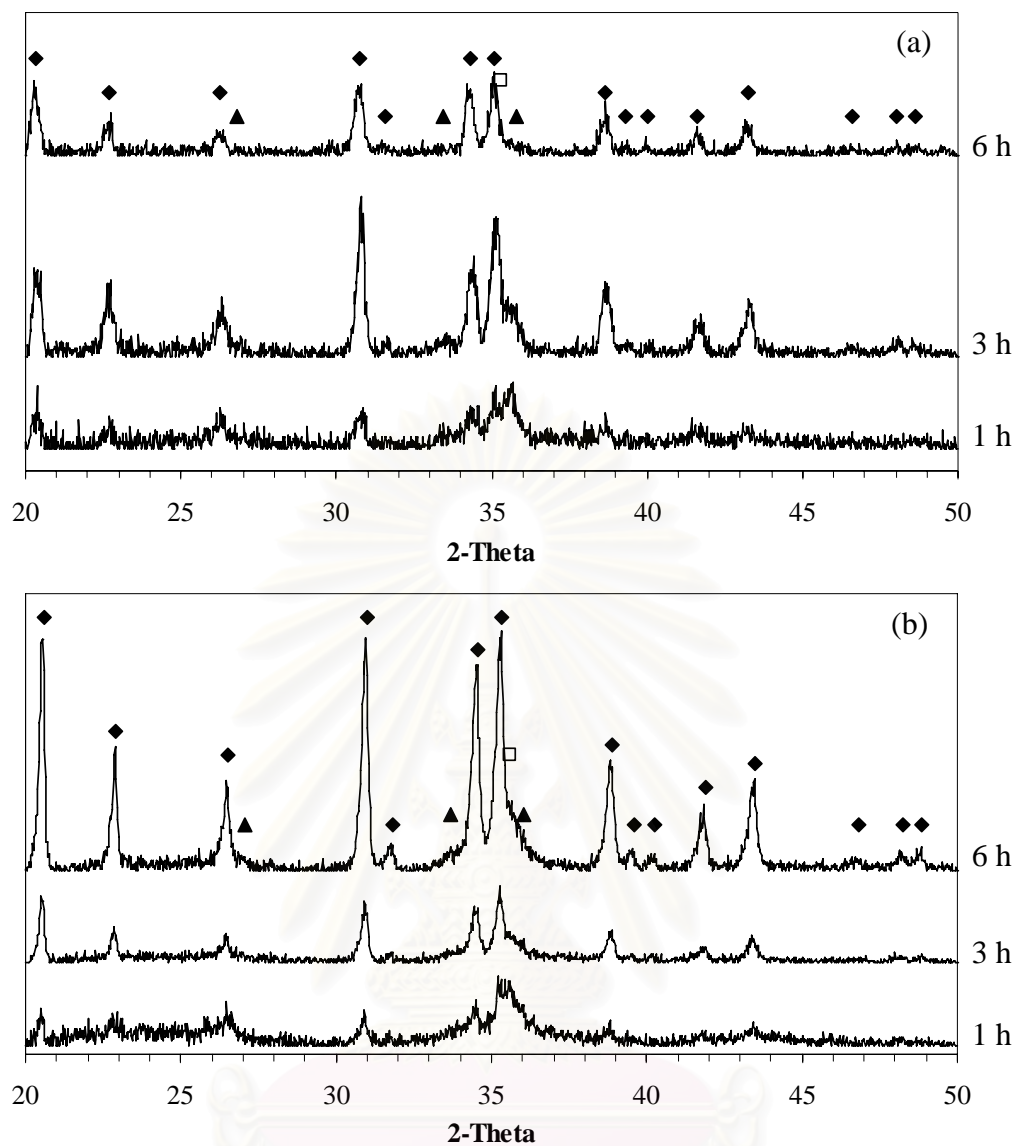reduction and nitridation of RHA impregnated with yttrium under
various reaction times: (◇) top portion of the product, (◆) bottom
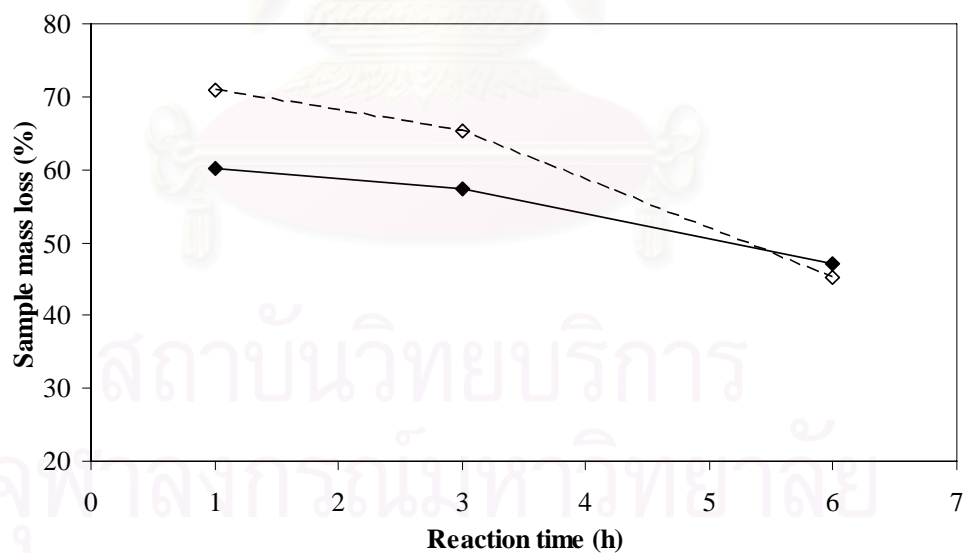portion of the product.

CHAPTER V

CONCLUSION AND RECOMMENDATIONS

5.1 Conclusions

In this work, the catalytic effects of metals in the carbothermal reduction and nitridation of rice husk ash for silicon nitride synthesis were investigated. The results are summarized as the followings.

5.1.1 Effect of Hydrogen Pretreatment

- Hydrogen pretreatment is a crucial factor affecting the product from the carbothermal reduction and nitridation process. Silicon carbide is the major crystalline phase from the reaction of pretreated RHA, while those without pretreatment result in silicon nitride.

- The pretreatment during heating the sample up from room temperature can enhance the conversion of the subsequent carbothermal reduction and nitridation of RHA and also enhance the growth of the fibrous portion of the product.

5.1.2 Effect of Metal

- The crystalline phase of silicon nitride product is significantly influenced by the presence of metal in RHA.

- The fractions of α-phase are generally decreased when metal is added to the RHA. The higher the metal content, the lower the fraction of α-phase in both top and bottom portion of the product.

- Iron and copper promote both β-silicon nitride and silicon carbide formation. The reaction between silica and carbon in RHA is also enhanced by the presence of iron.

     - The fraction of α-phase is decreased with an increase in the amount of aluminium addition. The formation of β-silicon nitride is enhanced in much greater extent than the case of other metals.

     - Magnesium is another metal that promote the β-silicon nitride formation.

     - Yttrium enhances the formation of α-silicon nitride as well as the conversion of the carbothermal reduction and nitridation of RHA.

     - For the carbothermal reduction and nitridation of RHA, silicon carbide is initially formed before converted to silicon nitride.
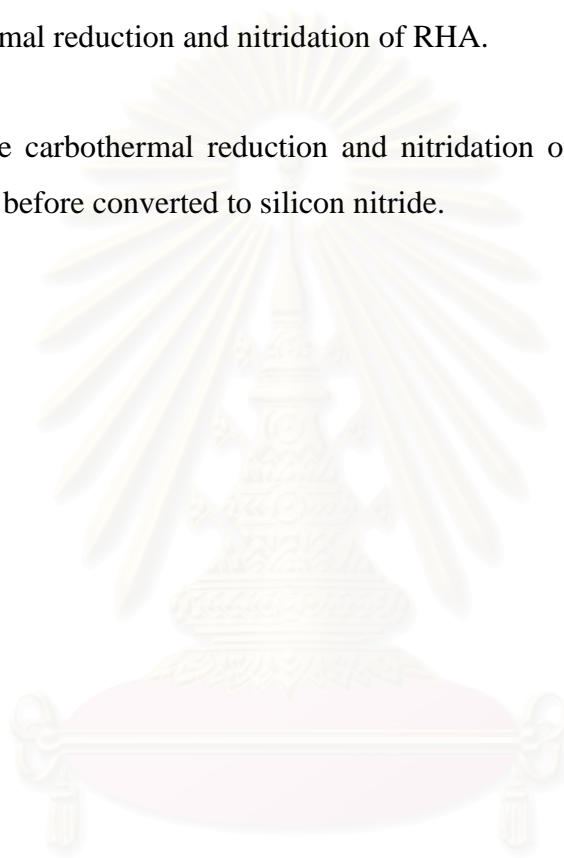
5.2 <u>Recommendations for Future Work</u>

The carbothermal reduction and nitridation of rice husk is an alternative way to produce silicon nitride. There are many critical factors involved in these processes that have not been fully investigated. Some recommendations for future work are listed as follows:

(1) The detailed mechanism for the carbothermal reduction and nitridation of rice husk ash impregnated with metals should be further investigated.

(2) The effect of reaction temperature should be investigated in detail.

(3) Silicon nitride product from each portion should be tested for physical properties.

(4) The kinetics of the carbothermal reduction and nitridation of RHA impregnated with metals should be investigated.

(5) The effects of acid pretreatment of rice husk before metal impregnation should be investigated.

(6) The impregnation of metal into rice husk before pyrolysis should be investigated.

(7) Quantity of carbon monoxide during the reaction of metal-impregnated RHA should be detected by Gas-Chromatography

REFERENCES

Alcala, M. D., J. M. Criado and C. Real (2001). "Influence of the experimental conditions and the grinding of the starting materials on the structure of silicon nitride synthesised by carbothermal reduction." Solid State Ionics **141-142**: 657-661.

Arik, H. (2003). "Systhesis of Si_3N_4 by the carbothermal reduction and nitridation of diatomite." Journal of the European Ceramic Society **23**: 2005-2014.

Atkinson, A., A. J. Moulson and E. W. Roberts (1976). "Nitridation of high-purity silicon." Journal of the American Ceramic Society **59**(7-8): 285-289.

Ault, N. N. and R. L. Yeckley (1994). "Silicon Nitride." American Ceramic Society Bulletin **73**(6): 129-133.

Barsoum, M., P. Kangutkar and M. J. Koczak (1991). "Nitridation Kinetics and Thermodynamics of Silicon Powder Compacts." Journal of the American Ceramic Society **74**(6): 1248-1253.

Bartnitskaya, T. S., P. P. Pikuza, I. I. Timofeeza, E. S. Lugovskaya and T. Y. Kosolapova (1983). "Thermodynamic Calculations for the Assessment of Possible Ways of Formation of Silicon Nitride." Sov. Powder Metallic Meterial **22**: 523.

Bondyopadhyay, S. and J. Mukerji (1991). "Reaction sequences in the synthesis of silicon nitride from quartz." Ceram. ht. **17**: 171-179.

Boyer, S. M. and A. J. Moulson (1978). "A Mechanism for the Nitridation of Fe-Contaminated Silicon." Journal of Materials Science **13**(8): 1637-1646.

Chang Zhang, S. and W. Roger Cannon (1984). Journal of the American Ceramic Society **67**: 691.

Cofer, C. G. and J. A. Lewis (1994). "Chromium Catalysed Silicon Nitridation." Journal of Materials Sciences **29**(22): 5880-5886.

Cutler, I. B. (1974). "Production Silicon Nitride from Rice Hulls." U.S.A.

Datton, V. and J. Drobeck (1986). "Structure and Sodium Migration in Silicon Nitride Films." Journal of the Electrochemical Society **115**: 865-868.

Deckwerth, M. and C. Russel (1994). "A New Polymeric Route to Silicon Carbide and Silicon Nitride using Elementary Silicon as Starting Material." Journal of Materials Sciences **29**(17): 4500-4504.

Della, V. P., I. Kuhn and D. Hotza (2002). "Rice husk ash as an alternate source for active silica production." Materials Letters **57**: 818–821.

Dervišbegovic, H. and F. L. Riley (1981). "The Role of Hydrogen in the Nitridation of Silicon Powder Compacts." Journal of Materials Science **16**: 1945-1955.

Ding, M. (1986). "Rice husk silicon and its applications." Inorganic chemistry industry **24**(6): 36.

Durham, B. G., M. J. Murtha and G. Burnet (1988). "Si_3N_4 by the Carbothermal Ammonolysis of Silica." Journal of American Ceramics Society **3**(1): 45-48.

Durham, S. J. P., K. Shanker and R. Drew (1991). "Carbothermal Synthesis of Silicon Nitride: Effect of Reaction Conditions." Journal of American Ceramics Society **74**(1): 31-37.

Ekelund, M., B. Forslund and T. Johansson (1990). "Si_3N_4 Powder Synthesis by High-Pressure Carbothermic Nitridation of SiO_2: Conversion as Function of Gas Flow Rate and Pressure." In Ceramic Powder Science III: 337-345.

Fang, M., L. Yang, G. Chen, Z. Shi, Z. Luo and K. Cen (2004). "Experimental Study on Rice Husk Combustion in a Circulating Fluidized Bed." Fuel Processing Technology **85**: 1273-1282.

Hanna, S. B., N. A. L. Mansour, A. S. Taha and H. M. A. Abd-Allah (1985). "Silicon Carbide and Nitride from Rice Hulls-III. Formation of Silicon Niride." British Ceramic Transactions Journal **84**(1): 18.

Houston, D. F. (1972). "Rice: Chemistry and technology." American Association of Cereal Chemists, Inc.:St Paul,MN.

James, J. and M. S. Rao (1986). "Silica from Rice Husk through Thermal Decomposition." Thermochimica Acta **97**: 329-336.

Jennings, H. M. (1983). "Review on Reactions between Silicon and Nitrogen : Part 1 Mechanisms." Journal of Materials Science **18**: 951-967.

Kawai, C. and A. Yamakawa (1998). "Crystal Growth of Silicon Nitride Whiskers Through a VLS Mechanism Using SiO_2-Al_2O_3-Y_2O_3 Oxides as Liquid Phase." Ceramic international **24**: 136-138.

Krishnarao, R. V. and M. M. Godkhindi (1992). "Distribution of silica in rice husk and its effect on the formation of silicon carbide." Ceramic international **18**: 243.

Kuskonmaz, N., A. Sayginer, C. Toy, E. Acma, O. Addemir and A. Tekin (1996). "Studies on Formation of Silicon Nitride and Silicon Carbide from Rice Husk." High Temperature Materials and processes **15**(1-2): 123-127.

Lange, F. F. (1979). "Fracture Toughness of silicon nitirde as a Function of the Initial a-Phase Content." Journal of the American Ceramic Society **62**(7-8): 428-430.

Lencart-silva, F. and J. M. Vieira (1999). "Carbothermal Reduction and Nitridation of silica: Nuclei Planar Growth Controlled by Silicon Monoxide Diffusion on the Reducer Surface." Journal of Materials Processing Technology **92-93**: 112-117.

Li, Y., L. Q. Liu and S. X. Dou (1991). "Kinetic of Si_3N_4 formation from rice hull." Journal Inorganic Material **6**(1): 45.

Lin, S.-S. (1977). "Comparative Studies of Metal Additives on the Nitridation of Silicon." Journal of the American Ceramic Society **60**(1-2): 78-81.

Liou, T.-H. (2004). "Evolution of chemistry and morphology during the carbonization and combustion of rice husk." Carbon **42**: 785-794.

Liou, T.-H. and F. W. Chang (1996). "The Nitridation Kinetics of Pyrolyzed Rice Husk." Ind. Eng. Chem. Res. **35**: 3375.

Mehta, P. K. (1996). International Congress on High-Performance Concreate and Performance and Quanlity of Concreate Structure, **Brazil**.

Mileweski, J. V., F. D. Gac, J. J. Petroiic and S. R. Skaggs (1985). "Growth of beta-silicon nitride whiskers by the VLS process." Journal of Materials Science **20**: 1160-1166.

Mitomo, M. (1977). "Effect of Fe and Al Additions on Nitridation of Silicon." Journal of Materials Science **12**(2): 273-276.

Mizuhara, Y., M. Noguchi, T. Ishihara and Y. Takita (1995). "Preparation of Silicon Nitride Whiskers from Diatomaceous Earth: I Reaction Conditions." Journal of American Ceramics Society **78**(1): 109-113.

Mukerji, J. and S. K. Biswas (1981). "Effect of Iron, Titanium, and Hafnium on Second-Stage Nitriding of Silicon." Journal of the American Ceramic Society **64**(9): 549-552.

Parr, N. L., R. Sands, P. L. Pratt, E. R. W. May, R. R. Shakespeare and D. S. Thompson (1961). "Structural Aspects of Silicon Nitride." Powder Metallurgy **8**: 152-163.

Pavarajarn, V. and S. Kimura (2001). "Catalytic Effects on Metals on Direct Nitridation of Silicon." Journal of the American Ceramic Society **84**(8): 1669.

Pavarajarn, V., R. Prechayutasin and P. Praserthdam (2005). "Silicon Nitride Synthesis via the Carbothermal Reduction and Nitridation of Rice Husk Ash."

Pigeon, R. G. and A. Varma (1993). "Quantitative Kinetic Analysis of Silicon Nitridation." Journal of Materials Science **28**: 2999-3013.

Pigeon, R. G., A. Varma and A. E. Miller (1993). "Some Factors Influencing the Formation of Reaction-Bonded Silicon Nitride." Journal of Materials Science **28**(7): 1919-1936.

Rahman, I. A. and F. L. Riley (1989). "The Control of Morphology in Silicon Nitirde Powder Prepared from Rice Husk." Journal of the European Ceramic Society **5**: 11-22.

Rahaman, M. N. and A. J. Moulson (1984). "The removal of Surface Silica and Its Effect on the Nitridation of High-Purity Silicon." Journal of Materials Science **19**: 189-194.

Real, C., M. D. Alcala and J. M. Criado (1996). "Preparation of Silica from Rice Husk." Journal of the Ceramic Society **79**: 2012-2016.

Real, C., M. D. Alcala and J. M. Criado (2004). "Synthesis of Silicon Nitride from Carbothermal Reduction of Rice Husks by the Constant-Rate-Thermal-Analysis (CRTA) Method." Journal of the American Ceramic Socity **87**(1): 75-78.

Riley, F. L. (2000). "Silicon Nitride and Related Materials." Journal of the American Ceramic Society **83**(2): 245-265.

Ruddlesden, S. N. and P. Popper (1958). "On the Crystal Structure of the Nitrides of Silicon and Germanium." Acta Crystallographica **11**(7): 465-468.

Segal, D. L. (1986). "A Review of Preparative Routes to Silicon Nitride Powders." British Ceramic Transaction **85**: 184.

Sharma, N. K., W. S. Williams and A. Zangvil (1984). "Formation and Structure of Silicon Carbide Whiskers frome Rice Hulls." Journal of the American Ceramic Socity **67**: 715.

Shimada, S. and T. Kataoka (2001). "Separate Growth of α- and β-Si_3N_4 Whiskers on or near a Carbon Substrate by Carbothermal Reduction." Journal of the American Ceramic Socity **84**(10): 2442-2444.

Siddiqi, S. A. and A. Hendry (1985). "The Influence of Iron on the Preparation of Silicon Nitride from Silica." Journal of Materials Science **20**: 3230.

Sugahara, Y., H. Hiraiwa, K. Kuroda and C. Kato (1988). "Nitride formation by the carbothermal reduction of a zeolite-polyacrylonitrile inclusion compound" Journal of Materials Science **23**: 3181.

Thomson, D. S. and P. L. Pratt (1967). "The Structure of Silicon Nitride." Science of Ceramics **3**: 35-51.

Tsuruto, H., M. Masuda, T. Soma and M. Matsui (1990). "Foreign Object Damage Resistance of Silicon Nitride and Silicon Carbide." Journal of the American Ceramics Society **73**(6): 1714-1718.

Turkdogan, E. T., P. M. Bills and V.A.Tippett (1958). "Silicon Nitrides: Some Physico-Chemical Properties." Journal of Apply Chemistry **8**: 296-302.

van Dijen, F. K. and E. Mayer (1996). "Liquid Phase Sintering of Silicon Carbide." Journal of the European Ceramic Society **16**: 413-420.

Wang, H. and Y. N. Dai (1996). "The charactor of reaction kinetics for producing ultrafine Si_3N_4 powder with rice husks." Refractories **30**(2): 77.

Weimer, A. W., G. A. Eisman, D. W. Susnitzky, D. R. Beaman and J. W. Mccoy (1997). "Mechanism and Kinetics of the Carbothermal Nitridation of a-Silicon Nitride." Journal of the American Ceramic Society **80**(11): 2853-2863.

Yalcin, N. and V. Sevinc (2001). "Studies on silica obtained from rice husk." Ceramics International **27**: 219-224.

Yamada, T. (1993). "Preparation and Evaluation of Sinterable Silicon Nitride Powder by Imide Decomposition Method." American Ceramic Society Bulletin **72**(5): 99-106.

Yamaguchi, A. (1986). "Effect of Oxygen and Nitrogen Partial Pressures on the Stability of Metals, Carbides, Nitrides, and Oxides in Refractories which Contain Carbon." Refractories **38**(4): 2-11.

Zhang, S. C. and W. R. Cannon (1985). "Preparation of silicon nitride from silica." J. American Ceramic Society **67**(10): 691-695.

Ziegler, G., J. Heinrich and G. Wotting (1987). "Relationships between processing, microstructure and properties of dense and reaction-bonded silicon nitride." Journal of Materials Science **22**: 3041.

APPENDICES

APPENDIX A

TEMPERATURE PROGRAMMED REDUCTION ANALYSIS OF
METAL-IMPREGNATED RICE HUSK ASH
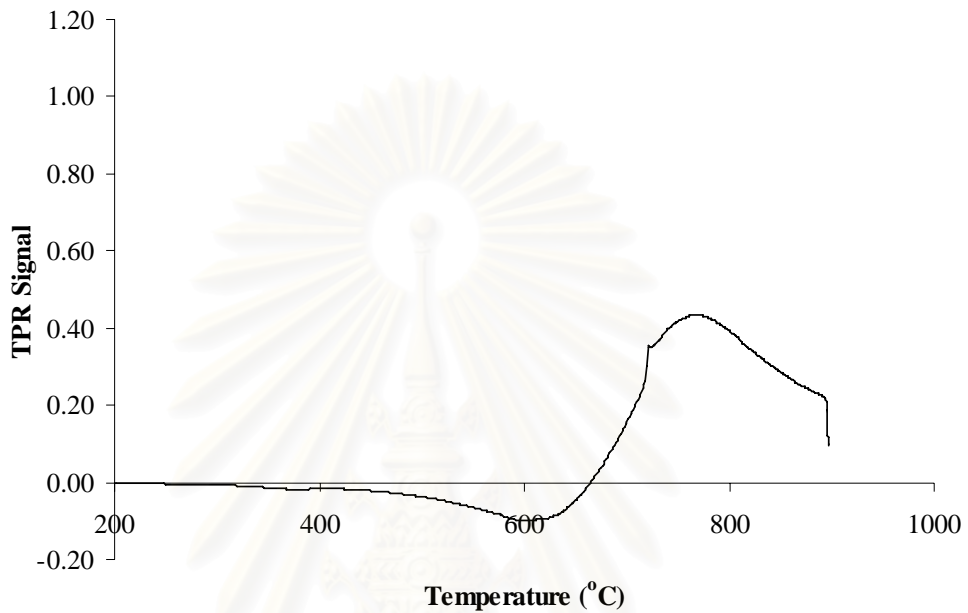
Figure A1 TPR of 0.5% iron impregnated RHA before nitridation.
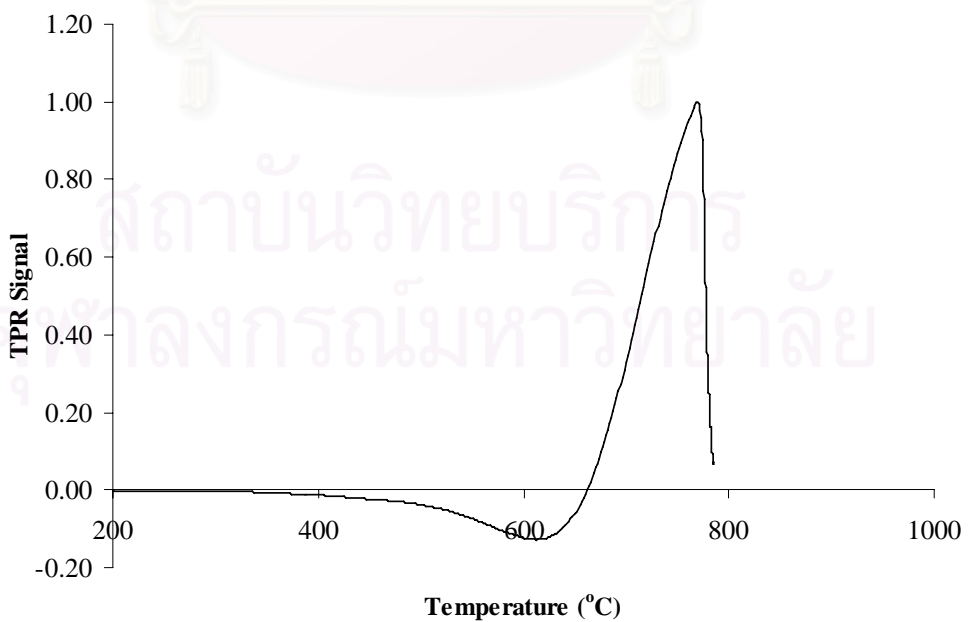
Figure A2 TPR of 0.5% aluminium impregnated RHA before nitridation.
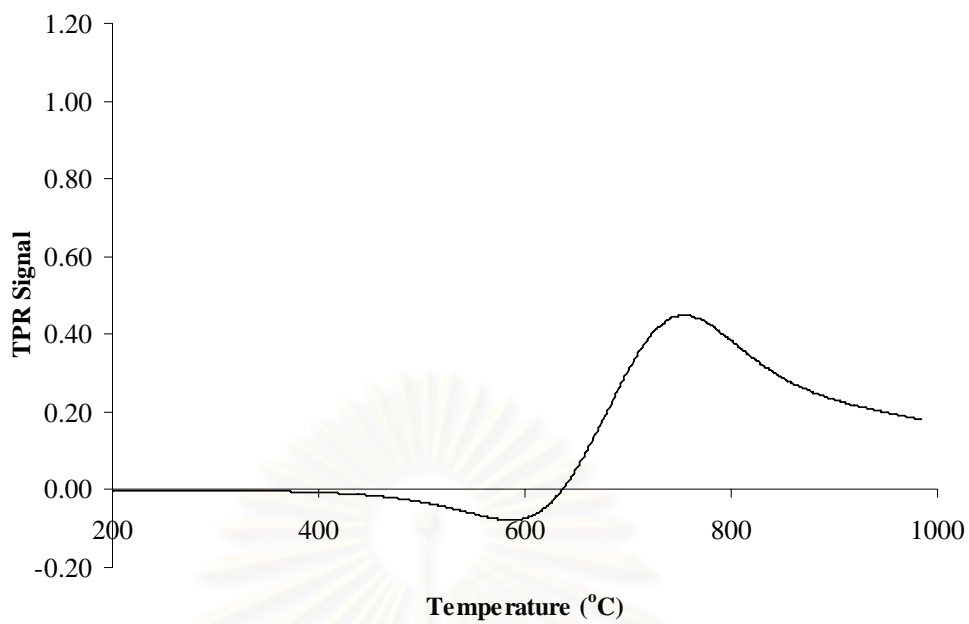
Figure A3 TPR of 0.5% magnesium impregnated RHA before nitridation.
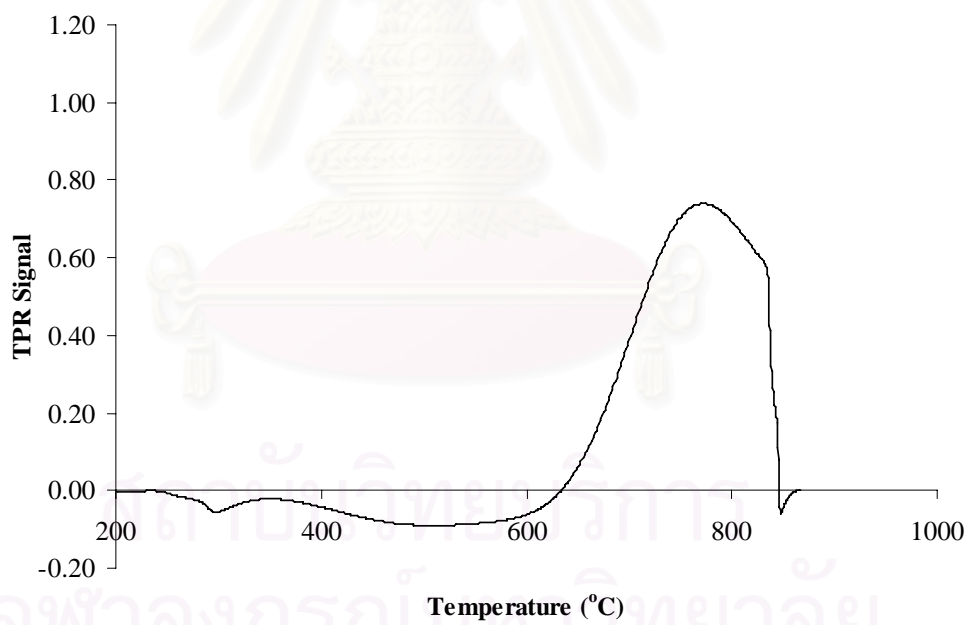
Figure A4 TPR of 0.5% copper impregnated RHA before nitridation.
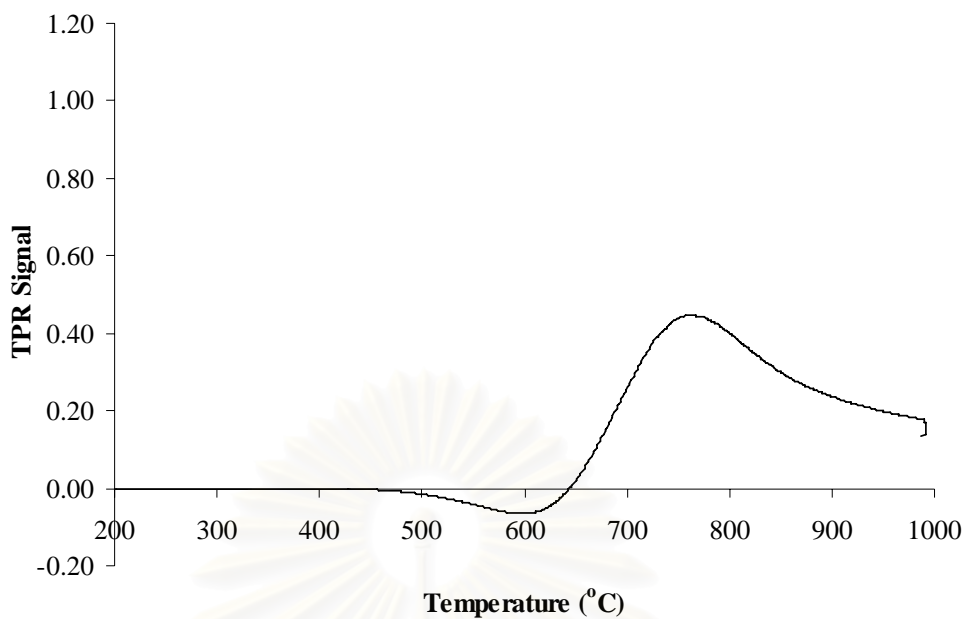
Figure A5 TPR of 0.5% yttrium impregnated RHA before nitridation.

APPENDIX B

ELEMENTAL ANALYSIS BY X-RAY PHOTOELECTRON SPECTROSCOPY

Table B1 XPS analysis of metal-impregnated RHA.

Element	Position BE (eV)	FWHM (eV)	Raw Area (CPS)	Atomic Mass	Mass Conc%
bare RHA					
O 1s	535.577	2.87	31078.7	15.999	25.48
N 1s	394.637	1.68	1936	14.007	2.24
C 1s	288.902	3.142	32596.1	12.011	57.18
Si 2p	99.712	2.503	3201.6	28.086	15.1
0.5% iron					
Fe 2p	725.855	3.376	17064.3	55.846	8.58
O 1s	530.582	1.644	39343.8	15.999	31.75
C 1s	287.208	4.694	27620.4	12.011	47.69
Si 2p	103.9	2.705	2581.3	28.086	11.98
0.5% Aluminium					
O 1s	532.744	2.865	35024.6	15.999	29.14
C 1s	285.733	4.22	29828	12.011	53.1
Si 2p	103.239	2.63	2470.6	28.086	11.82
Al 2p	74.817	2.844	847.3	26.982	5.94
0.5% Magnesium					
O 1s	532.803	3.034	38488.9	15.999	30.42
C 1s	286.714	4.499	29005.3	12.011	49.06
Si 2p	103.444	2.917	2993.9	28.086	13.61
Mg 2p	55.687	3.783	726.6	24.312	6.91
0.5% Copper					
Cu 2p	936.741	7.201	5315.4	63.549	2.06
O 1s	530.366	1.363	32452.1	15.999	26.69
C 1s	286.85	4.33	31970.3	12.011	56.26
Si 2p	103.638	3.278	3168.6	28.086	14.99
0.5% Yttrium					
O 1s	532.769	2.966	35378.1	15.999	25.94
Y 3s	395.929	3.072	1598	88.906	11.52
C 1s	286.822	4.395	32648.5	12.011	51.21
Si 2p	103.405	2.895	2686.7	28.086	11.33

Table B2 XPS analysis of silicon nitride product from RHA impregnated with iron at different contents:

Element	Position BE (eV)	FWHM (eV)	Raw Area (CPS)	Atomic Mass	Mass Conc%
0.5% iron					
Fe 2p	710.889	2.076	5812	55.846	4.82
O 1s	537.964	2.802	20864.6	15.999	27.81
N 1s	402.938	1.771	9069.2	14.007	17.04
Si 2p	98.652	1.759	6567.1	28.086	50.33
1.0% iron					
Fe 2p	707.26	1.164	11726.4	55.846	10.67
O 1s	529.967	1.071	22902	15.999	33.46
N 1s	397.717	2.691	6539.6	14.007	13.47
Si 2p	103.984	0.943	5045.1	28.086	42.39
3.0% iron					
Fe 2p	713.477	3.076	4133.9	55.846	4.02
O 1s	529.897	1.101	23777.7	15.999	37.13
N 1s	399.833	1.005	3567.5	14.007	7.85
Si 2p	106.4	0.638	5677.7	28.086	50.99

สถาบันวิทยบริการ
จุฬาลงกรณ์มหาวิทยาลัย

Table B3 XPS analysis of silicon nitride product from 0.5% iron impregnated RHA at different reaction times:

Element	Position BE (eV)	FWHM (eV)	Raw Area (CPS)	Atomic Mass	Mass Conc%
1 h					
Fe 2p	706.679	1.769	3256.2	55.846	2.85
O 1s	535.189	2.768	21930.4	15.999	30.82
N 1s	403.657	2.715	6220.8	14.007	12.32
Si 2p	103.742	2.438	6683.5	28.086	54.01
3 h					
Fe 2p	710.524	3.056	3295.6	55.846	2.62
O 1s	532.496	0.879	21930.3	15.999	28.01
N 1s	395.956	2.098	6749.6	14.007	12.15
Si 2p	103.266	1.083	7789.7	28.086	57.22
6 h					
Fe 2p	710.889	2.076	5812	55.846	4.82
O 1s	537.964	2.802	20864.6	15.999	27.81
N 1s	402.938	1.771	9069.2	14.007	17.04
Si 2p	98.652	1.759	6567.1	28.086	50.33

Table B4 XPS analysis of silicon nitride product from RHA impregnated with aluminium at different contents:

Element	Position BE (eV)	FWHM (eV)	Raw Area (CPS)	Atomic Mass	Mass Conc%
0.5% aluminium, top portion					
O 1s	530.479	1.157	36533.2	15.999	28.92
N 1s	402.045	2.107	16258	14.007	18.14
Si 2p	104.983	2.04	10711.4	28.086	48.77
Al 2p	78.299	2.17	623.5	26.982	4.16
0.5% aluminium, bottom portion					
O 1s	535.941	4.16	22008.1	15.999	31.6
N 1s	394.848	1.386	6045.3	14.007	12.24
Si 2p	106.546	2.245	5699.4	28.086	47.06
Al 2p	77.941	2.44	751.7	26.982	9.1
1.0% aluminium, top portion					
O 1s	537.394	3.206	34578.6	15.999	28.11
N 1s	396.569	1.879	14090.4	14.007	16.15
Si 2p	105.834	2.711	10552.7	28.086	49.33
Al 2p	72.477	0.427	935.9	26.982	6.42
1.0% aluminium, bottom portion					
O 1s	535.902	3.982	30061.8	15.999	31.7
N 1s	401.684	2.403	7768.3	14.007	11.55
Si 2p	107.914	1.453	7903.2	28.086	47.93
Al 2p	77.032	2.212	991.2	26.982	8.81
3.0% aluminium, top portion					
O 1s	537.04	3.221	40253.7	15.999	32.41
N 1s	401.982	2.55	12312.3	14.007	13.97
Si 2p	104.652	2.545	8559.2	28.086	39.62
Al 2p	79.088	1.286	2062	26.982	14
3.0% aluminium, bottom portion					
O 1s	536.167	2.771	36495.6	15.999	30.97
N 1s	401.062	1.811	9648.5	14.007	11.54
Si 2p	103.992	2.412	8568.4	28.086	41.81
Al 2p	78.739	1.059	2191.8	26.982	15.68

Table B5 XPS analysis of silicon nitride product from 0.5% aluminium impregnated
RHA at different reaction times:

Element	Position BE (eV)	FWHM (eV)	Raw Area (CPS)	Atomic Mass	Mass Conc%
1 h, top portion					
O 1s	530.377	1.536	38728.8	15.999	35.02
N 1s	403.353	0.968	10101.4	14.007	12.87
Si 2p	101.707	1.111	9072.3	28.086	47.17
Al 2p	75.159	6.372	648.4	26.982	4.94
1 h, bottom portion					
O 1s	537.417	3.26	19818.8	15.999	32.65
N 1s	395.196	1.25	6287.1	14.007	14.6
Si 2p	101.662	0.914	5075.4	28.086	48.09
Al 2p	74.661	4.028	335.4	26.982	4.66
3 h, top portion					
O 1s	530.201	1.716	38640	15.999	28.28
N 1s	402.385	1.652	16752.4	14.007	17.28
Si 2p	106.575	1.383	11655.8	28.086	49.05
Al 2p	75.302	2.339	872.5	26.982	5.38
3 h, bottom portion					
O 1s	528.251	2.311	22923	15.999	34.19
N 1s	403.028	1.287	5783.9	14.007	12.16
Si 2p	101.109	0.746	5423	28.086	46.51
Al 2p	74.519	4.039	568.4	26.982	7.15
6 h, top portion					
O 1s	530.479	1.157	36533.2	15.999	28.92
N 1s	402.045	2.107	16258	14.007	18.14
Si 2p	104.983	2.04	10711.4	28.086	48.77
Al 2p	78.299	2.17	623.5	26.982	4.16
6 h, bottom portion					
O 1s	535.941	4.16	22008.1	15.999	31.6
N 1s	394.848	1.386	6045.3	14.007	12.24
Si 2p	106.546	2.245	5699.4	28.086	47.06
Al 2p	77.941	2.44	751.7	26.982	9.1

Table B6 XPS analysis of silicon nitride product from RHA impregnated with
magnesium at different contents:

Element	Position BE (eV)	FWHM (eV)	Raw Area (CPS)	Atomic Mass	Mass Conc%
0.5% magnesium, top portion					
O 1s	530.655	2.678	35168.4	15.999	27.57
N 1s	399.141	2.097	14892.6	14.007	16.46
Si 2p	105.858	1.937	10010.9	28.086	45.13
Mg 2p	55.931	3.866	1149.7	24.312	10.84
0.5% magnesium, bottom portion					
O 1s	529.839	1.311	20417.8	15.999	30.64
N 1s	399.7	1.134	4705	14.007	9.95
Si 2p	106.759	1.618	5092	28.086	43.94
Mg 2p	54.941	7.159	856.8	24.312	15.47
1.0% magnesium, top portion					
O 1s	531.968	0.88	36781.9	15.999	29.92
N 1s	397.571	2.642	8660.9	14.007	9.93
Si 2p	99.973	2.19	6360.7	28.086	29.76
Mg 2p	56.717	2.928	3104.5	24.312	30.38
1.0% magnesium, bottom portion					
O 1s	530.025	1.385	21056.7	15.999	28.39
N 1s	402.788	1.349	6768.6	14.007	12.86
Si 2p	103.714	0.959	5123.8	28.086	39.72
Mg 2p	57.137	2.825	1173.2	24.312	19.03
3.0% magnesium, top portion					
O 1s	529.919	1.083	22664.7	15.999	28.4
N 1s	396.592	1.625	7334.1	14.007	12.95
Si 2p	100.885	1.156	5799.6	28.086	41.79
Mg 2p	55.785	4.584	1118.4	24.312	16.86
3.0% magnesium, bottom portion					
O 1s	537.08	3.942	21697.1	15.999	29.27
N 1s	401.782	1.254	6700.7	14.007	12.74
Si 2p	102.419	3.2	5002.6	28.086	38.8
Mg 2p	52.742	2.504	1182.8	24.312	19.19

Table B7 XPS analysis of silicon nitride product from 0.5% magnesium impregnated RHA at different reaction times:

Element	Position BE (eV)	FWHM (eV)	Raw Area (CPS)	Atomic Mass	Mass Conc%
1 h, top portion					
O 1s	530.045	1.512	39587.8	15.999	34.51
N 1s	403.835	3.889	8800.2	14.007	10.81
Si 2p	101.551	0.984	8587.3	28.086	43.05
Mg 2p	54.668	5.255	1109.2	24.312	11.63
1 h, bottom portion					
O 1s	532.422	0.92	18781.7	15.999	30.61
N 1s	402.442	1.478	4938.1	14.007	11.34
Si 2p	106.121	2.952	4689.8	28.086	43.95
Mg 2p	53.897	7.647	718.6	24.312	14.09
3 h, top portion					
O 1s	530.164	1.717	28265.3	15.999	31.5
N 1s	395.611	1.881	8493.2	14.007	13.34
Si 2p	101.348	1.107	6799.4	28.086	43.58
Mg 2p	54.43	4.836	863.4	24.312	11.58
3 h, bottom portion					
O 1s	536.311	3.064	20988.3	15.999	31.68
N 1s	402.292	0.806	4017.2	14.007	8.55
Si 2p	103.222	1.004	4356.3	28.086	37.81
Mg 2p	54.388	5.551	1210.2	24.312	21.97
6 h, top portion					
O 1s	530.655	2.678	35168.4	15.999	27.57
N 1s	399.141	2.097	14892.6	14.007	16.46
Si 2p	105.858	1.937	10010.9	28.086	45.13
Mg 2p	55.931	3.866	1149.7	24.312	10.84
6 h, bottom portion					
O 1s	529.839	1.311	20417.8	15.999	30.64
N 1s	399.7	1.134	4705	14.007	9.95
Si 2p	106.759	1.618	5092	28.086	43.94
Mg 2p	54.941	7.159	856.8	24.312	15.47

Table B8 XPS analysis of silicon nitride product from RHA impregnated with
copper at different contents:

Element	Position BE (eV)	FWHM (eV)	Raw Area (CPS)	Atomic Mass	Mass Conc%
0.5% Copper					
Cu 2p	931.788	1.49	4509.9	63.549	2.27
O 1s	538.649	2.319	26854.2	15.999	28.73
N 1s	402.971	2.853	12339.2	14.007	18.61
Si 2p	101.325	1.595	8188.9	28.086	50.39
1.0% Copper					
Cu 2p	933.618	2.019	3055.2	63.549	1.95
O 1s	529.917	1.087	24198.7	15.999	32.86
N 1s	402.705	0.832	6355	14.007	12.17
Si 2p	98.985	0.991	6789.1	28.086	53.02
3.0% Copper					
Cu 2p	939.3	5.666	1803.7	63.549	1.48
O 1s	536.119	3.735	23527.8	15.999	41.11
N 1s	397.898	0.839	3814.4	14.007	9.4
Si 2p	101.333	0.808	4777.2	28.086	48.01

Table B9 XPS analysis of silicon nitride product from 0.5% copper impregnated
RHA at different reaction times:

Element	Position BE (eV)	FWHM (eV)	Raw Area (CPS)	Atomic Mass	Mass Conc%
1 h					
Cu 2p	934.409	1.544	3098.6	63.549	1.94
O 1s	532.723	0.969	23549	15.999	31.34
N 1s	400.488	0.833	8363.1	14.007	15.69
Si 2p	99.009	1.095	6666.5	28.086	51.02
3 h					
Cu 2p	938.354	6.654	2590.8	63.549	1.65
O 1s	535.457	3.094	21736	15.999	29.49
N 1s	397.15	2.42	8029.8	14.007	15.36
Si 2p	100.836	1.238	6855.7	28.086	53.49
6 h					
Cu 2p	931.788	1.49	4509.9	63.549	2.27
O 1s	538.649	2.319	26854.2	15.999	28.73
N 1s	402.971	2.853	12339.2	14.007	18.61
Si 2p	101.325	1.595	8188.9	28.086	50.39

Table B10 XPS analysis of silicon nitride product from RHA impregnated with
yttrium at different contents:

Element	Position BE (eV)	FWHM (eV)	Raw Area (CPS)	Atomic Mass	Mass Conc%
0.5% yttrium, top portion					
O 1s	537.797	2.495	43159.2	15.999	13.88
N 1s	401.8	1.641	17851.3	14.007	8.09
Y 3s	396.914	1.654	17948.7	88.906	56.77
Si 2p	105.409	1.993	11500.4	28.086	21.26
0.5% yttrium, bottom portion					
O 1s	535.341	1.586	25169.8	15.999	20.2
N 1s	401.319	0.597	5359.4	14.007	6.06
Y 3s	397.623	0.481	4910.6	88.906	38.77
Si 2p	106.082	2.492	7574.2	28.086	34.96
3.0% yttrium, top portion					
O 1s	534.478	1.659	34746.5	15.999	18.29
N 1s	402.632	2.281	10692.9	14.007	7.93
Y 3s	402.1	1.581	10213.9	88.906	52.87
Si 2p	101.405	1.249	6909.4	28.086	20.91
3.0% yttrium, bottom portion					
O 1s	530.405	1.569	25684.9	15.999	19.25
N 1s	401.41	2.49	5749.6	14.007	6.07
Y 3s	394.864	7.483	6479.9	88.906	47.77
Si 2p	105.938	1.678	6244.6	28.086	26.91

Table B11 XPS analysis of silicon nitride product from 0.5% yttrium impregnated RHA at different reaction times:

Element	Position BE (eV)	FWHM (eV)	Raw Area (CPS)	Atomic Mass	Mass Conc%
1 h, top portion					
O 1s	537.986	2.362	34750.5	15.999	19.63
N 1s	404.532	2.127	9234.8	14.007	7.35
Y 3s	394.912	1.557	8428.8	88.906	46.83
Si 2p	105.078	1.135	8065.2	28.086	26.19
1 h, bottom portion					
O 1s	536.298	2.809	21985.2	15.999	15.66
N 1s	402.846	2.608	8081.8	14.007	8.11
Y 3s	400.036	2.138	7271	88.906	50.94
Si 2p	104.169	2.618	6176.2	28.086	25.29
3 h, top portion					
O 1s	531.091	2.835	44939.7	15.999	14.11
N 1s	397.483	1.957	18295.9	14.007	8.1
Y 3s	401.84	1.348	18305.9	88.906	56.54
Si 2p	105.513	1.883	11773.2	28.086	21.26
3 h, bottom portion					
O 1s	536.713	1.928	22632.7	15.999	22.96
N 1s	394.515	2.489	4626.9	14.007	6.62
Y 3s	394.642	2.981	4024.1	88.906	40.16
Si 2p	106.844	2.233	5185.7	28.086	30.26
6 h, top portion					
O 1s	537.797	2.495	43159.2	15.999	13.88
N 1s	401.8	1.641	17851.3	14.007	8.09
Y 3s	396.914	1.654	17948.7	88.906	56.77
Si 2p	105.409	1.993	11500.4	28.086	21.26
6 h, bottom portion					
O 1s	535.341	1.586	25169.8	15.999	20.2
N 1s	401.319	0.597	5359.4	14.007	6.06
Y 3s	397.623	0.481	4910.6	88.906	38.77
Si 2p	106.082	2.492	7574.2	28.086	34.96

APPENDIX C

EDX MAPPING OF RAW MATERIALS AND SILICON NITRIDE PRODUCTS
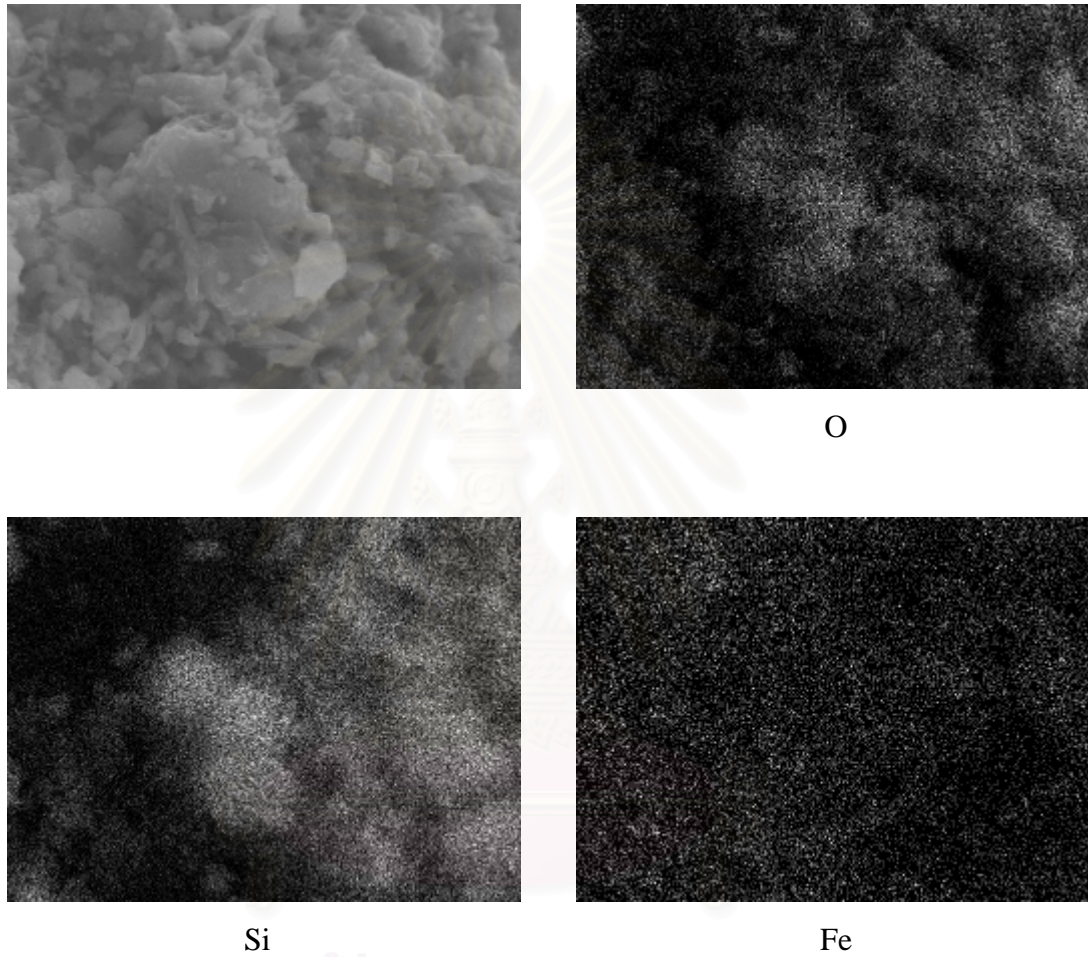

O

Si

Fe

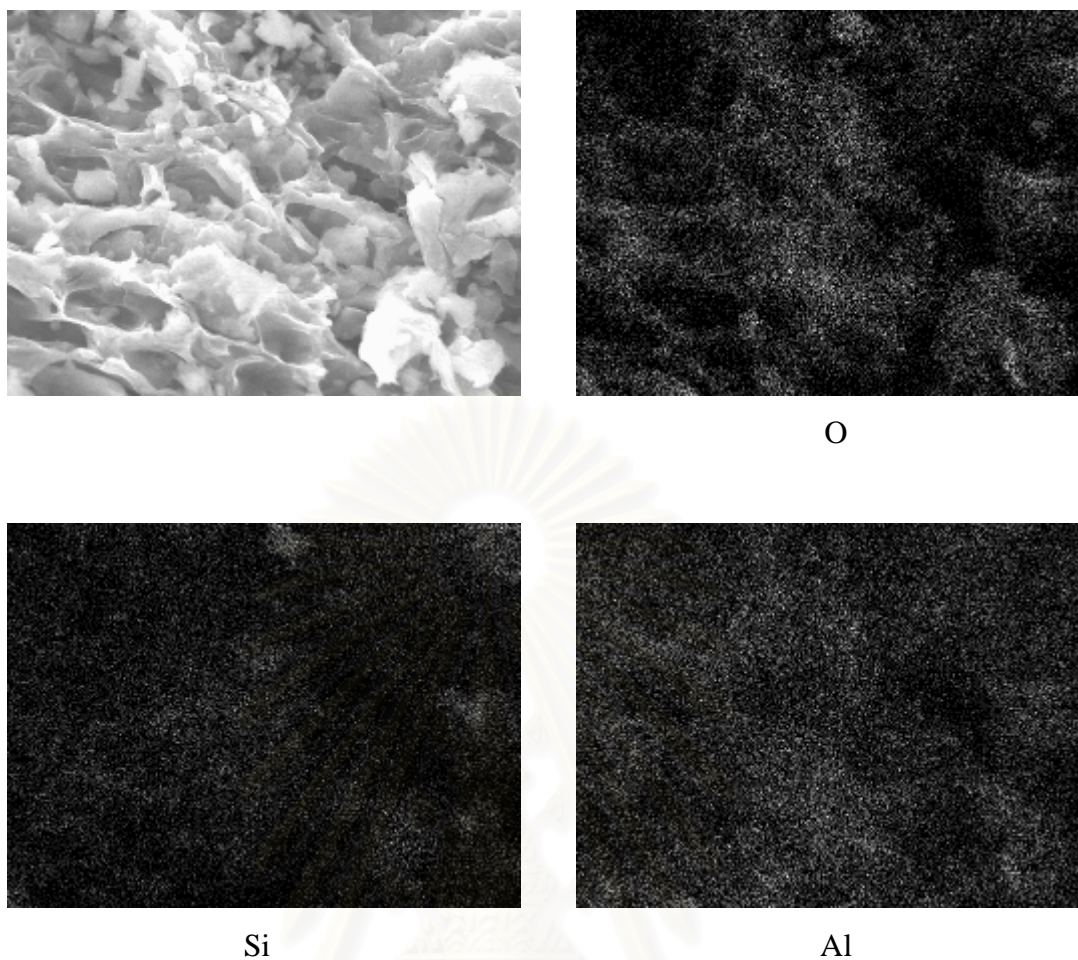**Figure C1** EDX mapping of 3.0% iron impregnated RHA before nitridation.

O

Si

Al

Figure C2 EDX mapping of 3.0% aluminium impregnated RHA before nitridation.

O

Si

Mg
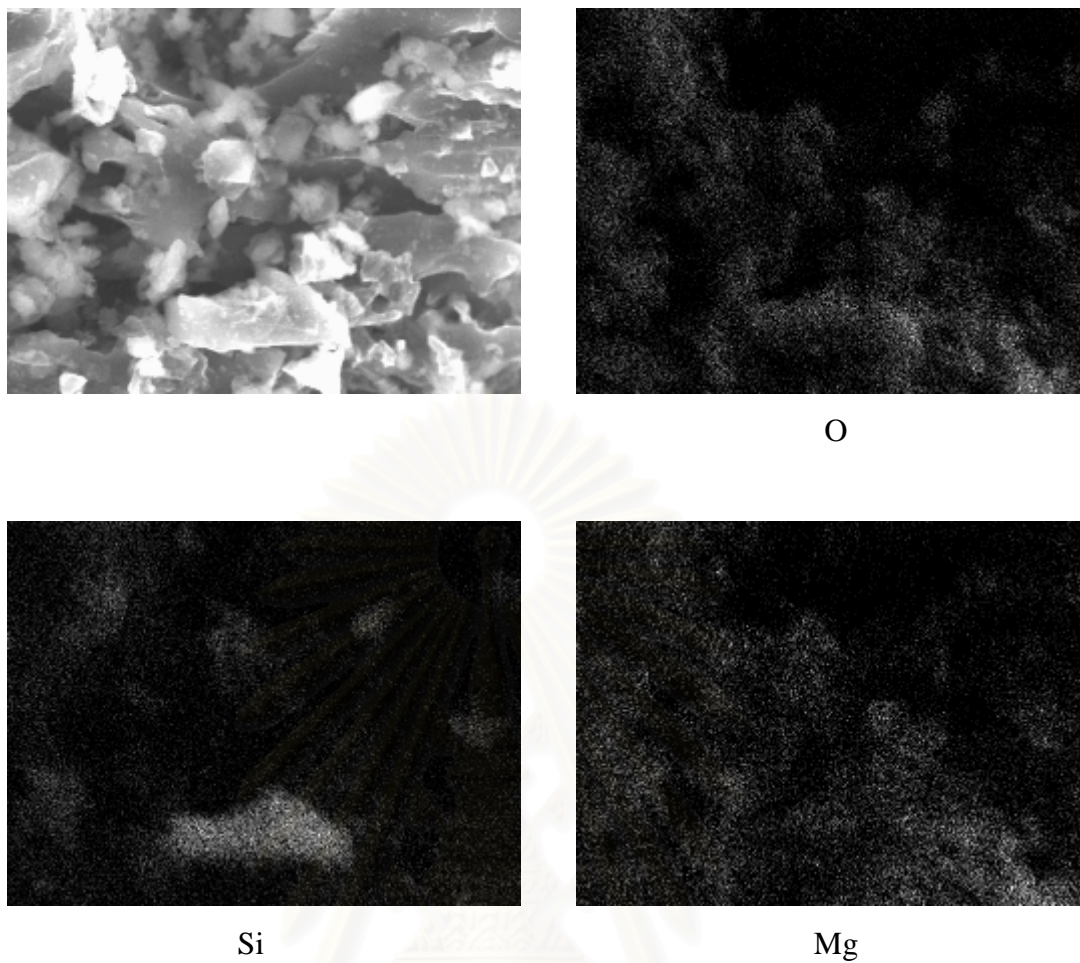
Figure C3 EDX mapping of 3.0% magnesium impregnated RHA before nitridation.

O

Si

Cu
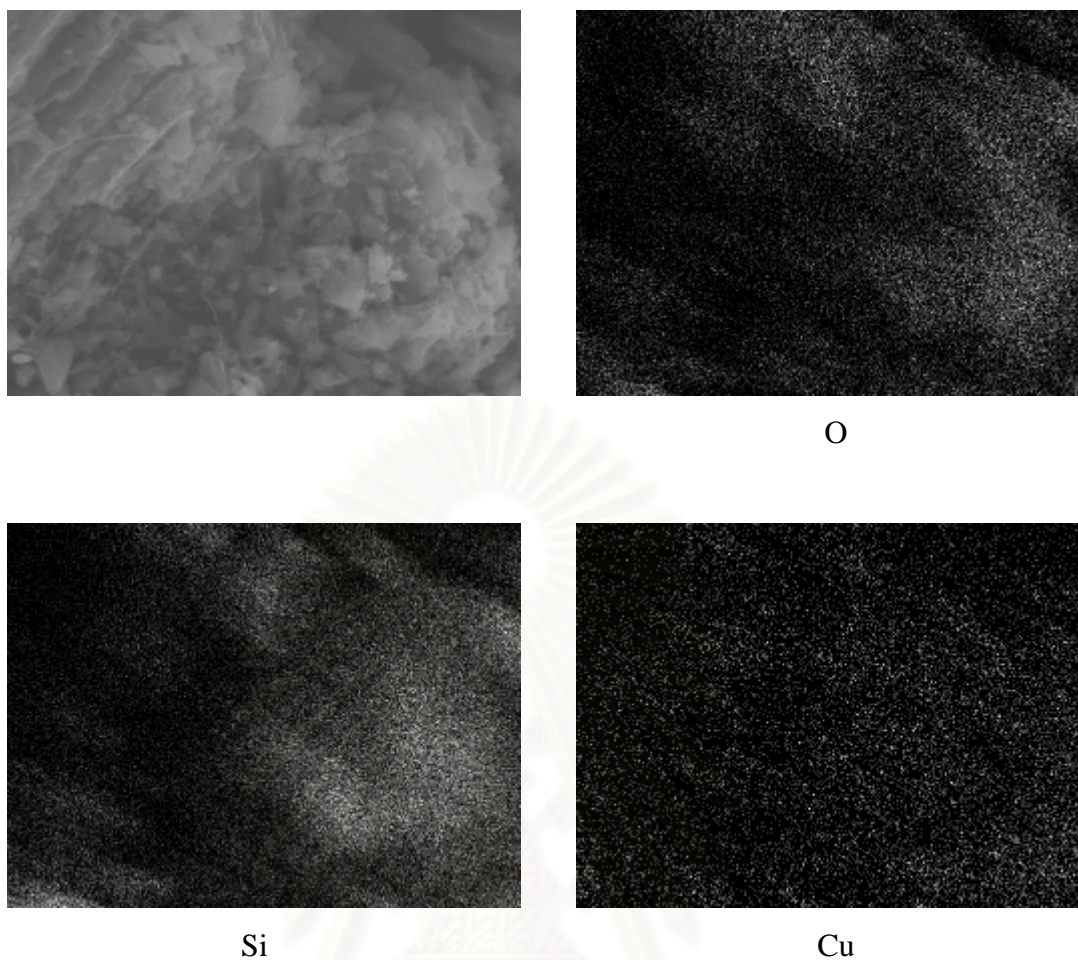
Figure C4 EDX mapping of 3.0% copper impregnated RHA before nitridation.

O

Si

Y
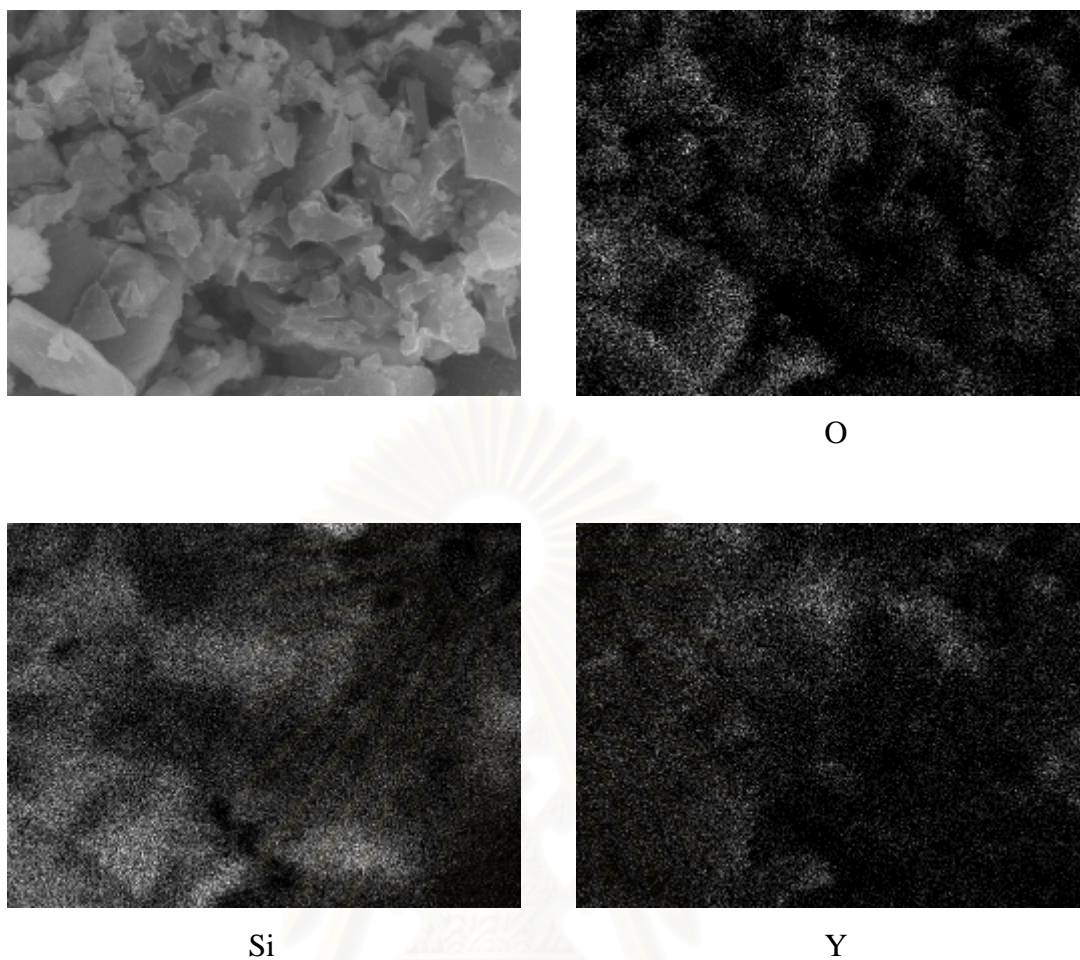
Figure C5 EDX mapping of 3.0% yttrium impregnated RHA before nitridation.

O

Si

Fe

N
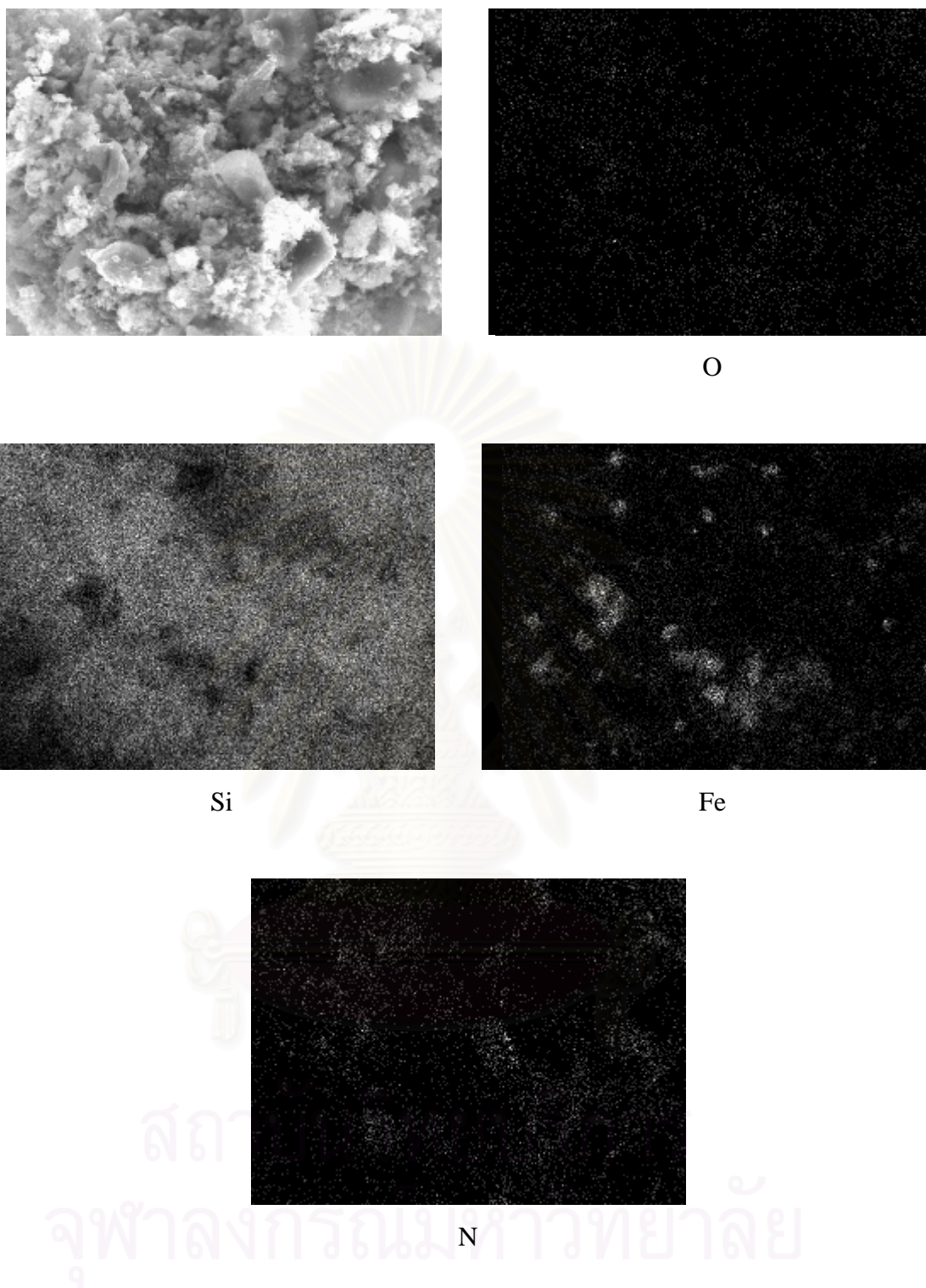
Figure C6 EDX mapping of silicon nitride product from 3.0% iron impregnated RHA
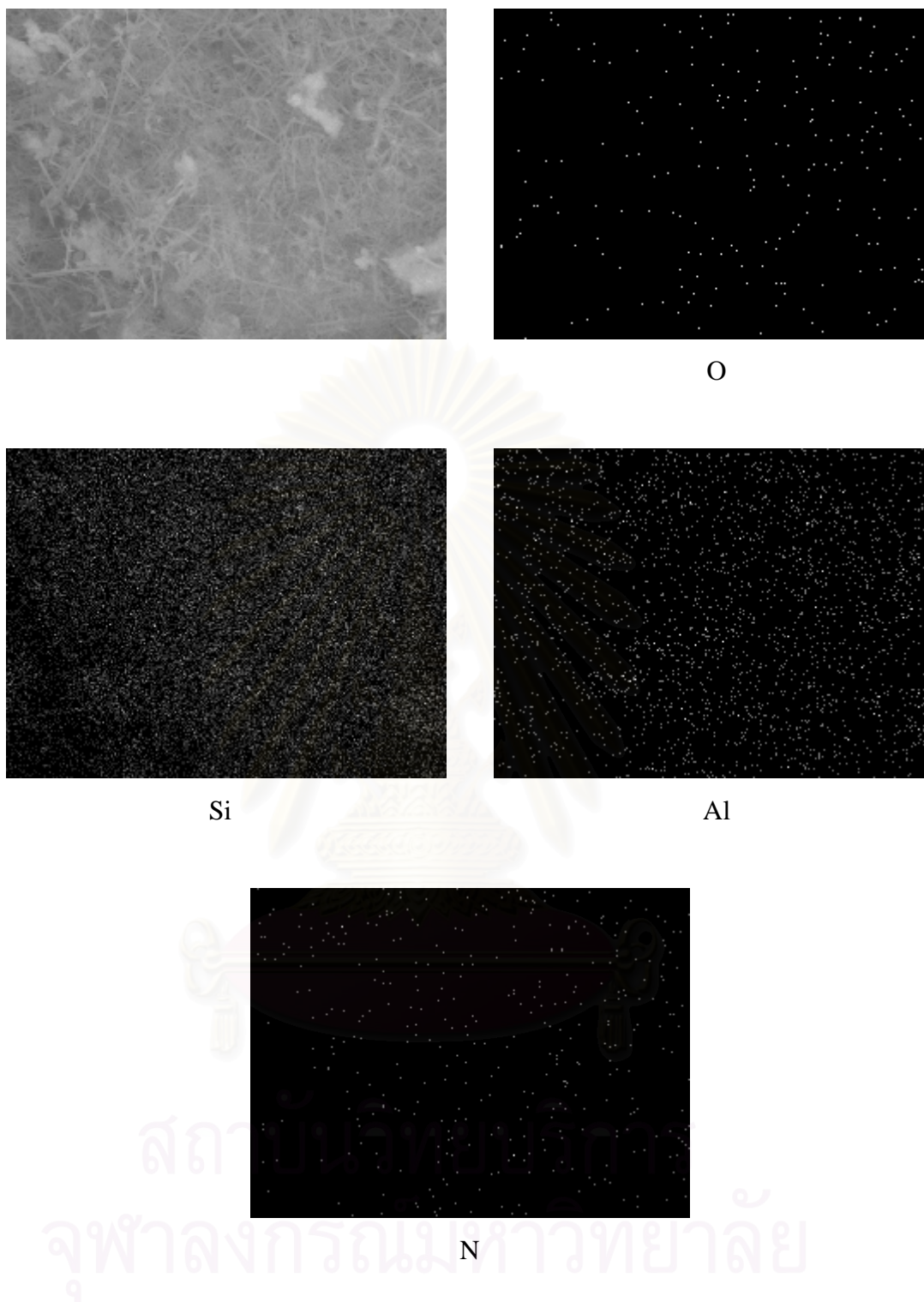
Figure C7 EDX mapping of silicon nitride product from 3.0% aluminium
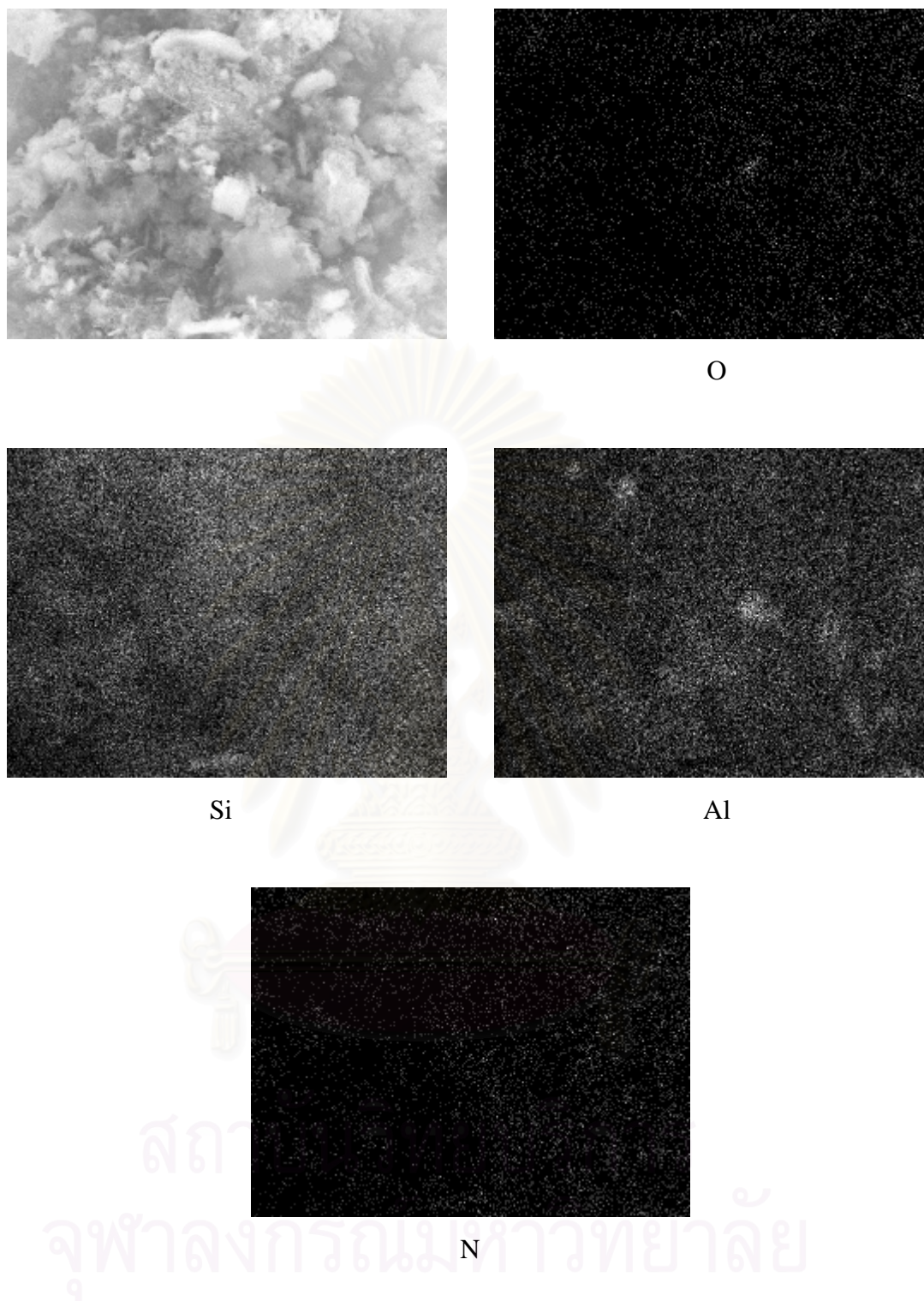impregnated RHA in top portion.

O

Si

Al

N

Figure C8 EDX mapping of silicon nitride product from 3.0% aluminium
impregnated RHA in bottom portion.

Figure C9 EDX mapping of silicon nitride product from 3.0% magnesium impregnated RHA in bottom portion.
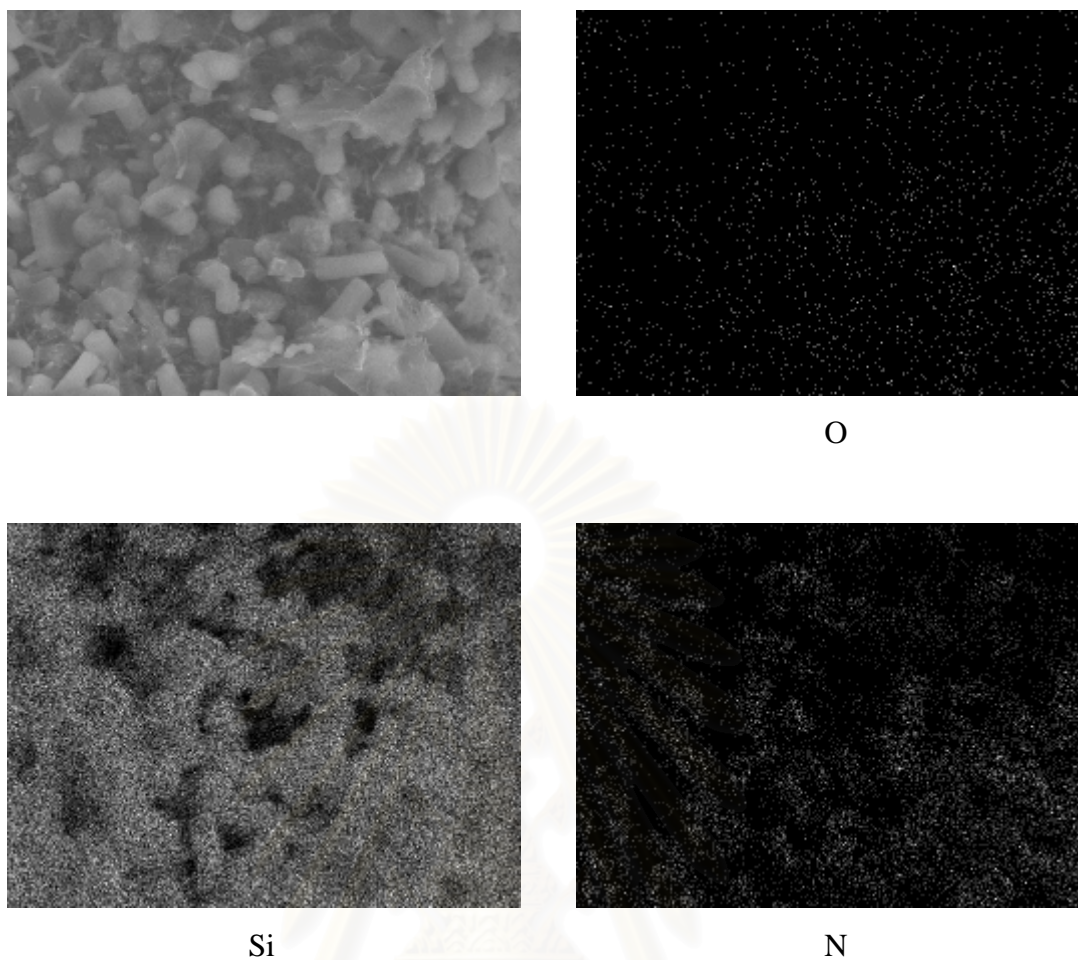
O

Si

N

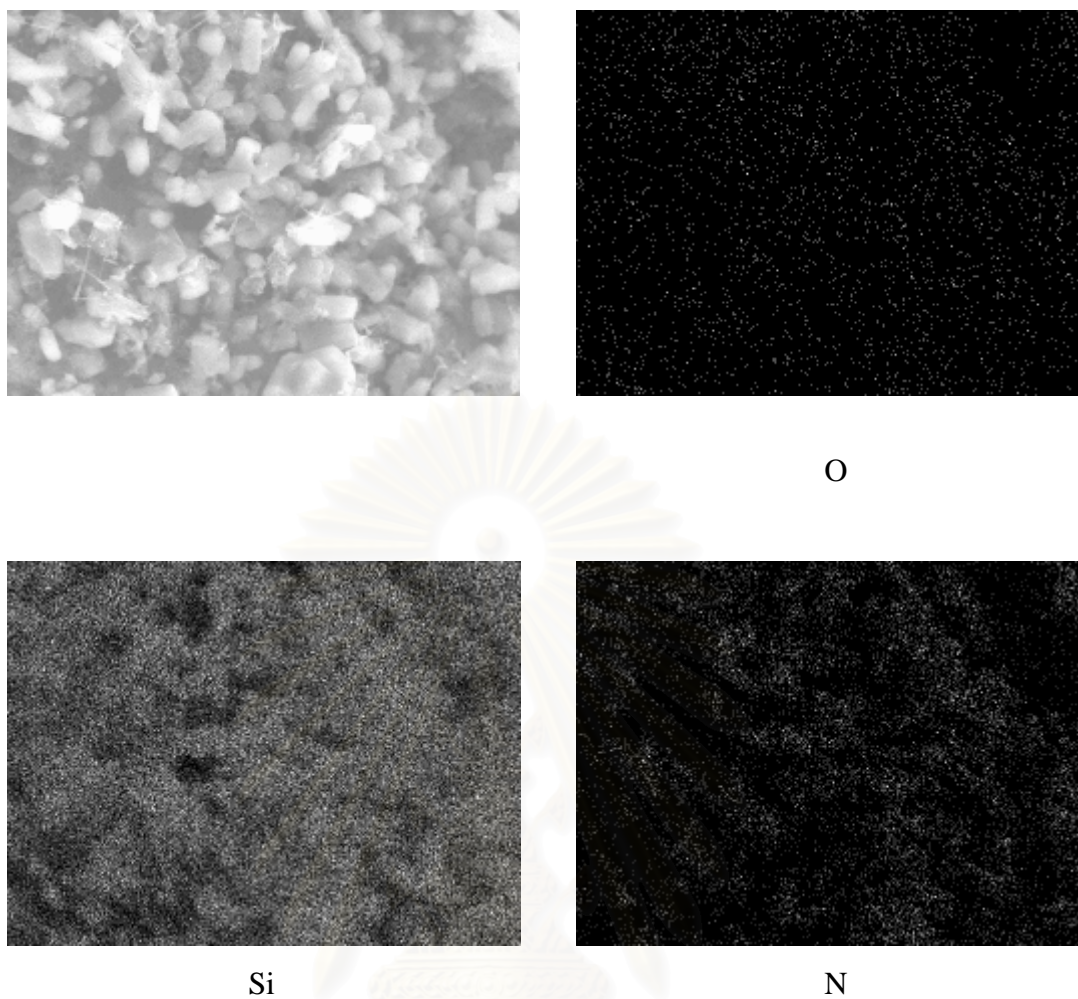**Figure C10** EDX mapping of silicon nitride product from 3.0% copper impregnated
RHA in bottom portion.

O

Si

N
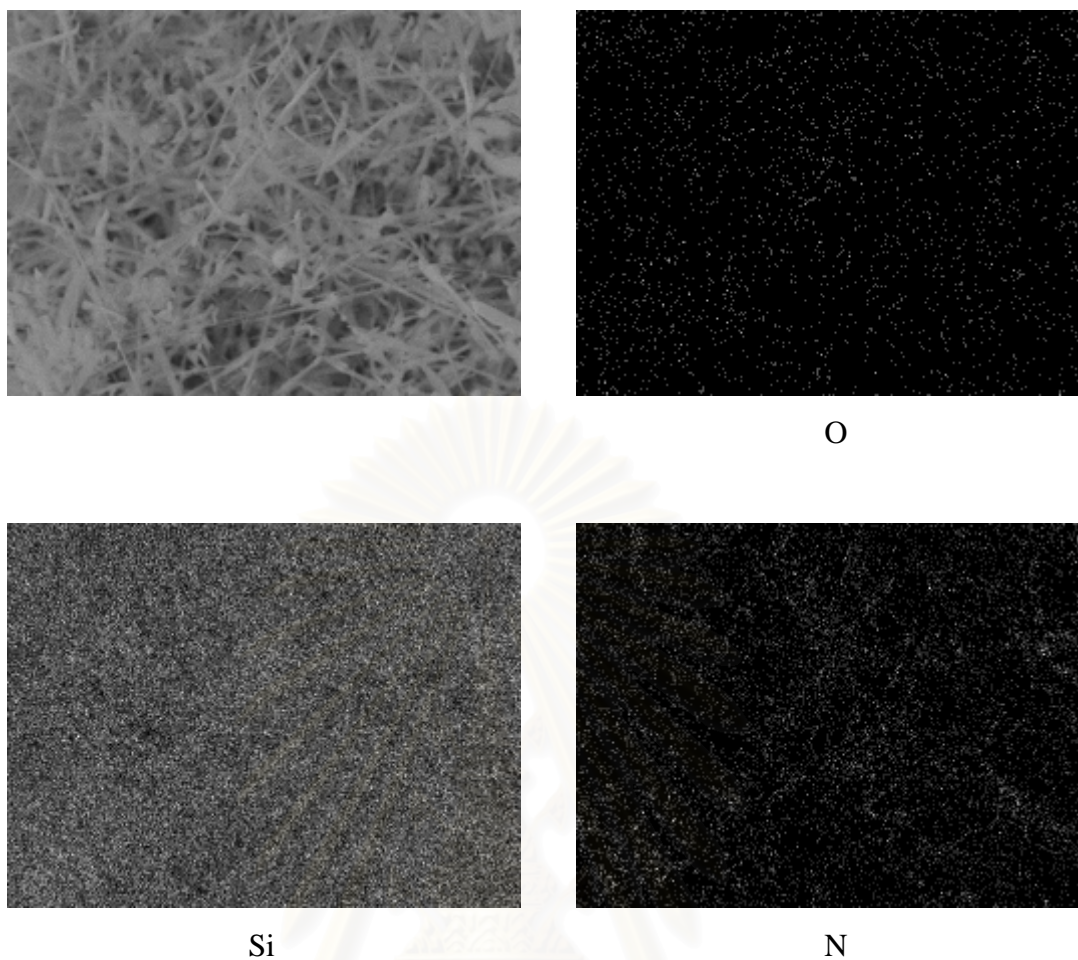
Figure C11 EDX mapping of silicon nitride product from 3.0% yttrium impregnated
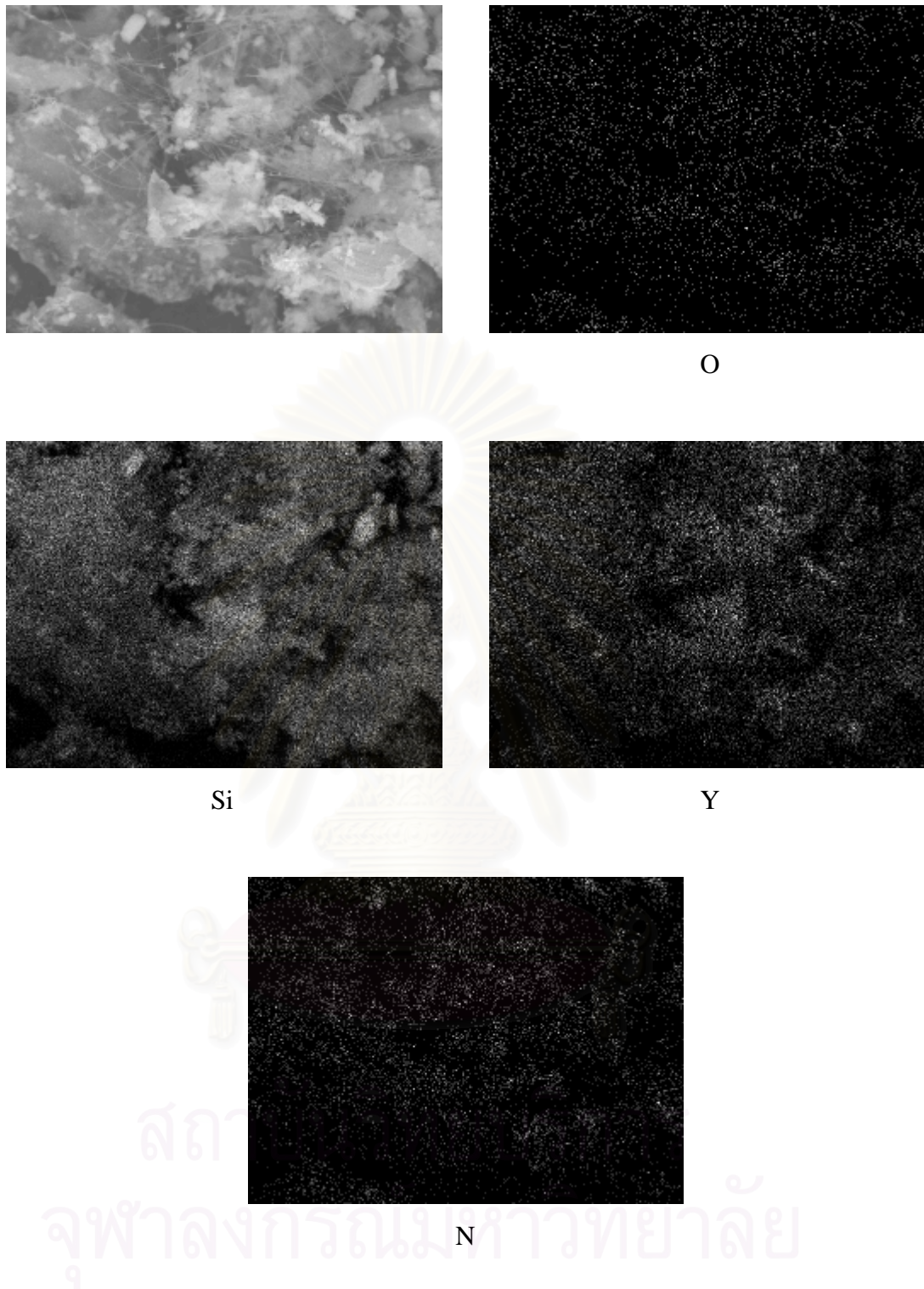RHA in top portion.

O

Si

Y

N

Figure C12 EDX mapping of silicon nitride product from 3.0% yttrium impregnated
RHA in bottom portion.
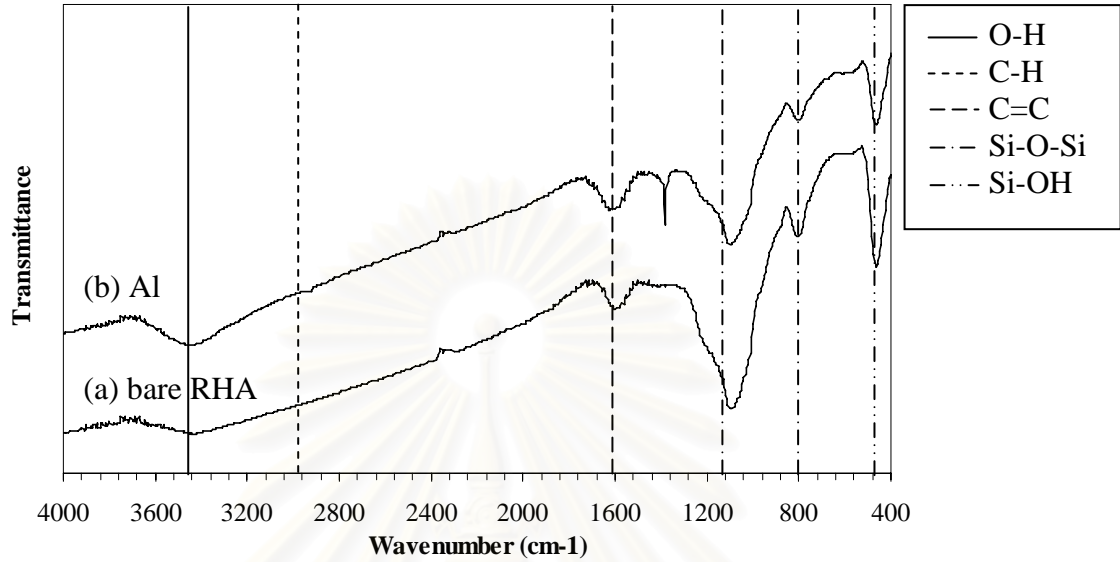
FT-IR ANALYSIS OF SAMPLES

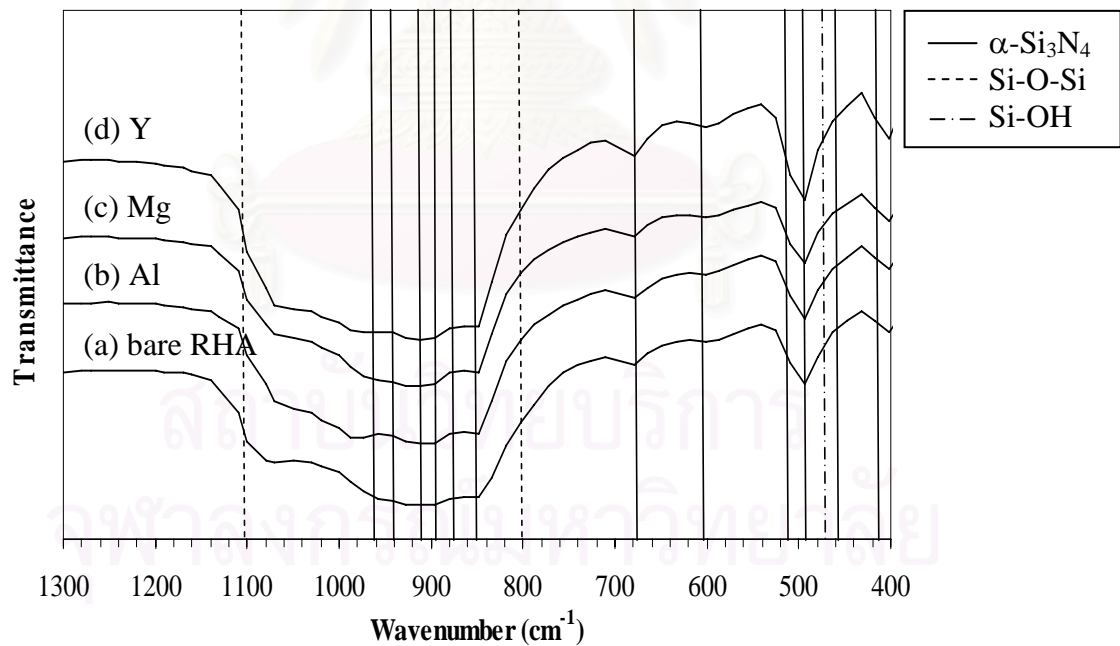**Figure D1** FT-IR spectra of metal-impregnated RHA: (a) bare RHA and (b) 0.5% Al.

Figure D2 FT-IR spectra of product from the carbothermal reduction and nitridation

in top portion: (a) bare RHA, (b) 0.5% Al, (c) 0.5% Mg, (d) 0.5% Y.
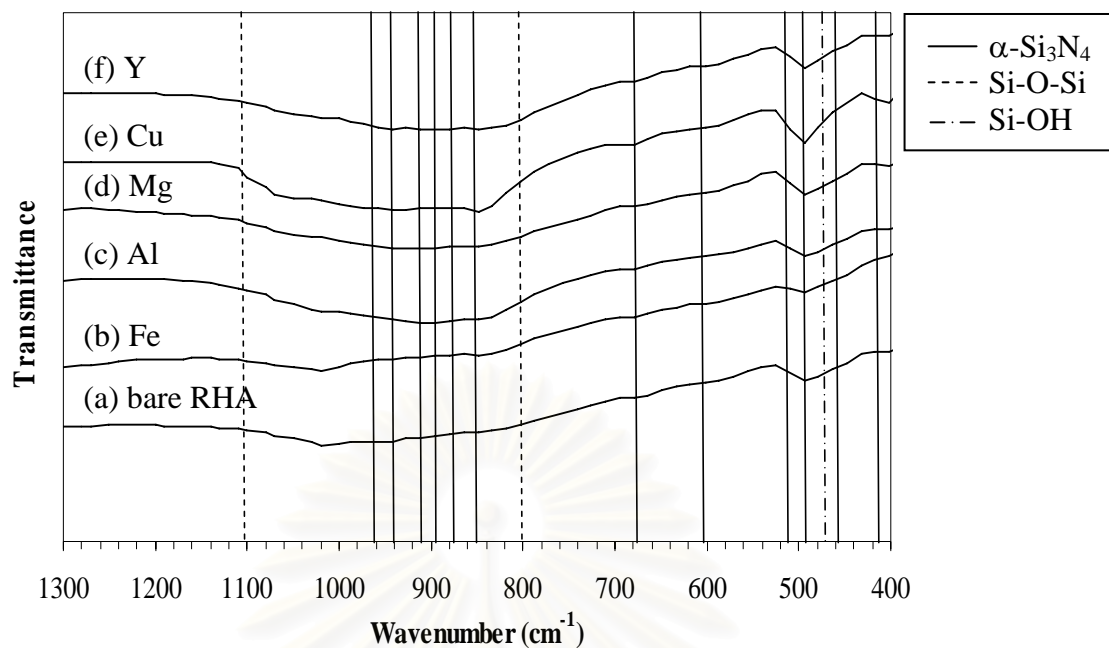
Figure D3 FT-IR spectra of product from the carbothermal reduction and nitridation
in bottom portion: (a) bare RHA, (b) 0.5% Fe, (c) 0.5% Al, (d) 0.5% Mg,
(e) 0.5% Cu and (f) 0.5% Y.

APPENDIX E

LIST OF PUBLICATION

1. Praphat Thanongkongsawad, Piyasan Praserthdam and Varong Pavarajarn, "Catalytic Effects of Metals in the Carbothermal Reduction and Nitridation of Rice Husk Ash", The Fourth Thailand Materisls Science and Technology Conference, Bangkok, Thailand, March 31-April 1, 2006, 46-48.

Catalytic Effects of Metals in the Carbothermal Reduction and Nitridation of Rice Husk Ash

Praphat Thanongkongsawad, Piyasan Praserthdam and Varong Pavarajarn*

Center of Excellence on Catalysis and Catalytic Reaction Engineering,

Department of Chemical Engineering, Chulalongkorn University, Bangkok 10330

*Corresponding author: (Phone 0-2218-6890, Fax. 0-2218-6877, E-mail: fchvpv@eng.chula.ac.th)

Abstract

Silicon nitride could be synthesized by carbothermal reduction and nitridation of rice husk ash (RHA). In this work, catalytic effects of various metals, i.e. aluminum, magnesium, yttrium, copper and iron were investigated. It was found that magnesium enhanced the formation of β-silicon nitride, while yttrium enhanced the formation of α-silicon nitride. Beside the catalytic activity toward the formation of silicon nitride, some of the impregnated metal also enhanced the formation of silicon carbide.

1. Introduction

Silicon nitride (Si_3N_4) is one of the most promising structural materials for high-temperature and high mechanical stress applications because of many excellent high temperature related properties. Silicon nitride exists in two common crystalline phases, i.e. α- and β-phase. One common method for silicon nitride synthesis is the carbothermal reduction and nitridation process, according to the following overall reaction:

$$3SiO_2\ (s) + 6C\ (s) + 2N_2\ (g) \rightarrow Si_3N_4\ (s) + 6CO\ (g)$$
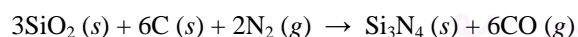
Since rice husk ash (RHA) naturally contains both silica and carbon which are well mixed to each other, it is considered to be a good candidate for the carbothermal reduction and nitridation process. It is also economical to produce high-valued silicon nitride from low-valued agricultural waste. However, despite the extensive studies, the production of silicon nitride from RHA has not been commercially implemented because of the problem associated with impurities as well as the very long reaction time required [1].

Many parameters contribute to the extent of the nitridation process, such as temperature, particle size, reaction time, heating rate and reactant gas composition [2,3]. Addition of metals to RHA, for their catalytic effects, is also an effective approach to regulate the subsequent reaction of silica in RHA [4,5]. In this study, the catalytic effect of various metals such as iron, aluminum, copper, yttrium and magnesium on the carbothermal reduction and nitridation process of RHA is investigated.

2. Experimental

Rice husk used in this work was jasmine rice husk from Nakornratchasima province in Thailand. The husk was thoroughly soaked in distilled water at 90°C for 3 h, subsequently dried in an oven at 110°C for 24 h and pyrolyzed at 600°C under argon flow rate of 10 ml/sec for 3 h to form RHA. Metal was added to RHA by impregnation. About 2 g of RHA was immersed in 10 ml of solution of metal-nitrate compound (e.g. $Fe(NO_3)_3 \cdot 9H_2O$, $Cu(NO_3)_2 \cdot 2.5H_2O$, $Mg(NO_3)_2 \cdot 6H_2O$, $Al(NO_3)_3 \cdot 9H_2O$ and $Y(NO_3)_3 \cdot 6H_2O$, all of which had 99.9% purity and were used as received) in methanol. The amount of metal-nitrate compound used was adjusted according to the desired level of metal impregnation. After all methanol was naturally evaporated, the samples were put in an oven at 110°C for 24 h to ensure the elimination of all possibly remaining methanol and moisture.

Silicon nitride was synthesized via the carbothermal reduction and nitridation of RHA. The RHA was put into an alumina tray (25 mm × 15 mm × 5 mm deep), which was placed in the uniform temperature zone of a horizontal tubular flow reactor. The reactor was continuously purged with argon and heated up to the reaction temperature (1450°C) at constant heating rate of 10°C/min. Then, the nitridation was initiated by

switching the supplying gas to a gas mixture of 90% nitrogen and 10% hydrogen. The flow rate of the gas was maintained at 50 l/h (measured at room temperature). The reaction was maintained at constant temperature for 6 h. The product was characterized by various techniques, such as powder X-ray diffraction (XRD), Scanning electron microscopy (SEM), Fourier transform infrared spectrometry (FTIR), Thermogravimetric analysis (TGA) and X-ray photoelectron spectroscopy (XPS).

3. Results and Discussion

The product obtained from the carbothermal reduction and nitridation of undoped RHA was similar to the results reported earlier in our previous work [2]. Generally, the product residing in the sample holder can be categorized into two portions, i.e. dark gray powder at the bottom of the holder and thin layer white fibrous materials on the top, all of which were confirmed by XRD analysis to have silicon nitride as the major crystalline phase. For all experiments, mass fraction of the dark gray portion of the product was much higher than the top layer. Examples of SEM image for each portion of the product are shown in Figure 1.
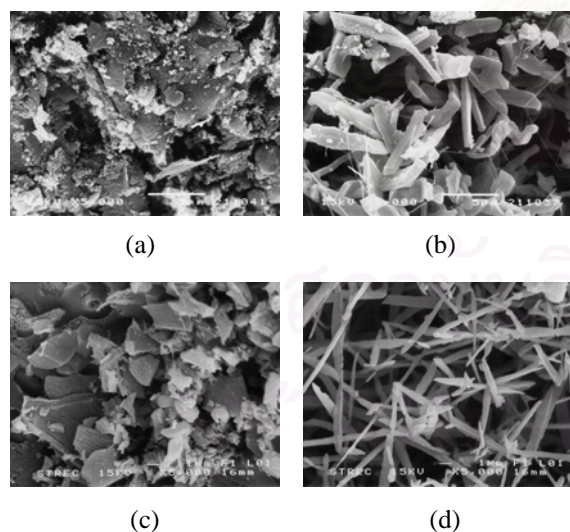

(a)   (b)

(c)   (d)

Figure 1. SEM micrographs of products from the carbothermal reduction and nitridation of RHA impregnated with 0.5% aluminum: (a) bottom portion, (b) top portion; comparing with products from non-impregnated RHA: (c) bottom portion, (d) top portion.

According to Figure 1, the dark gray powder consists of irregular shape aggregates, while the top layer of white fibrous material is rod-like grains. This observation is in agreement with the report in our previous work [2]. However, when metal was present in the system, grains in top layer were much bigger than that of bare RHA.

Figure 2 shows the XRD patterns of products from the nitridation of RHA impregnated with various metals (0.5% wt.). It is clearly indicated that metal has catalytic effect toward the phase formation of silicon nitride. Addition of magnesium enhanced the formation of β-Si_3N_4, especially in the top portion of the product. On the other hand, yttrium enhanced the formation of α-Si_3N_4. No silicon nitride in β-phase was observed from the top layer of the product when yttrium was used.
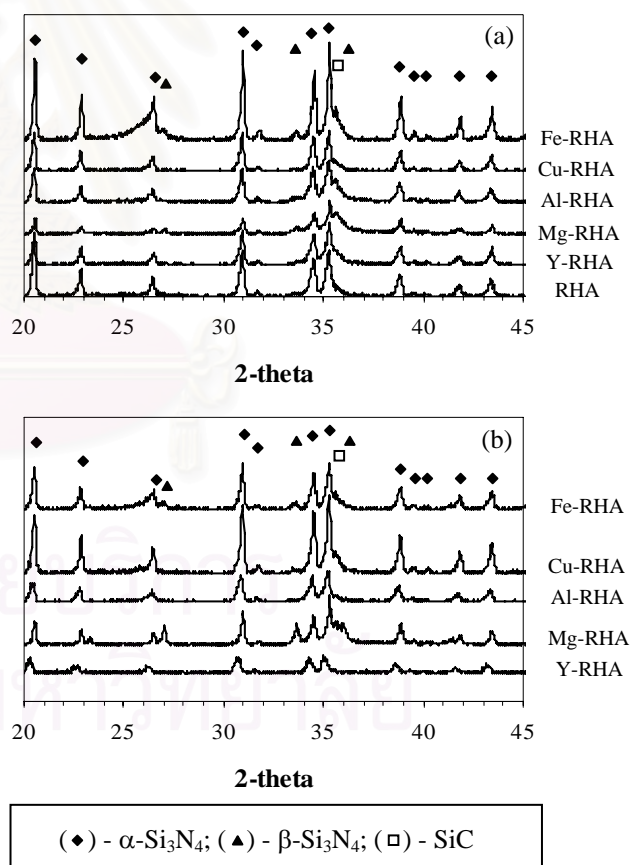

Figure 2. XRD patterns of products from carbothermal reduction and nitridation of RHA impregnated with various metals: (a) bottom portion of product, (b) top portion of product.

The results shown in Figure 2 also suggest that metal impregnated to RHA regulates the reaction for silicon carbide formation. Many metals, such as magnesium, aluminum and iron tend to have catalytic effect toward silicon carbide. Although, it has been generally accepted that the reaction between silica and carbon to form silicon carbide takes place at temperature higher than 1500°C [6], the presence of these metals can result in high fraction of SiC in the product (as observed from high XRD peak at 2-theta around 35.5°). It should be noted that, in case when SiC was detected in the product, SiC was present in both portions of the product. This observation is particularly interesting because silicon carbide-silicon nitride composite formed from RHA usually has non-fibrous morphology [7,8].

The catalytic activity of metal was increased when the amount of impregnated metal was increased. As seen in Figure 3, for the case of aluminum impregnation, the higher the aluminum content, the more β-silicon nitride as well as silicon carbide was produced. Very high content of β-silicon nitride/silicon carbide composite was obtained from the carbothermal reduction and nitridation of 3% aluminum impregnated RHA.
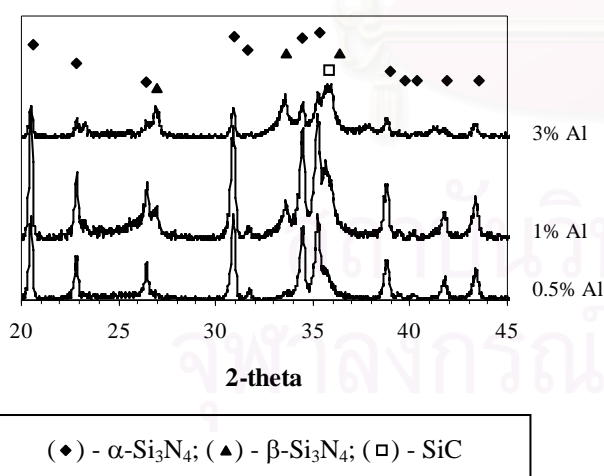
4. Conclusion

Catalytic activity of metal for the carbothermal reduction and nitridation of RHA was investigated. The crystalline phase of silicon nitride product was significantly influenced by the presence of metal in RHA. Moreover, formation of silicon carbide was also enhanced by metal, such as magnesium, aluminum and iron.

5. Acknowledgement

References

[1] Riley, F.L., Journal of the American Ceramic Society, 83, 245, 2000.
[2] Pavarajarn, V., Precharyutasin, R. and Praserthdam, P. Proceedings of. the 7th World Congress of Chemical Engineering, Glasgow, Scotland.2005.
[3] Arik, H., Journal of the European Ceramic Society, 23, 2005, 2003.
[4] Rahman, I.A. and Riley, F.L., Journal of the European Ceramic Society, 5, 11, 1989.
[5] Liou, T.H., Carbon, 42, 785, 2004.
[6] Krishnarao, R.V. and Godkhindi, M.M., Ceramics International, 18, 243, 1992.
[7] Hnatko, M., Galusek, D. and Sajgalik, P., Journal of the European Ceramic Society, 24, 189, 2004.
[8] Kuskonmaz, N., Sayginer, A., Toy, C., Acma, E., Addemir, O. and Tekin, A., High Temperature Materials and Processes, 15, 123, 1996.

($\blacklozenge$) - α-Si_3N_4; ($\blacktriangle$) - β-Si_3N_4; ($\square$) - SiC

Figure 3. XRD patterns of bottom products from carbothermal reduction and nitridation of aluminum-impregnated RHA in various concentrations.

VITA

Mr. Praphat Thanongkongsawad was born on 29th September, 1982, in Bangkok, Thailand. He received him Bachelor degree of Engineering with a major in Chemical Engineering from Srinakharinwirot University (SWU), Nakhon Nayok, Thailand in 2004. He continued him Master study in the same major at Chalalongkorn University, Bangkok, Thailand in June 2004.